UNIVERSITY OF CAPE TOWN

Thesis submitted in fulfilment of the requirements for the degree of Master of Science in Engineering in the Department of Electrical Engineering

---

Energy Efficiency Analysis of Converter-Fed Induction Motors

Author
John Mushenya

Supervisor
Prof. Azeem Khan

August 2018

Declaration

"I know the meaning of plagiarism and I declare that all the work in this dissertation, save for that which is properly acknowledged, is my own. This thesis/dissertation has been submitted to the Turnitin module and I confirm that my supervisor has seen my report and any concerns revealed by such have been resolved with my supervisor."

Signed by candidate

John Mushenya

August 2018

Acknowledgements

I am very thankful to God Almighty for the grace that has made it possible for me to complete this master's dissertation. This journey has been the most turbulent, and yet the most thrilling experience of my academic endeavours.

I wish to express my heartfelt-thanks to my supervisor, Professor Azeem Khan for his invaluable guidance, consistent encouragement and financial support throughout the course of this work. He has been a great mentor and I am very glad to have pursued my master's studies in the Advanced Machines and Energy Systems (AMES) research group, under his supervision.

I would also like to thank my incredible parents, Mr. and Mrs. Daniel and Regina Mushenya, and my wonderful siblings, Daniel, Peter, Francis, James and Selina, for their love and moral support during my time away from home. Special thanks also to my best friends Prisca Bupe and Richard Siakuba for their constant messages of goodwill.

I am extremely grateful to Mr. Chris Wozniak for his overwhelming technical guidance throughout the experimental phase of this work. I am also thankful to Riyaad, Tashrique, Bongi, Hossein and all technicians in the Machines lab for always being on hand to assist me during my lab tests. This work would have been impossible to complete without you all.

Special thanks to Mr. Michael Sparenberg from HBM Netherlands and Mr. Peter Nakha from Ametek USA for their technical support at various stages of the hardware implementation for this project. I am also grateful to the AMES Research Administrator, Ms. Shireen Sabodien, for her tremendous support regarding all admin issues related to my research.

Finally, I would like to thank all my friends from the AMES research group, Akinola, Sampath, Olakunle, Darren, Moloa, Dolly and Emmanuel, for their contributions to this project in one way or another and for making my stay in Cape Town extremely memorable.

Abstract

Electric motor systems are the largest consumers of industrial electrical energy. As Variable Speed Drives continue to dominate various industrial processes, there is need for stakeholders to fully understand and quantify the converter-fed motor losses over a wide range of operating conditions. Such knowledge is crucial for both manufacturers and end-users in performing energy-efficiency optimizations for motor-drive applications. Although there is an increase in legislative activities, particularly in Europe, toward classification and improvement of energy efficiency of electric motor-drive systems, the available standards for quantifying the various losses are still in their early stages of development. None of these standards have yet passed through all the required phases for them to be considered full international standards, owing to a lack of consensus on many technical issues. Therefore, the need for researchers to provide feedback to the relevant standards committees cannot be over-emphasized.

One of the most challenging issues in estimating the efficiency of converter-fed motors is the accurate determination of additional harmonic losses due to the PWM voltages and currents. Although the recently introduced IEC 60034-2-3 Technical Specification has proposed a method of determining these losses through experimental testing, the approach is still undergoing validation. Moreover, it only considers the rated motor frequency and voltage whereas induction motor drives are usually operated over a wide range of speed and torque.

The main emphasis of the work presented in this dissertation was to develop a thorough understanding of various converter-fed induction motor losses, and hence efficiency, when fed from a 2-level Voltage Source Inverter. In particular, the dissertation provides a healthy questioning of some concepts in the proposed IEC method, with a view to providing useful feedback for improving the standard. Comparisons are also drawn between the related standards to identify areas for improvement. This study further attempts to explain some conflicting reports cited in literature regarding the nature of additional harmonic losses.

The experimental results obtained by testing three induction motors demonstrate some of the technical issues associated with the determination of additional harmonic losses. To mitigate the adverse effect of varying technical skill and competence levels on efficiency test results, an automated testing procedure was developed and implemented on the 110kW test rig in the UCT Machines Lab. The test rig, which boasts of a *Genesis 7i* high-speed Data Acquisition System, also provides an energy-efficient platform for investigating the steady-state and dynamic characteristics of converter-fed motors. By utilizing the capability of the Data Acquisition System to segregate the fundamental and harmonic components of measured input electrical power, it was found that a PWM power supply can be used in place of a conventional Variac to estimate the sinusoidal supply efficiency of an induction motor. This is a welcome development for both laboratory and field efficiency testing applications.

This page intentionally left blank

Contents

List of Figures

List of Tables

Nomenclature

DC	–	Direct Current
EMI	–	Electromagnetic Interference
IEC	–	International Electrotechnical Commission
IEEE	–	Institute of Electrical and Electronic Engineers
IM	–	Induction Motor
NEMA	–	National Electrical Manufacturers Association
PWM	–	Pulse-Width Modulation
RMS	–	Root Mean Square
SCIM	–	Squirrel Cage Induction Motor
SLL	–	Stray-Load Loss
TS	–	Technical Specification
VFD	–	Variable Frequency Drive
VSI	–	Voltage Source Inverter

1. INTRODUCTION

1.1 BACKGROUND TO THE STUDY

Electric motor systems account for about 60 to 70 percent of industrial electricity consumption, and about 40 percent of global electricity consumption. They are the main source of mechanical energy in various industrial processes and systems [1]. Although this figure is much smaller in domestic applications and the tertiary industry, electric motors find application in a host of household appliances and public amenities. These range from very small motors used in computers, food mixers, washing machines and air conditioning units, to the large motors used in electric trains. Consequently, even small improvements in the design and operation of these motors can potentially lead to significant global energy savings. This is what makes electric motors an attractive target for energy efficiency studies.

Although there is a wide variety of electric motor types available in industry today, the three-phase Squirrel-Cage Induction Motor (SCIM) is the most widely used motor type, occupying, by far, the largest market share [2]. This is due to its robustness, low cost and simplicity in construction. However, owing to the constant-speed nature of Induction Motors (IMs) when fed from a mains supply, DC motors were for a long time the obvious choice for variable speed applications. This was due to the relative ease with which their speed can be controlled. Nonetheless, the presence of brushes and commutators which required periodic maintenance made the DC motor unfavourable for high speed operations or for use in harsh environments [3]. Therefore, the emergence of the Variable Frequency Drive (VFD) in the late 1980's provided the much-needed variable speed operation in IMs, hence consolidating their reputation as the 'workhorse' of industry.

Fig.1. 1. Application of motorised systems for industrial process control. [*Source: www.electronicproducts.com*]

Although VFDs have become so popular in the last two decades owing to their energy saving capability and ease of process control, they introduce additional harmonic losses in electric motors. Therefore, while considering the overall energy savings potential of VFDs, it is equally important to quantify the harmonic losses introduced by the PWM voltages and currents, and the associated degradation in motor efficiency [4]. Such knowledge can then be used to optimize various industrial processes, and to improve the design of these motors and VFDs. Moreover, as more and more manufacturing companies are established, it becomes necessary for regulation authorities to ascertain the quality and energy efficiency of the motor and VFD systems being supplied on the market. However, this determination of converter-fed motor losses and efficiency must be performed according to a standardized procedure to ensure a fair comparison of motors from different manufacturers.

While there is an increase in legislative activities toward the classification and improvement of energy efficiency in motor-VFD systems [5], the available standards for quantifying the various losses are still in their development phase. Therefore, researchers are constantly looking for ways to improve these standards by proposing more accurate test methods, motivated by the advancements in power measurement technology and a better understanding of the machine losses under variable operating conditions.

1.2 ENERGY EFFICIENCY IMPROVEMENT

Different regional and international organizations have intensified their efforts to promote a competitive electric motor market transformation. Although the approach varies from one organization to another, the aim is to accelerate the transition towards high-efficiency motor systems. For instance, the European Union has taken a more radical and mandatory transition while the South African electricity supply utility has opted for a subtler approach by providing incentives to energy-efficient industrial customers in South Africa. Each of these two approaches is briefly described in the following sections:

1.2.1 European Community

The European Community regulation CE 640/2009 [5] imposes that all motors introduced in the European market will have to respect the minimum efficiency IE classes, following the scheduled agenda which has been summarised in [6] as reported in Table 1.1. The various efficiency classes referred to in this regulation are defined in the International Electrotechnical Commission (IEC) 60034-30 standard [7] and are reported in Fig 1.2.

A similar classification for converter-fed motors will soon be launched. However, for this to happen, there is need for a well-established international test standard for quantifying the motor-drive system efficiency. It is only a matter of time before similar policies are implemented in South Africa as part of the National Energy Efficiency Program.

Table 1.1 Timeline for the application of IEC 60034-30 as imposed by the regulation CE 640/2009 [6]

Phase	Starting date	Requirements
1	16 June 2011	All motors must have a minimum efficiency equal to the IE2 class
2	01 January 2015	All motors with rated power between 7.5 – 375 kW must have a minimum efficiency equal to IE3 class or IE2 class if with inverter supply
3	01 January 2017	All motors with rated power between 0.75 - 375 kW must have a minimum efficiency equal to IE3 class or IE2 class if with inverter supply

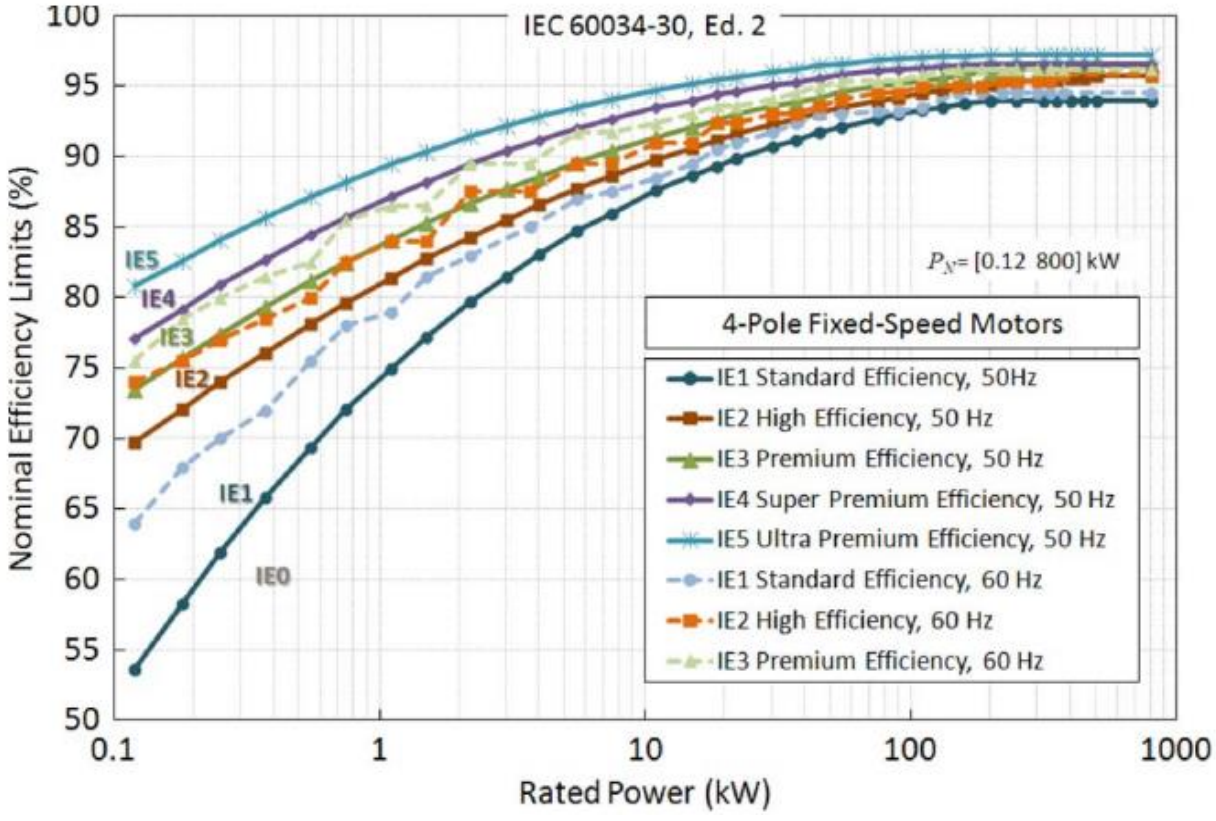

Fig.1. 2. IEC Nominal Efficiency class limits for 4-pole motors in the 0.12 – 800 kW power range. [2]

1.2.2 South African Scenario

In 2007, the South African Electricity Supply Utility (Eskom) introduced an Energy-Efficient motor programme in its Demand Side Management strategy to improve the energy efficiency. How this program worked was that electric motor users in industry were offered an instant once-off rebate on the purchase price of a new Eff1 motor when purchasing it to replace an old inefficient motor, which was to be traded for scrapping. The programme was nationwide and offered to customers via the accredited suppliers on the programme. All these efforts were aimed at encouraging energy efficiency in industrial applications. By implementing energy-efficient motors in all industrial applications, Eskom estimated that enough electricity could be saved to meet the demand needs of 1500 average households in South Africa [8].

Table 1.2 Eskom subsidy table for the Energy-Efficient Motor Program [8]

kW Rating	4-pole Eff 1	2-pole Eff 1	DSM Subsidy
	Eff (%)		
1.1	≥ 83.8	≥ 83.8	R 400
1.5	≥ 85	≥ 84.1	R 400
2.2	≥ 86.4	≥ 85.6	R 500
3	≥ 87.4	≥ 86.7	R 500
4	≥ 88.3	≥ 87.6	R 500
5.5	≥ 89.2	≥ 88.5	R 700
7.5	≥ 90.1	≥ 89.5	R 700
11	≥ 91	≥ 90.6	R 700
15	≥ 91.8	≥ 91.3	R 700
18.5	≥ 92.2	≥ 91.8	R 1,000
22	≥ 92.6	≥ 92.2	R 1,300
30	≥ 93.2	≥ 92.9	R 1,400
37	≥ 93.6	≥ 93.3	R 1,700
45	≥ 93.9	≥ 93.7	R 2,200
55	≥ 94.2	≥ 94	R 2,600
75	≥ 94.7	≥ 94.6	R 3,000
90	≥ 95	≥ 94.6	R 3,500

The subsidy amount was calculated to cover most of the cost of the difference between the average motor supplier's catalogue price of Eff1 (premium efficiency) motors and Eff2 (high efficiency) motors, thus incentivising the purchase of Eff1 motors over Eff2 motors. Table 1.2 shows the full-load efficiency values of 2- and 4-pole Eff1 motors with the respective subsidies which, depending on the size of the motor, would range from R400 to R3500. The figures shown in Table 1.2 were revised on a regular basis, and the efficiency classes Eff1, Eff2 and Eff3 (standard efficiency) were adopted from the IEC efficiency classes defined in [7].

In the first year of the Energy-Efficient motor programme, its impact was low as only 164 motors were collected by Eskom. A case study [51] reports that activities were accelerated in

the second year as 1088 standard motors were replaced with energy-efficient motors, with a combined output power of 15.99MW. However, the program was stopped in 2009 because monitored results indicated that expected energy savings were not achieved whereas Eskom was running into cash flow problems. Furthermore, replacing the motors without optimizing the system loads was not adequate. Therefore, Eskom's recent Demand Side Management strategies have focussed on promoting the installation of VFDs for energy savings.

Although Eskom is no longer offering any direct subsidies to motor users in industry on the purchase of VFDs, it has partnered with the National Treasury, the South African Revenue Services and the Department of Energy to offer a tax allowance that supports start-up or expanding businesses that practice and adhere to energy productivity. This Income Tax Act, referred to as the *12L Tax Allowance*, enables businesses to claim a tax deduction for the efficient use of energy and for investing in modern energy-efficient equipment. Through this act, businesses can claim 95 cents per kilowatt hour of energy saved, which could have been used if energy-efficient technologies and processes had not been implemented [52]. However, this tax allowance falls off 12 months from the time it was approved on a client. A similar Tax Allowance Act (*12I Tax Allowance*) is available for new industrial projects or expansions that meet, among other criteria, energy efficiency and cleaner production requirements.

1.3 MOTIVATION FOR DISSERTATION

The test methods for efficiency estimation in IMs fed from a mains supply are well-established after going through several improvements over the years. The most commonly used international standards are the IEEE 112 [9] and the IEC 60034-2-1 [10]. However, for converter-fed induction motors, there is only a handful of draft standards, none of which has attained the level of consensus required to be considered a full international standard. Given the influx of VFDs on the market in the last two decades, there is a demand for test facilities to critically analyse these draft standards and provide feedback that can be used to refine them. The 110kW test rig available in the UCT machines lab provides a suitable platform for testing the practical applicability of the recently introduced IEC Technical Specification (IEC/TS) 60034-2-3 [11], as well as studying the dynamic operation of induction motors.

The IEC/TS, which attempts to characterize converter-fed induction motor losses, has made good progress by specifying the test methods, reference drive parameters, and introduces the concept of additional harmonic losses. However, the experimental determination of these

harmonic losses is still a challenge for researchers as evidenced by conflicting reports cited in literature [12], [13], [22], [29], on the dependency of harmonic losses on motor load. Such inconsistencies are expected because the measurement of non-sinusoidal power quantities is more complex than that of sinusoidal ones as shown in [14]. Furthermore, in addition to establishing test facilities with appropriate instrumentation for analysing harmonic losses, it is imperative to eliminate errors due to varying technical skill and competence levels of the individuals performing the efficiency tests. One way to achieve this is by implementing automated efficiency testing procedures.

1.4 OBJECTIVES OF STUDY

The main objectives of this research work are:

- To review the available standards for efficiency estimation of converter-fed machines and highlight some of the recent improvements in the testing procedure and analysis.
- To test the practical applicability of the recently introduced IEC 60034-2-3 Technical Specification and identify any technical issues that can influence the proposed determination of harmonic losses.
- To provide feedback on these issues to the relevant IEC standards committee in the form of a technical paper.
- To use the advanced Data Acquisition System on the 110kW Test rig in the UCT machines lab to study some dynamic operations of converter-fed induction motors.
- To minimize human errors in the back-to-back efficiency estimation process by developing an automated testing procedure.

1.5 SCOPE AND LIMITATIONS OF STUDY

Although various topologies of electric motors can be supplied from a converter, the IEC/TS procedure, in its current form, is only valid for IMs fed by a 2-level Voltage-Source Inverter (VSI). Therefore, only IMs motors will be considered in this research work.

In addition to operating at rated voltage and frequency, IMs can also operate above and below the base speed, when supplied by a VFD. When considering the performance characterisation of converter-fed induction motors, it is therefore vital to analyse the motor losses over a wide range of operating speeds. However, the work presented in this dissertation

is limited to IM operation at base speed (frequency), to establish a firm understanding of the IEC/TS procedure. Future studies will then attempt to extend the proposed IEC procedure to other regions of the torque-speed plane of IMs.

In this study, all no-load tests with a converter supply were performed by maintaining a constant dc bus voltage, that is, by employing a variable modulation index technique. This aspect of the testing procedure will be discussed in detail in the proceeding chapters of the dissertation.

1.6 OUTLINE OF DISSERTATION

The research presented in this dissertation is divided into nine chapters as follows:

Chapter—1: This chapter presents an overview of energy efficiency in electric motors and a few examples of deliberate policies that different organizations have put in place to promote the use of high-efficiency electric motors.

Chapter—2: An overview of international standards for efficiency estimation of converter-fed IMs is presented in this chapter, with additional details on the limitations and technical issues surrounding the IEC/TS.

Chapter—3: This chapter presents an in-depth discussion on the various categories of losses in a converter-fed induction motor.

Chapter—4: The IEC/TS procedure for the experimental determination of additional harmonic losses in converter-fed IMs is presented in this chapter. The chapter also highlights recent technical improvements in the methods proposed by the different standards.

Chapter—5: In this chapter, the 110kW test rig that was used for experimental work is described. To demonstrate the test rig's suitability for the analysis of transient operations, the chapter also presents a report on the dynamic operation of converter-fed IMs.

Chapter—6: This chapter describes the developed automated testing procedure for estimating the efficiency of converter-fed IMs, in accordance with the proposed IEC/TS procedure.

Chapter—7: This chapter presents details of the performed experimental tests, the objectives, and the adopted methodology. The experimental data collected from these tests is presented in this chapter and appendix A of the dissertation.

Chapter—8: In this chapter, the test results presented in chapter 7 are analysed and discussed in detail to highlight the key findings of this study.

Chapter—9: In this chapter, conclusions and recommendations are drawn from the presented results and discussions.

The research outline is summarized in Fig. 1.3.

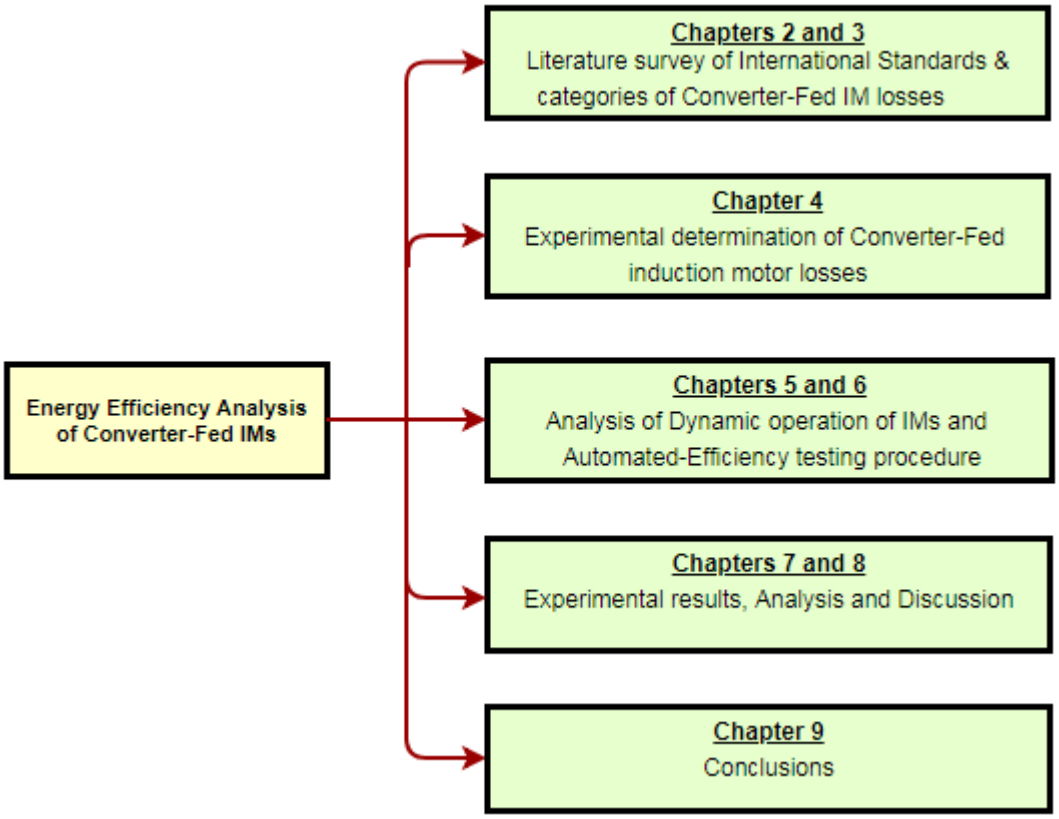

Fig.1. 3 Organization of dissertation

1.7 RESEARCH OUTPUTS

Conference Publications:

(a) J. Mushenya and M.A. Khan, "Automated Efficiency Testing of Converter-Fed Induction Motors," IEEE Power Africa Conference, Cape Town, South Africa, June 2018.

Papers in Preparation:

(a) J. Mushenya and M.A. Khan, "Simple Method for Estimating Converter-Fed Induction Motor Efficiency," intended for publication in IEEE Transactions on Energy Conversion.

2. OVERVIEW OF INTERNATIONAL STANDARDS FOR CONVERTER-FED MOTOR EFFICIENCY

This chapter presents an overview of international standards that relate to the determination of converter-fed motor efficiency. In this discussion, emphasis is placed on the recently introduced IEC 60034-2-3 Technical Specification as it is the basis of the experimental work presented in this dissertation.

2.1 REVIEW OF STANDARDS FOR CONVERTER-FED MOTOR EFFICIENCY

The methods for the performance characterization of induction motors fed from a mains supply are well established after going through several improvements over the years. The most relevant international standards widely used in industry are the IEEE 112 [9] and the IEC 60034-2-1 [10]. Others like the Canadian standard CSA C390-2010 and the Japanese standard JEC 37 are mostly used in their respective countries. In recent times, revisions to the above standards have been largely minor in nature, which is a sign that the standards have matured.

On the other hand, test standards for motor-drive systems are just beginning to appear. At present, the handful of standards that deal with motor-variable frequency drive systems can hardly be said to have matured. Many of them relate to specifications rather than tests, and those that are test standards have barely been applied in industry [14]. Of these draft standards, the most promising one is the IEC 60034-2-3 [11], which was released in 2013 by the Electrical Drives committee of the International Electrotechnical Commission (IEC). The objective of this standard is to define test methods for determining the additional harmonic losses of converter-fed induction motors.

Although the work presented in this dissertation is mostly based on the IEC Technical Specification, it was necessary to review the other related standards to establish a basis for comparison and endorsement. The following sections briefly outline existing standards related to efficiency estimation in converter-fed motors as well as complete motor-VFD systems. The discussions presented in each section highlight the primary focus of each standard and the limitations associated with it.

2.1.1 IEEE Standard 995

This is one of the earliest standards to have been produced for converter-fed motor efficiency determination. It was published in 1987 by the Drives Committee of the Industry Applications Society (IAS), to propose a method for determining the efficiency of large adjustable-speed alternating current motor-drive systems. This standard was primarily directed to synchronous motor-drive systems exceeding 1000hp, in which a dc-liked converter is connected between the line and the load [17]. According to this standard, the additional harmonic losses in synchronous machines due to the non-sinusoidal voltages and currents were calculated as a fixed percentage of the fundamental sine wave losses according to (2.1).

$$P_h = k_1.(SL + I^2RS) \tag{2.1}$$

where P_h is the harmonic loss, k_1 = 0.3 and $SL + I^2RS$ is sine wave load losses which is a combination of the Stray-Load losses and armature copper loss.

As reported in the appendix of the IEEE 995 standard, the fixed multiplier k_1 = 0.3, which represents approximately 15% additional electrical losses over the sinusoidal losses, was a reasonable estimate given the limited information available on the subject at the time. This published recommended practice was only part 1 of the task – the other part was never published. According to the author of [14], it appears the task was never completed. Moreover, it is not clear for how long this standard became available as there are no existing revisions to it. Currently, the IEEE 995 has been withdrawn and has been in this state for many years.

2.1.2 CSA C838

The CSA C838 standard [18] was published in 2013 by the Canadian Standards Association (CSA). This standard establishes the testing procedure for determining the efficiency of Variable Frequency Drive systems under varying loads and speeds. It applies to voltage source inverter (VSI) pulse-width modulated (PWM) drives for induction motors and other three phase VFD technologies with a voltage rating not exceeding 750V.

Although the standard provides procedures for estimating losses under converter supply by taking the losses under sinusoidal supply as a reference, its primary focus is the measurement of system efficiency [14]. In addition, this standard is only used in Canada and is generally not recognized internationally. Therefore, this standard was not particularly applied in this research.

2.1.3 EN 50598-2

The European Standard EN 50598-2 [19] is another recently published standard that deals with motor-VFD systems. The standard was proposed by the European Manufacturers Association (CEMEP), similar to the National Electrical Manufacturers Association (NEMA), and has been undergoing revisions on a yearly basis since it was first introduced in September 2013. The aim of the standard is to specify the Energy Efficiency indicators for Power Drive Systems PDS, motor starters, and power electronic converters used in motor-driven applications in the power range of 0.12kW up to 1000kW. According to this standard, the power drive system (PDS) consists of the motor, loading device and variable frequency drive, which is referred to as a complete drive module (CDM) as illustrated in Fig. 2.1.

The European standard does not specify its own test methods for determining the additional harmonic losses but refers to the draft IEC/TS 60034-2-3 [11]. Nonetheless, it offers mathematical models for estimating the various losses in the motor system, the PDS and the CDM at non-rated motor frequency. This aspect gives it a slight advantage over the related IEC/TS as will be discussed further in section 2.2 of this dissertation. As these mathematical models are based on certain assumptions, they are only intended to give rough estimates of the motor losses at non-rated speed and must therefore be treated with caution.

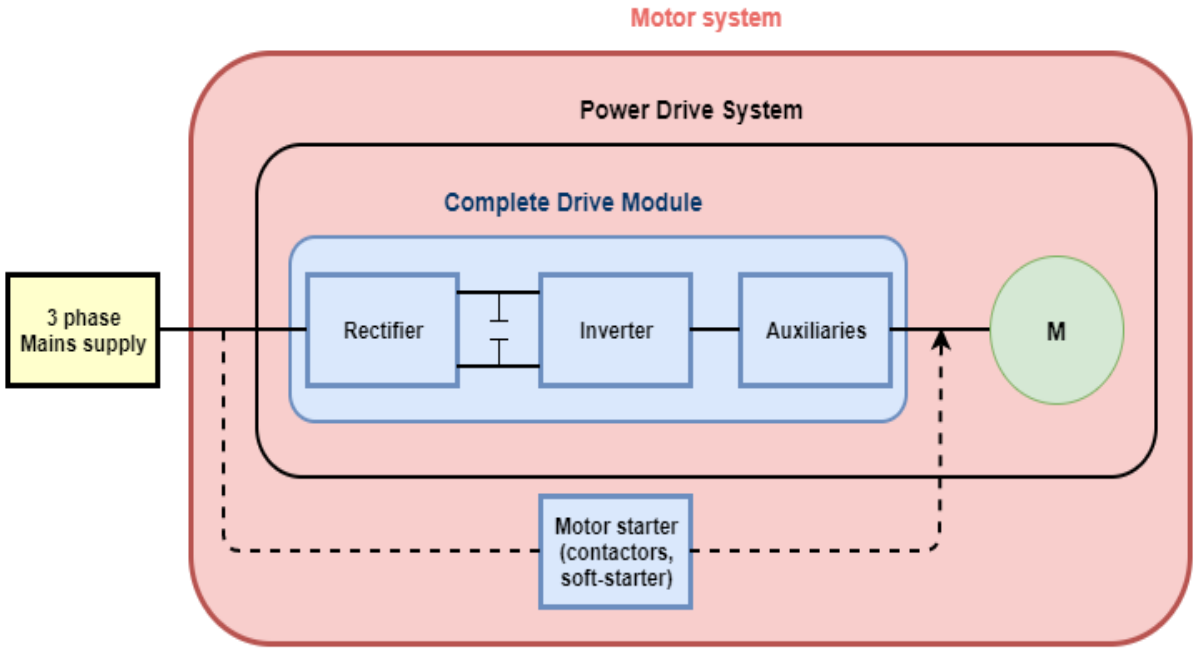

Fig.2. 1. Definitions of power drive system (PDS), complete drive module (CDM) and motor system as defined by EN 50598-2 [19]

2.1.4 IEC 60034-2-3

This standard was published in 2013 by the Rotating Machinery committee of the International Electrotechnical Commission (IEC) as a technical specification. The objective of the IEC/TS is to define test methods for determining the additional harmonic motor losses and efficiency of voltage-source inverter-fed induction motors. The results obtained using this standard are intended to allow for efficiency ranking of different IMs when they are fed by converters. In contrast to the other standards discussed above, the emphasis of the IEC/TS is on test methods, instrumentation requirements and converter parameterization to establish comparable testing conditions. It specifies four test methods, all based on experimental activity.

The IEC/TS defines the additional harmonic losses as the increase in motor losses in moving from a sinusoidal supply to a PWM supply. Therefore, the proposed procedure requires that the fundamental motor losses are first determined with a sinusoidal supply using the already established IEC 60034-2-1 standard [10], and then repeating the tests with a converter. Although the proposed procedure is valid, there are certain limitations and technical considerations that need to be addressed if this technical specification is to mature into a full international standard in the next few years.

To acknowledge that the subject area is relatively new and that a consensus has not been met regarding certain aspects of the test procedure and requirements, [11] has been released in the light form of a Technical Specification. A technical specification, by IEC procedures, is a standard that has not fully passed through all required stages for it to be considered a full standard. This normally happens when the subject is still under technical development where there is a lack of consensus on certain aspects of the standard. Therefore, there is a call for test facilities to test the practical applicability of the proposed procedure and to provide feedback that will assist in refining the standard.

As the IEC/TS is the core of this study, the following section presents an in-depth discussion regarding its methodology, merits and limitations.

2.2 TECHNICAL CONSIDERATIONS AND LIMITATIONS OF IEC/TS 60034-2-3

Both the Canadian Standard CSA C838 and the European Standard EN 50598-2 have made some progress in providing some guidance on the determination of motor-drive system efficiency as well as component motor and converter efficiencies using experimental

procedures and mathematical models. However, most of the recent technical discussions have focused on the IEC/TS as it provides more details on the experimental test methods. Moreover, EN 50598-2 does not provide its own method but rather refers to the IEC/TS procedure for determining the additional harmonic losses. Therefore, although the IEC/TS procedure still needs some refinements as will be highlighted in this section, it seems likely to mature into a full standard in the next few years as it is based on the already-established IEC 60034-2-1 standard. It is for this reason that the IEC/TS was selected for this research.

The aim of the IEC/TS is to evaluate the additional harmonic losses and efficiency of an induction motor when it is fed by a PWM supply, taking the motor losses under sinusoidal supply as a reference. This draft standard specifies the test methods, reference converter parameters and calculation procedures to be followed in determining the converter-fed motor losses at rated frequency. A detailed discussion on the available test methods and calculation procedures can be found in [22] and will be presented in chapter 4 of this dissertation.

To establish repeatable test conditions that can be used to rank motors in terms of efficiency on converter supply, the IEC/TS requires a strict parameterization of the introduced two-level *test-converter*. The standard specifies drive parameters such as switching frequency, fundamental motor voltage and frequency, and other drive settings shown in Table 2.1. This strict parameterization is justifiable since each of these parameters can significantly influence the obtained motor losses. However, while the parameterization is easy to implement on the test-converter, challenges arise when testing a motor with a generic VFD bought from a random manufacturer. This is because different manufacturers impose different limits and control flexibility on their products.

Table 2.1 IEC/TS test-converter parameters

Parameter	Required setting
Fundamental motor frequency	Rated value (50Hz or 60Hz)
Fundamental motor voltage	Rated motor voltage at 50/60Hz
Switching frequency	4kHz for output powers < 90kW 2kHz for output powers > 90kW
Slip compensation	Off
Current feedback	Off

The four test methods for determining losses and efficiency of converter-fed IMs defined in IEC/TS are briefly explained below:

Method 2-3-A: Summation of losses with test converter supply

This loss segregation method requires an IEC-defined test-converter parameterized according to Table 2.1. The term *test-converter* as used in the IEC/TS refers to a 2-level voltage source frequency converter capable of producing a strictly defined PWM waveform, according to Annex A of the standard. The purpose of the test-converter setup is only to establish comparable test conditions for motors designed for operation with commercially available converters. In addition to a test converter, method 2-3-A also requires a sinusoidal power supply. To determine the additional harmonic losses and efficiency, no-load and load tests are performed with both a sinusoidal supply and a test converter.

Method 2-3-B: Summation of losses with specific converter for final application

This method is similar to the test-converter method, but it is intended to be used when testing with a generic converter for the final application, or simply a commercially available converter. This means that with this method, the converter can be parameterized slightly different from the specified settings to suit a particular drive's capabilities. This method has been the subject of many discussions [2], [15], [16], [22] owing to the many restrictions imposed by the IEC/TS.

Method 2-3-C: Input – Output

The input – output (or direct) method is the simplest of all four and is intended for a specific converter supply. All that is required is a loading dynamometer and direct measurement of input power, load torque and speed. Although the direct method is generally considered less accurate than the loss segregation, some studies have shown that it has a smaller associated uncertainty than the later owing to the limited number of measurements it requires [21].

Method 2-3-D: Calorimetry

The calorimetric method uses the temperature rise in the coolant, usually a liquid, to determine the motor losses according to IEC 60034-2-2. Although this method is regarded as very accurate, it is only suitable for motors cooled by a liquid.

The following sections discuss some of the technical issues regarding the IEC/TS that have generated a lot of technical debates and criticism from the research community.

2.2.1 Converter input voltage

Under test-converter setup, the IEC/TS states as a reference condition that "*fundamental motor voltage must be equal to rated motor voltage at rated frequency, that is 50Hz or 60Hz. The input voltage of the test-converter shall be set to a value that allows rated motor voltage to be applied without going into overmodulation operation. However, the converter input voltage shall not be higher than just needed to fulfil the above*." The above reference condition is one of the critical issues in the discussions relating to the IEC/TS. This is because the avoidance of overmodulation is difficult to achieve in most converter topologies.

Reference [2] clearly illustrates the challenges in avoiding overmodulation by considering a typical VFD integrating a three-phase diode rectifier at the input and a two-level VSI with PWM at the output. If a 400V input voltage is applied to the rectifier-end and the VFD is set to produce 400V fundamental line-to-line voltage (equal to rated motor voltage), the VFD will slightly operate in the non-linear or overmodulation region. This will be the case even if third harmonic injection or space vector PWM (SVPWM) technique is utilized. Therefore, the author suggested that the only way to guarantee linear operation would be to boost the converter input voltage by means of an autotransformer. However, it is important to note that such a technique increases the PWM pulse peak values, leading to higher order harmonics as shown in Fig 2.2.

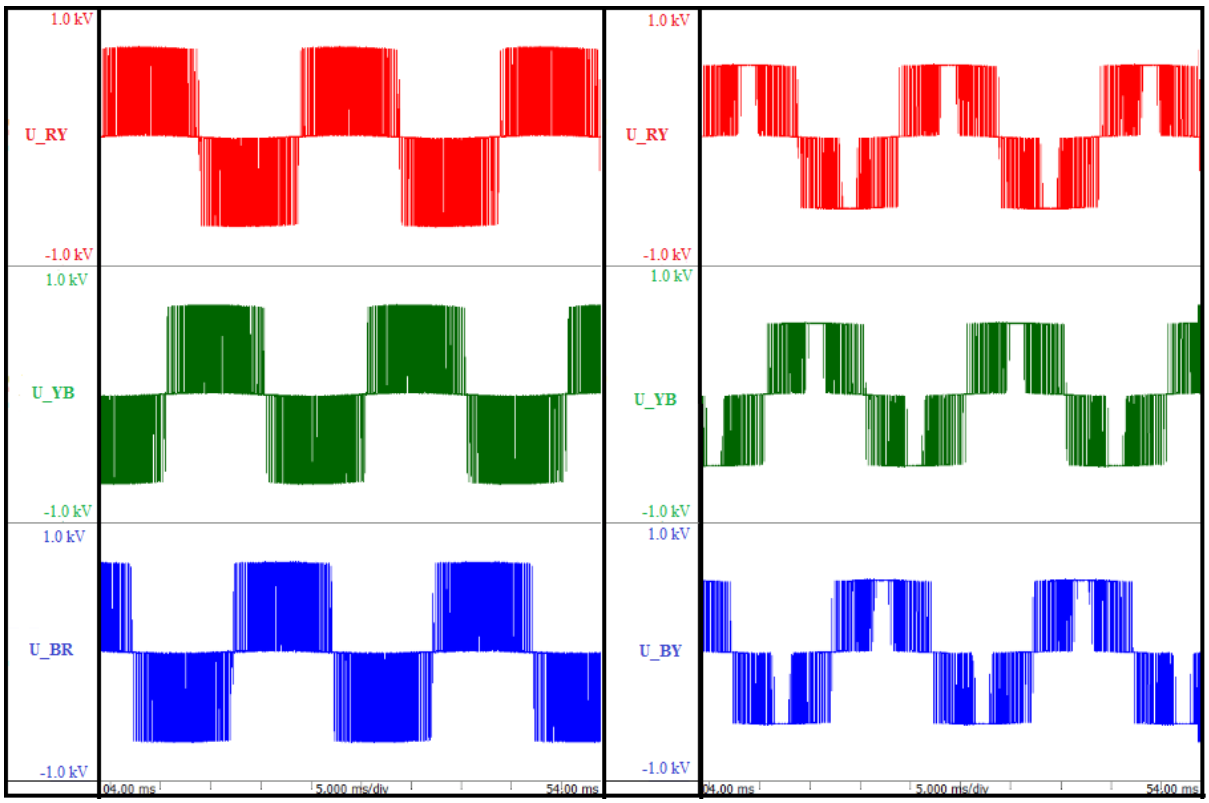

Fig.2. 2. Motor voltage waveforms: (Left) with no overmodulation (right) slightly into overmodulation operation

The waveforms shown in Fig. 2.2 were captured when the converter was delivering motor-rated fundamental voltage of 400V at different dc bus voltages. As shown, setting a lower dc bus of 540V (right graph) results in lower peak values but some pulses are missing, compared to a boosted dc of 700V (left), which is the standard input voltage for this converter.

The avoidance of overmodulation has also been justifiably criticized in [22] because it can only be achieved in cases where the converter has an active dc voltage-boosting rectifier, like the one used in this research. The complexity of this issue has been highlighted in the same study [22] in which the authors demonstrated that the indirect method did not give a realistic estimate of the converter-fed motor losses with a specific converter for final application. This was attributed to the fact that motor voltage, load and frequency cannot reach their rated values simultaneously when considering a practical VFD application without a boost rectifier.

The other issue with the above reference condition regarding fundamental motor voltage is that it is somewhat ambiguous, leading to different interpretations within the research community. For example, the interpretation according to [15] and [16], is that both the no-load and load tests must be performed by varying the dc bus voltage to keep a constant modulation index. However, the general practice when performing no-load tests is to keep the dc bus constant as adopted in studies [2], [6] and [14], resulting in a variable modulation index. Since it is well-known that a higher modulation index generally leads to lower core losses as shown in several studies [24] - [25], there is need to clarify the issue of converter input voltage.

While the choice of modulation technique may have negligible influence on the motor losses obtained during the load test, owing to the minor variation in motor voltage, its effect on the no-load losses cannot be neglected. Adopting a constant modulation index as shown in [15] and [16] requires a pre-evaluation of the required dc bus voltages for each no-load voltage. However, the process of evaluating and applying the optimum dc voltage, if using a manual autotransformer, can make the testing slower, leading to significant temperature variations. Perhaps this is why the method is not favoured in practical testing.

From a practical point of view, most VFDs operate using a fixed dc bus level. Therefore, it is logical that efficiency tests are also performed in the same manner to get core losses that reflect the actual operating conditions. This is the approach that has been adopted in this study. However, it is important to note that performing a no-load test under constant dc bus results in much higher core losses and presents challenges in the determination of friction and windage losses. This will be discussed later in chapter 4 of this dissertation.

2.2.2 Converter-fed motor frequency and voltage

In variable speed applications, induction motors are operated over a wide range of speed and torque. In fact, certain applications require the motor to be driven above its rated speed. Therefore, to optimize motors for such applications, it is necessary to determine their losses over a wider operating range. Although it is impossible to cover the entire torque-speed plane of a motor, several operating speeds must be considered below and above the rated speed of the motor to obtain an indication of the motor losses. This entails analysing the converter-fed motor losses in the constant-flux as well as the flux-weakening (constant power and high-speed) regions of the torque-speed plane shown in Fig. 2.3.

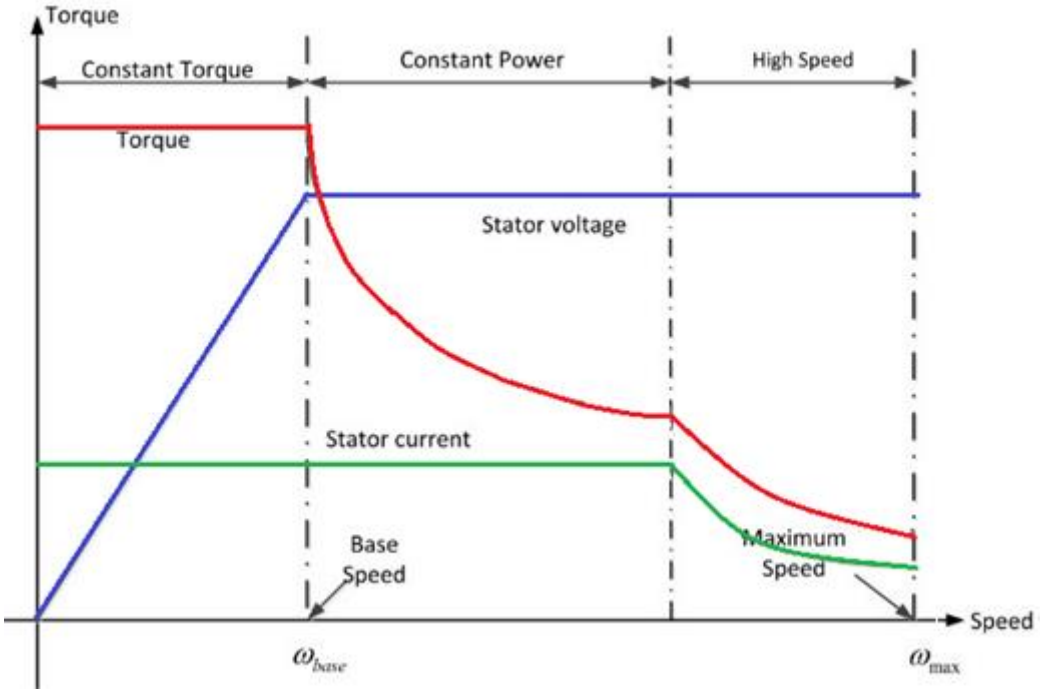

Fig.2. 3 Torque-speed plane of an induction motor showing the constant-torque and flux-weakening regions [3]

Although the IEC/TS has made good progress towards standardization of the methods for determining additional harmonic losses in converter-fed IMs, its limitation to motor-rated voltage and frequency has been identified as one of its main weaknesses [2], [22]. Despite not offering its own method of determining additional harmonic losses, the European standard EN 50598-2 [19] goes a step further than the IEC/TS by providing a calculation-based approach for estimating the motor losses at non-rated motor frequency. This is achieved by converting the losses determined from experimental tests at rated frequency to equivalent losses at any other frequency using mathematical models. Although the European standard only specifies a matrix of 8 operating points on the torque-speed profile as shown in Fig. 2.4, the mathematical

models can be used for any operating point on the torque speed plane, provided its corresponding losses with a sinusoidal supply are known.

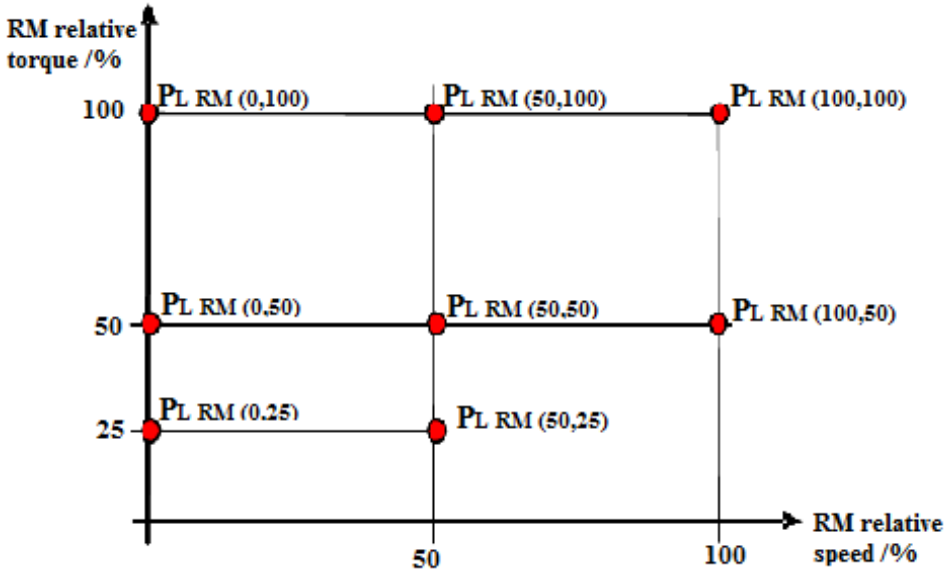

Fig.2. 4 Specified operating points for speed versus torque to determine relative power losses for converter-fed motor, CDM and PDS [19]

A few studies [13], [26] – [28] have attempted to analyse the converter-fed induction motor losses and efficiency under a wide range of operating speeds. However, most of these works are only based on the input-output method. Some loss segregation analysis is presented in [13] but the authors do not provide adequate information regarding the additional harmonic losses, citing the lack of practical methods for separating the iron losses, friction and windage losses, and additional harmonic losses. Therefore, the determination of additional harmonic losses under variable frequencies is still a challenge for researchers and requires further studies [30].

2.2.3 Determination of additional harmonic losses

The IEC/TS defines the additional harmonic losses as the losses produced in the motor by the non-sinusoidal voltage and current waveforms due to the converter supply. These losses are in addition to the fundamental losses of iron, rotor-winding, stator-winding, and stray-load loss. The standard adds that these harmonic losses increase with the motor load and can therefore be divided into a constant component and a load-dependent one. The latter is obtained from the difference in stray-load losses for operation with a converter and with sinusoidal supply.

The determination of stray-load losses is one aspect of electrical machine loss-segregation that has been extensively studied over the last two decades. Although the incorporation of linear regression analysis, emphasized by imposing a strict value of regression co-efficient, has greatly improved the procedure in recent years, the determination of stray-load losses is still considered a delicate process. This is because these losses are not measured directly but are simply deduced from the other measured losses. Therefore, any measurement errors in the stator resistance, torque, speed and electrical power generally lead to errors in stray-load losses [32]. Detailed discussion on stray-load losses can be found in [31] - [34] in which all authors stressed the difficulty of determining stray-load losses.

Based on the stray-load sensitivity analysis presented in [31], it was concluded that an accurate prediction of the stray-load losses is very difficult even if the instrumentation used matches the standard requirements. Since the IEC/TS procedure defines a load-dependent component of additional harmonic losses as the increment in stray-load losses between load tests performed with a sinusoidal supply and with a converter supply, the two tests must be performed under identical conditions. Otherwise, any minor mismatch, say in loading, between the two tests will potentially amplify the difference in stray-load loss values This difference will thus be misinterpreted as load-dependent additional harmonic losses. Therefore, although the IEC/TS procedure is theoretically valid, the obtained load-dependent harmonic losses may not be so accurate due to the delicate nature of the experimental determination of stray-load losses.

Taking the foregoing discussion into account, it is not surprising that there are contrasting reports in literature on the dependency of harmonic losses on motor load. Whereas the IEC/TS explicitly asserts that the harmonic losses increase with load and is supported by reports in [13] and [22], other reports [12], [29] indicate otherwise. Furthermore, several studies on the subject have been inconclusive. For example, [2] reports that the harmonic losses increased with load in an IE2 and IE3 Line-start Permanent Magnet motor (LSPM) but decreased in an IE4 motor. Another study [6] demonstrated an increase in stray-load losses between the sinusoidal and converter load tests, which suggests an increase in harmonic losses. However, the same study showed a constant difference between absorbed power on load and on no-load condition, suggesting that the harmonic losses are not affected by load. From these reports, there is need for further works on this aspect of converter-fed motor losses.

2.3 SUMMARY

In this chapter, an overview of international standards for the determination of converter-fed motor efficiency was presented. Although there are several draft standards undergoing different phases of development, the main discussion focused on the IEC/TS methodology, limitations and some of the technical considerations surrounding the determination of additional harmonic losses.

The main limitations of the IEC/TS include its applicability only to induction motors supplied by 2-level voltage source inverters at rated motor frequency and voltage. However, it is hoped that the final version of the standard will also apply to higher-level converters and other motor topologies. Other notable technical issues include the difficulty in realizing and validating the reference converter voltage waveforms and the lack of a clear explanation on the required variation of converter input voltage. The final section of the chapter presented a healthy questioning of the load-dependent component of additional harmonic losses, based on challenges reported in existing literature on the experimental determination of stray-load load losses.

3. INDUCTION MOTOR LOSSES UNDER SINUSOIDAL AND CONVERTER SUPPLIES

The determination of induction motor losses and efficiency is a key factor in any optimization process that involves electric motor drives. Knowledge of the machine losses and efficiency enables machine design personnel to improve their designs by consciously identifying ways to minimize these losses. It also enables regulation authorities, manufacturers and end-users to classify and rank induction motors according to efficiency classes.

This chapter discusses the various categories of induction motor losses under sinusoidal and converter supplies. The losses in induction motors fed by a three-phase mains (sinusoidal) supply are mainly due to the fundamental frequency components of voltage and current at 50Hz or 60Hz while the losses in a converter-fed induction motor are a combination of losses caused by fundamental frequency and those caused by the converter harmonics.

3.1 INDUCTION MOTOR LOSSES UNDER SINUSOIDAL SUPPLY

Induction motors are the workhorse of industry owing to their low-cost, robustness and simplicity of construction. They convert the input electrical energy into mechanical energy at the shaft of the motor, to which a load can be directly coupled or by means of a transmission system. However, as is the case in all practical systems, this energy conversion process is not ideal – not all the input electrical energy is converted into useful mechanical energy at the motor shaft. This is because some energy is needed to overcome external influences like friction and windage, in addition to that lost due to the electrical and magnetic properties of the materials used for the motor core and windings. All these losses are usually dissipated as heat. The energy conversion process in induction motors is summarized in Fig. 3.1.

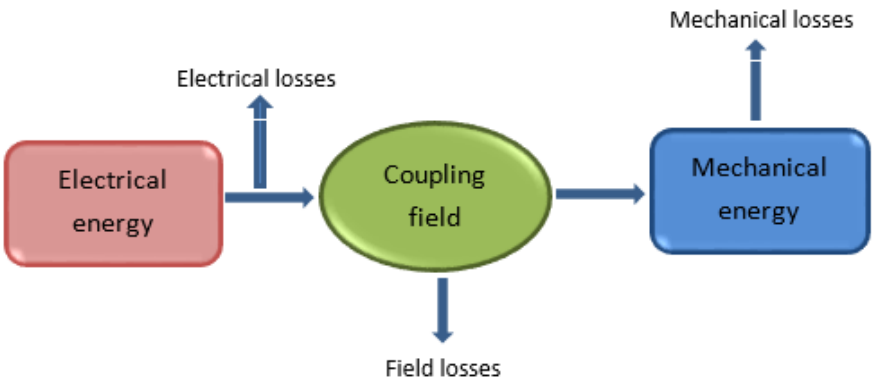

Fig.3. 1 Energy conversion process in induction motors

The losses in a line-fed polyphase induction motor can be typically grouped into five categories. These are:

- Stator copper losses
- Rotor copper losses
- Iron (core) losses
- Friction and windage losses
- Stray-load losses

The main components of an induction motor which influence its performance can be classified into the active and non-active parts. The active parts, which constitute the stator and rotor, can be modelled by equivalent circuit elements as shown in Fig. 3.2. These carry the conductors and magnetic core. The non-active components include the motor frame, the cooling fan and its cover, the shaft, terminal box and the bearing end shields. These components are difficult to model in the induction motor equivalent circuit [35].

The five categories of IM losses can further be classified as being load-dependent or load-independent (constant). However, experience has shown that even the so-called load independent ones exhibit some tendency to vary with load. Therefore, although the constant losses are obtained from the no-load test, they are often corrected to account for the loading effects. Each of loss component is discussed in the following sections.

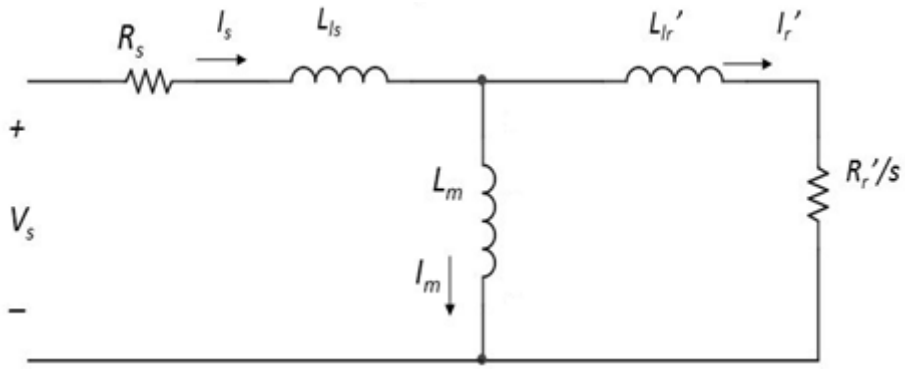

Fig.3. 2 IEEE recommended equivalent circuit of an induction motor [20]

3.1.1 Stator Copper losses

The stator copper losses are simply the resistive losses in the stator windings of the IM. They are proportional to the square of the current flowing through the stator windings and are modelled on the IM equivalent circuit by means of a resistor R_s as shown in Fig.3.2. In a typical

induction motor, the stator copper loss is the dominant loss component, accounting for 25 – 40 percent of the total motor losses [36].

The stator copper losses also depend on the cross-section area, length, and resistivity of the conductor material used for the windings. Typical conductor materials for the stator winding conductors are copper and aluminium. As the resistivity of copper and aluminium are a function temperature, it necessary to model the stator losses at a specific temperature. For efficiency tests, these losses are determined when the motor achieves thermal steady-state operation, that is, when the average temperature of the stator winding changes by 1°C or less per half an hour [10]. The stator copper losses, denoted by P_s, are calculated according to (3.1).

$$P_s = 1.5.I_1^2.R_{ll} \tag{3.1}$$

where I_1 is the line current and R_{ll} is the average line-to-line resistance for a wye-connected stator winding, determined according to the requirements of [10].

3.1.2 Rotor Copper losses

The rotor copper loss is the power dissipated in the resistance of the rotor circuit and is very similar to the stator copper loss. In the equivalent circuit of Fig. 3.2, the rotor circuit is modelled by means of a variable resistor $R_r/_S$ and a reactance X_r at line frequency. Since the real power dissipated across the effective rotor resistance $R_r/_S$ represents the real power crossing the airgap, the rotor copper loss can be expressed as a fraction of the airgap power according to (3.2). Therefore, the rotor copper losses depend on the actual resistance of the rotor circuit and vary with the square of current flowing in the rotor windings [20].

$$P_r = s.P_{ag} = 3.I_r^2.R_r \tag{3.2}$$

where P_r denotes the rotor copper loss, s the motor slip, P_{ag} the electromagnetic power developed in the motor's airgap and I_r the current flowing in the rotor windings.

Although rotor copper losses can be minimized by reducing the resistance of the rotor circuit, a high rotor resistance is needed to maximize the starting torque and minimize starting current. Therefore, a compromise must be made between the rotor resistance value required for a good starting performance and minimal losses during operation. At full-load condition, rotor current and hence rotor copper losses can be minimized by increasing the airgap flux. However, care must be taken to avoid saturating the machine. In a typical induction motor, the rotor copper losses account for about 15 – 25 percent of the total losses [36].

3.1.3 Iron (core) losses

The iron losses (or core losses) occur in the laminations that make up the stator and rotor cores. These losses can be separated into the hysteresis and eddy-current components. As explained in [4], the hysteresis component is due to the 'memory effect' exhibited by the relationship between the magnetic flux density (B) and the magnetic field intensity (H) in soft magnetic materials. The area of the BH loop shown in Fig. 3.3 represents the energy lost in traversing these locations in the BH plane. The hysteresis loss is proportional to frequency and is given by (3.3).

$$P_h = k_h.(B_{\max})^n f \tag{3.3}$$

Where k_h and n are empirical constants, B_{max} is the maximum flux density and f is the frequency of variation of current [20].

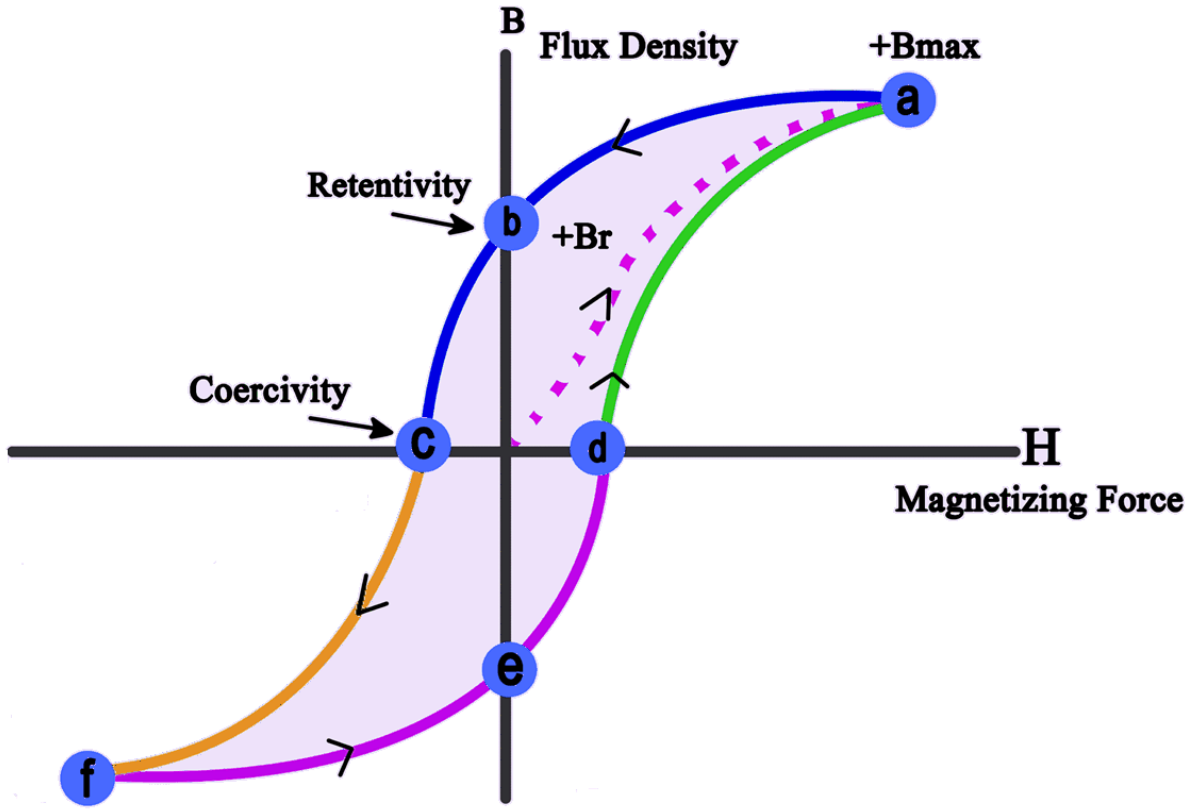

Fig.3. 3 BH loop of a soft magnetic material [37]

The eddy-current component of iron loss comes about due to the time-varying nature of the magnetic field. The time variation in B causes real currents to flow in the core of the stator and rotor, resulting in I^2R loss known as eddy current loss [20]. One way to limit the eddy-current

loss is by increasing the effective resistance of the core through the addition of small amounts of high-resistivity materials such as silicon. Another method is by creating the stator and rotor core using thin laminations which are insulated from each other. The eddy current loss component is proportional to the square of frequency and is given by (3.4).

$$P_e = k_e.(B_{\max})^2 f^2 \tag{3.4}$$

where k_e is a constant whose value depends on the type of material and its thickness, B_{max} is the maximum flux density and f is the frequency of variation of current [20].

From (3.3) and (3.4), both the hysteresis and eddy-current losses increase with frequency. Since the fundamental frequency of the magnetic fields in the stator core is at line frequency whereas the rotor core is at slip frequency, the iron losses are primarily associated with the stator rather the rotor.

According to [4], there is a third component of iron loss that accounts for aspects that are not accurately described by the hysteresis and eddy-current models. This is often referred to as the anomalous loss and is sometimes attributed to the movement of magnetic domain walls. However, not much information is available in literature regarding this loss component.

3.1.4 Friction and Windage losses

The friction and windage losses, collectively known as mechanical losses, are generally accounted for by subtracting from the available shaft torque. The friction losses mainly account for the losses in the bearings that support the rotor shaft while the windage losses are primarily due to the air resistance experienced by the cooling fans which remove the heat generated in the machine.

Friction losses can be minimized by lubricating the bearings and other moving mechanical parts. The windage losses can be minimized by generally improving the design of the fan, such as by reducing its size. Obviously, the friction and windage losses are higher at higher motor speeds. These losses typically account for 5 – 15 percent of the total motor losses [36].

3.1.5 Stray-Load losses

The stray-load losses (or additional load losses) represent those losses that are not accounted for in any of the four loss categories described previously. Although this seems to imply a lack

of understanding of the motor loss mechanisms, some of the stray-load losses can be explained but they do not fit into the other four categories. For example, the presence of load currents tends to distort the magnetic fields within the laminations, creating additional iron losses that would not be present in the no-load testing that is used to determine the no-load iron losses. Therefore, although these are iron losses, they are considered in the stray-load loss because of the way they appear during the testing sequence [4].

Stray load losses are mainly caused by imperfections in the design and construction and induction machines. For instance, flaws can occur in the design of the teeth and slots for the windings, the transverse inclination of the rotor bars (skewing), the airgap size, and the end-winding connections. Such design imperfections will lead to rotor end leakage loss, belt leakage, skew leakage, stator end loss, rotor zigzag pulsation and other non-defined losses [35].

Since stray-load losses cannot be measured experimentally, they are determined by subtracting the conventional losses (stator copper losses, rotor copper losses, iron losses and friction and windage losses) from the total measured losses according to (3.5) and (3.6).

$$P_{SLL} = P_1 - P_2 - P_{conventional} \tag{3.5}$$

with

$$P_{conventional} = P_s + P_r + P_c + P_{fw} \tag{3.6}$$

where P_{SLL} denotes stray-load losses, P_1 is the input electrical power, P_2 is the mechanical power at the shaft, P_s is the stator copper loss, P_r is the rotor copper loss, P_c is the core loss, and P_{fw} is the friction and windage loss.

In general, the stator and rotor copper losses (I^2R loss) dominate the overall breakdown of induction motor losses. However, the relative contributions of the core loss and stray-load losses increase with an increase in motor rating. This is expected because larger motors use large-sized conductors for the windings, hence reducing the resistance. The five loss categories and their relative contributions to the total losses in an induction motor fed by a sinusoidal supply are summarized in Table. 3.1.

Table 3.1 Classes of motor losses and their relative contributions [36]

Loss category	% of total loss	Load dependent/ independent	Description	Mitigation procedures
Stator copper loss (P_s)	Approximately 25-40%	Dependent on area, length and resistivity; increase with load	Caused by finite stator resistance of the motor for a given current	Optimal design, increasing cross-sectional area and reducing length of conductors
Rotor copper losses (P_r)	Approximately 15-25%	Load dependent	Caused by heating as a result of I^2R losses in the rotor bars	Use large conductive bars and end rings to reduce resistance
Core losses (P_c)	Approximately 5-15%	Varies only slightly with load	Core magnetization energy	Lengthen the steel structure, increased permeability steel and thinner laminations
Friction and windage losses (P_{fw})	Approximately 5-15%	Load independent	Results from bearing friction and air resistance on the cooling fan	Improving fan design, air flow and using lower friction bearings
Stray-load losses (P_{SLL})	Approximately 10-20%	Load dependent	Mostly due to imperfections in the motor design	Optimization of design and manufacturing detail

3.2 INDUCTION MOTOR LOSSES UNDER NON-SINUSOIDAL SUPPLY

In addition to the fundamental losses of iron, rotor winding, stator winding and stray-load losses, harmonic losses are also produced when the motor is fed by a non-sinusoidal power supply [11]. These additional harmonic losses are due to the harmonic voltages and currents produced by the power electronics converter. Therefore, the total motor losses in converter-fed motors are much higher than during operation with a nominally sinusoidal supply.

Reference [4] broadly categorizes the sources of additional losses in converter-fed motors according to the following causes:

- **Non-fundamental frequency components of voltage and current**

The presence of voltage harmonics due to the converter result in harmonic currents, which produce additional I^2R losses in the rotor and copper windings. These harmonic currents also produce harmonic torque pulsations in the airgap, which may lead to troublesome speed fluctuations and shaft fatigue [3]. However, given that the current in a converter-fed motor is typically sinusoidal due to the filtering effect of the motor's inductance, the increase in the rms value of the current is marginal. Therefore, the increment in copper losses obtained during experimental testing is generally negligible – especially when the converter has an additional filter at the output.

In addition, the higher frequencies due to the converter force the current to flow on the outer rims of the conductor – a phenomenon known as skin effect. In induction motors, this effect is predominantly present in the rotor bars and is usually referred to as the 'deep-bar effect.' The deep-bar effect results in a reduction in the active surface area, thus increasing the current density towards the outer radius [46]. Although the increase in apparent resistance due to skin effect can be easily modelled, the characterization by testing on converter waveforms is more challenging [4].

- **Operation above or below base speed (frequency)**

Besides operation at rated frequency and voltage, converter-fed IMs can also be operated above or below the base speed. Thus, the combined friction and windage losses are reduced when the motor is operated below base speed but are significantly increased at speeds greater than rated speed. Therefore, motors intended for operation at speeds well above base speed often have separately powered cooling to reduce windage losses [4]. Furthermore, the fundamental frequency component of iron losses is expected to decrease during operation below base speed. However, the converter waveforms at harmonic frequencies greatly increase the overall iron losses [24].

- **Operation above or below optimal flux**

Although converter-fed induction motors can easily be operated over a wide range of flux, separating the iron losses during the no-load test becomes a challenge. This is because the eddy-current losses generated in the rotor bars during no-load operation are not technically iron losses, although they occur during this part of the testing [4].

- **Operation with unbalanced voltages or current**

The effects of distorted supply voltages are numerous as they influence most operational parameters of the machine such as output torque, torque ripple, motor temperature, vibrations, and bearing stress [46]. While voltage imbalance is a reality of life in mains-fed induction motors, converters used in VFDs generally produce identical voltages and currents in each phase, except for the 120^{o} phase displacement [3]. Therefore, converters generally make some of the above operational conditions better.

Although any induction motor can be operated from a converter supply, the degree of success varies with both the motor design and converter design. Therefore, motors intended for use with converters are optimized accordingly. The following sections discuss some of the design optimizations for motors intended for converter supply.

3.2.1 Motor design optimization for converter supply

The additional harmonic losses can be influenced significantly by the induction motor design characteristics. The design of an induction motor intended for operation with a converter can be optimized to minimize the losses caused by the non-sinusoidal waveforms. For example, the airgap length, bridge thickness, and rotor slot shape can be optimized to reduce rotor bar losses. The converter waveforms will induce high losses in the rotor bars if an inappropriate rotor slot shape is used, or if the airgap and bridge thickness used are too small. These rotor bar losses consequently degrade the motor efficiency and tend to raise the rotor bar temperature. This causes the slip to increase, compounding the loss on converter supply [4].

The other design optimization is in the motor cooling assembly. Although windage losses are reduced when operating the converter-fed motor at low speeds, the increased core losses result in increased heat generation in the core of the motor. Therefore, motors designed for converter operation usually have a separate power supply to the fan to ensure adequate cooling even at lower speeds. On the other hand, general induction motor designs utilize the fan mounted on the motor shaft to cool the motor. Thus, the cooling depends on the speed of the motor and is lowest at low speed operation.

Further studies are still being done to find more ways of optimizing the design of induction motors for converter operation. For example, a study [38] reports that the additional stray-load losses due to PWM switching are less significant in a machine with higher saturation level because saturation effects reduce the change in flux density caused by the high frequency

current harmonics. Further studies [39] – [41] have also investigated other rotor design factors that affect slip frequency losses.

3.2.2 Impact of converter characteristics on additional motor losses

Several power quality issues such as harmonic distortion, noise, and transient voltage spikes have been reported as some of the major issues affecting the smooth operation of VFDs [41], [42]. AC inverters use a fast switching PWM technique to create variable frequency AC output. The fast switching of the output voltage of the drive, when connected with long motor cables, results in a reflected voltage at the motor which can be up to 3 times the AC supply voltage, with a very fast rise time. This high dV/dt increases the stress on the motor insulation, leading to induction motor failures. To prevent the above issues, output reactors (chokes) are often installed at the drive output terminals.

The chokes reduce harmonic distortion of line current, nuisance drive over-voltage trips caused by transient voltage spikes and minimize motor insulation failure by increasing the rise time. Although these reactors are typically sized for slopping off the high-frequency edges of the voltage signal and have no meaningful impact on the fundamental frequency waveform, the filter and motor will likely have at least one natural frequency where resonance will occur. Operation near this resonance frequency will result in poor current waveforms, excessive vibrations and poor motor efficiency, and must therefore be avoided [4].

Very often, the VFDs used for IM drives allow the user to set operating parameters suitable for the application. These parameters can either minimize or increase the harmonic losses. For example, a high switching frequency reduces the torque ripple and results in a more sinusoidal waveform. However, the switching losses in the converter obviously increase with switching frequency. Therefore, both the motor and converter must be considered to achieve optimal operation.

Other VFD features like slip compensation and current feedback may yield superior performance over grid-fed motors in applications where the motor is expected to maintain a constant speed under fluctuating load conditions. The downside to this is that the motor draws more current to provide the additional torque, thus increasing the resistive losses in the windings. Another advantage of current feedback is that the currents can be regulated to maintain balance – even if it requires some voltage imbalance to achieve good current balance. This contrasts with line-powered systems where a small voltage imbalance can lead to a large imbalance in phase currents [4].

3.3 SUMMARY

In this chapter, the different categories of line-fed induction motor losses were presented. These losses are mainly due to the fundamental component of voltage and current at 50 or 60Hz. Under converter supply, the non-sinusoidal voltages and currents generate harmonic losses in the motor, in addition to the fundamental losses. It is these additional harmonic losses that are mainly responsible for the efficiency degradation in converter-fed motors.

The chapter also highlighted some design and operational considerations aimed at minimizing these harmonic losses. Although the sources and relative contributions of each fundamental loss component have been presented and summarized in Table 3.2 for low to medium-power induction motors, it is important to note that these percentages may change significantly with increase in motor rating. The next chapter discusses the test procedures for the experimental determination of fundamental losses as well as the additional harmonic losses according to the IEC/TS proposed methodology.

4. EXPERIMENTAL DETERMINATION OF ADDITIONAL HARMONIC LOSSES

In general, the use of motor-VFD systems can result in significant energy savings. This is more apparent in applications were the motor operates under light load conditions for a considerable amount of time. A typical example of such an application is a centrifugal pump system. If the motor is run at nearly constant speed and the flow rate is controlled using a throttling valve, there will be energy loss across the throttling valve. However, if the flow rate is controlled by driving the motor at a speed that results in the desired flow, by means of a variable speed drive, there is huge potential for saving energy [3].

Although energy savings can be realized by controlling an induction motor by means of a VFD, there is an associated degradation in motor efficiency due to the additional harmonic losses. These losses occur in addition to the fundamental losses that occur in the motor when it is fed from a sinusoidal supply. Several studies have proposed some 'rules of thumb' for estimating the induction motor efficiency when it is fed from a converter. For instance, [4] proposes a method for making reasonable estimates of the converter-fed motor efficiency from limited sinusoidal data. This method corrects the sinusoidal supply motor losses to equivalent losses under a non-sinusoidal supply by applying a multiplication factor, depending on the converter switching frequency and whether the motor has been optimized to operate with a converter. However, such a rule of thumb is only a first approximation and cannot be used for critical tasks such as ranking of converter-fed induction motors or checking their minimum efficiency requirements.

This chapter explains the IEC/TS method for the experimental determination of additional harmonic losses in a converter-fed induction motor with power ratings below 1000kW. As this procedure is based on quantifying the loss increment in moving from a sinusoidal supply to a converter, the IEC/TS keeps referring to the related IEC 60034-2-1 standard to determine the fundamental losses on both sinusoidal and converter supplies. As some of these references are ambiguous and quite confusing, this chapter will first describe the test procedures for determining the fundamental losses using the recommended method 2-1-1B – "*Summation of losses, additional load losses according to the method of residual loss*" of the IEC 60034-2-1, 2014. As this method is very similar to the loss segregation method of IEEE 112 standard, only the major differences in the methods will be highlighted.

4.1 DETERMINATION OF FUNDAMENTAL MOTOR LOSSES

For clarity, the term fundamental losses as used in this discussion refers only to the motor losses due the fundamental components of voltage and current. While the fundamental input power and voltage differ significantly from their total values when a motor is fed from a converter, the corresponding power and voltage quantities are nearly equal under sinusoidal supply. The determination of these fundamental losses using the IEC 60034-2-1 standard will form the basis for the determination of additional harmonic losses introduced in the IEC/TS. It is therefore important to understand the determination of each loss component to avoid erroneous values of additional harmonic losses. Where the approach used in method 2-1-1B – "*Summation of losses, additional load losses according to the method of residual loss*" of differs significantly from that of method B of the IEEE 112 standard, the differences will be discussed to highlight the more accurate approach.

The segregation of the five component motor losses discussed in the previous chapter, namely stator and rotor copper losses, iron losses, mechanical losses and stray-load losses, under sinusoidal supply requires a series of tests. Some of these losses are considered to be independent of load and are therefore determined by running the motor without any external load. These are referred to as the constant losses – although they actually vary with load to some extent as will be discussed shortly in this section. Other motor losses increase with load and thus require the motor-under-test to be coupled to a loading device. In addition to the load and no-load tests, the following tests are required to bring the motor to the required operating conditions and to establish the motor parameters needed for analysis of efficiency test results.

4.1.1 Measurement of winding resistance

The winding resistance is needed in the calculation of stator copper losses (I^2R). Its value must be measured using calibrated high accuracy instrumentation such as a Wheatstone bridge or digital instruments. For polyphase a.c machines, the line-to-line winding resistance R_{ll}, is the arithmetic average of the resistances measured between each pair of terminals. Therefore, the phase resistance in a delta-connected machine is 1.5 times the measured line-to-line resistance and 0.5 times the line-to-line resistance if the machine is wye-connected.

According to standard [10], the preferred method for determining the winding resistance to be used for calculating the stator copper loss during the load test is to measure it just before the highest and after the lowest load points during the load test. The resistance used for the rated load point and higher shall then be taken as the value measured just before the highest load

point. The resistance for loads below the rated value shall be interpolated as varying linearly with load using the reading before the highest load and below the lowest load. Clearly, this method introduces an error at the load points above the rated value and is only suitable if an online resistance measurement method is available.

An alternative and simpler approach is to correct the cold winding resistance, measured prior to the start of the rated load test, to the test temperature measured by installing sensing devices at strategic positions on the winding. The temperature correction is achieved using the well-known equation (4.1).

$$R_w = \frac{R_{w,o}\,(k+\theta_w)}{k+\theta_{w,o}} \tag{4.1}$$

where R_w is the winding resistance corrected to the required load test temperature θ_w, $R_{w,o}$is the cold winding resistance measured at a temperature $\theta_{w,o}$ before the start of the test, and k is a constant that depends on the material used for the winding (it is 235 for copper and 225 for aluminium windings).

4.1.2 Measurement of winding temperature

The winding temperature is monitored through-out the rated load test to ascertain whether the motor has achieved thermal stability; that is, when the motor winding temperature changes by 1°C or less in half an hour. During the load test, the recommended method to determine winding temperature is to extrapolate from the rated load curve test resistance as explained under the resistance measurement section. Of course, the winding resistance can be measured directly using temperature sensing devices such as thermocouples, as the arithmetic average of the three or more readings from the sensors placed on the windings.

Where the above recommended methods for temperature measurement are not available, the standard [10] provides additional methods for estimating the winding temperature. These include the use of information from a duplicate motor of the same construction and electrical design, or the rated motor temperature according to the insulation class.

Note that methods for measuring the winding temperature and resistance in the IEC and IEEE standards are very similar. The major difference is that the IEC standard 60032-2-1 introduces a further correction of the winding resistance to a reference coolant temperature of 25°C. This can be considered a minor improvement as it allows test results from different test dates to be compared since all temperature-dependent quantities are referred to a standard

coolant temperature. For induction machines, the factor required to the adjust the winding resistance and slip to a standard coolant temperature of 25°C is given by (4.2).

$$k_\theta = \frac{235+k_w+25-\theta_c}{235+\theta_w} \tag{4.2}$$

where $k_\theta$is the temperature correction factor for the windings, $\theta_c$is the inlet coolant temperature during the test, and θ_w is the winding temperature.

4.1.3 Rated Load test

The rated load test is the longest test in the series. For this test, the test motor is loaded by suitable means, usually a dynamometer, to its rated output power and operated until the rate of change of temperature is less than or equal to 2°C/hour. At this condition, the motor is said to be under thermal equilibrium. At this point, all test quantities are measured and recorded. Under thermal equilibrium, the temperature response of the motor is expected to be consistent. Fig. 4.1 shows traces of winding temperature over time during the rated-load test.

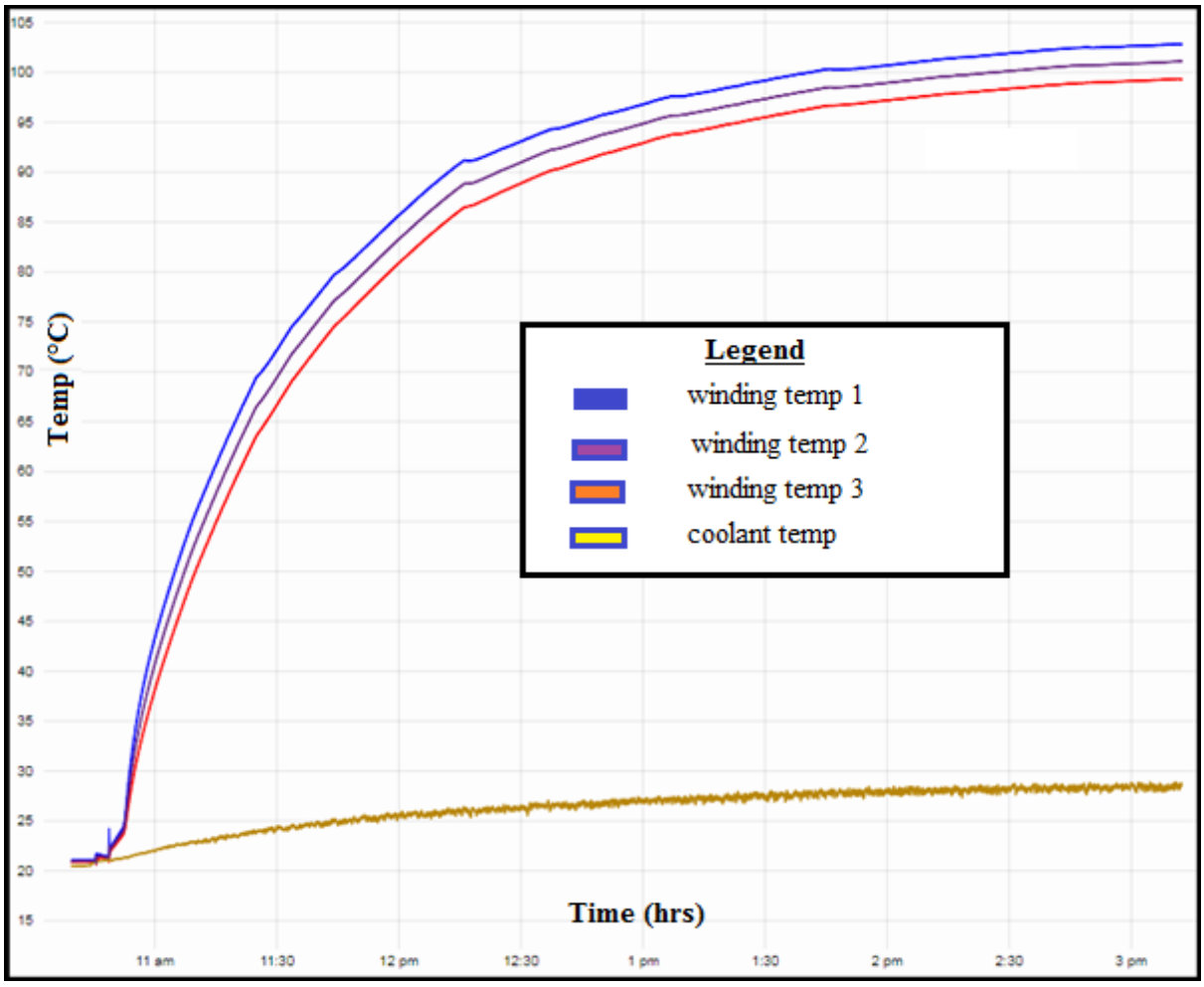

Fig.4. 1 Temperature variation during rated load test captured using a Pico 6 temperature transducer

4.1.4 No-Load test

The no-load test is performed at the end of the load curve test to determine the constant motor losses; that is, those losses that vary only slightly with motor load. For this test, the motor is decoupled from the dynamometer and is operated by varying the supply voltage at rated frequency. Method B of IEEE 112 standard is somehow vague regarding the no-load voltages because it simply states that: the motor voltage for the no-load test should range from 125% of rated value down to a point where further voltage reduction increases the current. The IEC 60034-2-1; 2014 standard clearly defines the required no-load voltages as 110%, 100%, 95%, 90%, 60%, 50%, 40%, and 30% of rated motor voltage.

By subtracting the no-load copper losses from the input power, the resulting constant losses, which are a combination of the mechanical and *conventional* iron losses, are obtained according to (4.3). The mechanical (friction and windage) losses at near-synchronous speed are determined at point c in Fig. 4.2, that is, at the intercept with the zero-voltage axis of the plot of constant losses against the square of voltage. Again, the IEEE 112B standard suggests that better results can be obtained by using the no-load voltages in the lower voltage range that do not show any saturation effects, but it does not specify what is considered low voltage. However, the IEC 60034-2-1 standard avoids any confusion by explicitly stating that only the voltages between 60% and 30% of rated value must be used to determine the mechanical losses.

$$P_{k\,sin} = P_{NL} - P_s = P_{fw} + P_{fe} \tag{4.3}$$

Where the $P_{k\,sin}$ is the constant losses, P_{NL} is the no-load input power, P_s is the stator copper loss, P_{fw} is the friction and windage (mechanical losses), P_{fe} is the no-load iron loss.

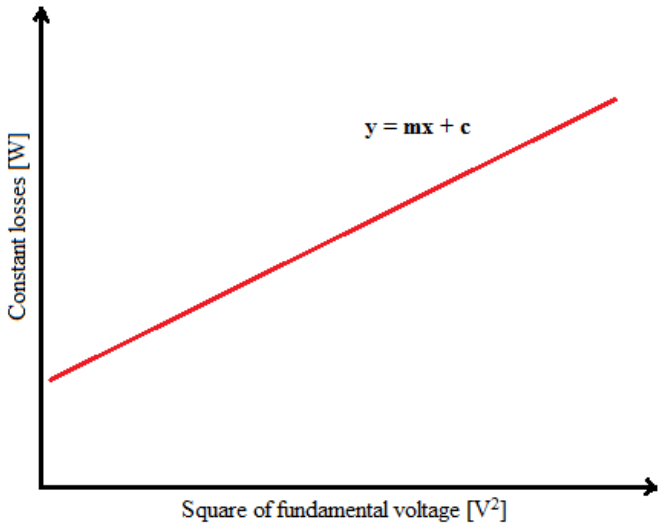

Fig.4.2 determination of mechanical losses at near-synchronous speed.

The remaining component of constant losses – the iron loss, is plotted against voltage to obtain the iron loss at any desired voltage. However, as the iron losses in an induction motor are directly related to the flux in the machine, which is a function of the magnetizing branch voltage, it means that the iron losses slightly decrease with load. This is because the magnetization voltage decreases with increasing load due to the increase in the voltage drop across the stator resistance. This correction of the iron losses with load is one of the major improvements in the IEC 60034-2-1 procedure over the more established IEEE 112B procedure. Furthermore, the IEC 60034-2-1 standard also clearly states that the iron losses on load are to be obtained using the higher no-load voltages between 90% and 110% of rated fundamental voltage. The magnetization voltage is determined according to (4.4) and (4.5).

$$U_i = \sqrt{(U - \frac{\sqrt{3}}{2} I.R.cos\emptyset)^2 + (\frac{\sqrt{3}}{2} I.R.\sin\emptyset)^2} \tag{4.4}$$

where

$$cos\ \emptyset = \frac{P_1}{\sqrt{3}\times U\times I}\ ; \quad \sin\emptyset = \sqrt{1-\sin^2\emptyset} \tag{4.5}$$

P_1 is the input power, U is the average line-to-line voltage, I is the average line current and R is the resistance measured during the load-curve test according to section 4.1.1.

Although the induced currents in the rotor cage due to the airgap m.m.f spatial harmonics produce some copper losses, the no-load analysis presented in this section does not provide a method for segregating these losses from the iron losses. Therefore, the iron losses obtained using the methodology provided in the IEEE 112B and the IEC 60034-2-1 standards are referred to as "conventional" iron losses since they are higher than the "actual" ones [48]. However, this wrong inclusion of rotor copper losses in the iron losses has a marginal effect on the efficiency determination.

4.1.5 Load-curve test

The load-curve test, or simply load test, is performed at the end of the rated load test to determine the stator and rotor copper losses. For this test, six load points are applied to the motor at approximately 125%, 115%, 100%, 75%, 50%, 25% of the rated torque *as quickly as possible* to minimize temperature changes in the machine.

The stator and rotor copper losses are determined using the resistance at the temperature of the load test obtained, as explained in sections 4.1.1 and 4.1.2. These uncorrected stator and

rotor copper losses obtained using (4.6) - (4.7) are then used to determine the residual losses, P_{Lr} according to (4.8).

$$P_s = 1.5.I^2.R \tag{4.6}$$

$$P_r = (P_1 - P_s + P_{fe}).s \tag{4.7}$$

$$P_{Lr} = P_1 - P_2 - P_s - P_r - P_{fe} - P_{fw} \tag{4.8}$$

where P_s is the stator loss, P_r is the rotor loss, I and R are the line current and line-to-line resistance, respectively, measured during the load test, s is the operating slip, P_1 and P_2 are the input electrical power and output mechanical power respectively.

The residual losses are simply those losses that are not accounted for in the other four loss categories. These residual losses are smoothed by linear regression analysis to determine the stray-load losses. This linear regression is important as it also serves as a quality assurance check for the entire efficiency test.

To obtain the stray-load losses, the residual losses are plotted against the square of load torque. The gradient of the resulting plot is then multiplied by the square of torque to obtain the stray-load losses at each load point. From the plot of residual losses against the square of load torque, the coefficient of correlation (R^2 value) is used to check if the test was performed satisfactorily. As a matter-of-fact, the IEC 60034-2-1 standard strictly requires a correlation coefficient of 0.95 or better for a test to be considered satisfactory, adding that anything less than this value could be indicative of errors in the instrumentation or test readings, or both. When the correlation coefficient is less than 0.95, the worst point is deleted, and the regression is repeated. If this new correlation is still less than 0.95, the test is rendered unsatisfactory, and the source of error must be investigated and corrected before repeating the test.

Although the IEEE 112B procedure for obtaining stray-load losses is the same as the one described above, it only requires a correlation coefficient of 0.9 or better. The only other difference is that the IEC 60034-2-1 standard corrects the friction and windage losses used in (4.8) to the operating slip at each load point using (4.9). The IEEE 112B standard on the other hand does not consider the variation of windage losses with operating speed. Therefore, based on the recent improvements highlighted above, namely the correction of iron losses to the magnetizing branch voltage and the correction of friction and windage losses, it is the author's opinion that the recent IEC procedure can be considered more accurate than the IEEE 112B.

$$P_{fw} = P_{fw,o}.(1 - s_\theta)^{2.5} \tag{4.9}$$

where $P_{fw,o}$ is the no-load friction and windage loss and $s_\theta = s.k_\theta$ is the slip value corrected to a standard coolant temperature of 25°C.

The corrected values of stator loss, rotor loss and input power used to determine the sinusoidal supply efficiency of the motor are given by

$$P_{s,\theta} = 1.5.I^2.R.k_\theta \tag{4.10}$$

$$P_{r,\theta} = (P_1 - P_{s,\theta} - P_{fe}).s_\theta \tag{4.11}$$

$$P_{1,\theta} = P_1 - (P_s - P_{s,\theta} + P_r - P_{r,\theta}) \tag{4.12}$$

The total losses and efficiency of the induction machine under a sinusoidal supply are then evaluated using 4.13 and 4.14 respectively. The standard includes a note that states that motor efficiency is usually determined using the first expression while generator efficiency is determined using the second expression in (4.14).

$$P_{Tsin} = P_{fe} + P_{fw} + P_{s,\theta} + P_{r,\theta} + P_{SLL} \tag{4.13}$$

$$\eta = \frac{P_{1,\theta} - P_{Tsin}}{P_{1,\theta}} = \frac{P_2}{P_2 + P_{Tsin}} \tag{4.14}$$

where P_{Tsin} is the total loss and η is the efficiency of the machine under a sinusoidal supply.

4.2 DETERMINATION OF ADDITIONAL HARMONIC LOSSES

When fed by a converter, motor losses are a combination of losses caused by fundamental frequency and those caused by the converter harmonics. Therefore, the IEC/TS has proposed a method of estimating the additional harmonic losses at rated voltage and frequency, as the loss increment in moving from a sinusoidal supply to a converter. The proposed approach first requires the determination of fundamental motor losses using the sequence of steps described in section 4.1 above. Thereafter, the same series of tests are repeated on the motor, this time fed by a converter.

Although the IEC/TS specifies that the converter supply load-curve and no-load tests must be performed immediately after the sinusoidal supply no-load test, the mechanical processes involved in coupling and decoupling two hot machines can be cumbersome. Therefore, it is

sometimes preferred to perform the two load tests first, before decoupling the test motor from the dynamometer for the no-load tests [6]. This is the approach that was adopted in this research. Note that there is a rapid loss of temperature when decoupling the two machines.

According to the IEC/TS, experience has shown that additional harmonic motor losses generally increase with load. Thus, the proposed method separates the obtained harmonic losses into a constant component and load-dependant component. However, as explained earlier in section 2.2.3, there is still no consensus on this aspect of harmonic losses. The following section discusses the determination of harmonic losses.

4.2.1 Constant additional harmonic losses

From the converter supply no-load test performed as explained in section 4.1.4, the constant losses are obtained in the same manner as was explained under sinusoidal supply using (4.3). The constant component of additional harmonic loss is then the difference between the converter supply no-load losses and sinusoidal supply no-load losses as shown in (4.15).

$$P_{HL\,no-load} = P_{k\,conv} - P_{k\,sin} \tag{4.15}$$

where $P_{k\,conv}$ is the converter supply no-load loss and $P_{k\,sin}$ is the sinusoidal supply no-load loss.

Since the constant additional harmonic loss varies with voltage, only the value obtained at the rated fundamental voltage of the motor is used in the final determination of converter-fed motor efficiency. Thus, one study [22] has proposed that the converter-supply no-load test must be performed at only one value of fundamental voltage, equal to the motor rated voltage. The problem with this approach is that the other higher voltage points in the no-load test are required in the determination of core losses, and hence stray-load losses on load.

4.2.2 Load-dependent additional harmonic losses

To determine the load-dependent component of additional harmonic loss, the stray-load losses on converter supply are first determined in the same manner as the sinusoidal supply stray-load losses. However, one of the challenges in determining the stray-load losses under converter supply is the determination of friction and windage losses. This is because under converter supply, the graph of constant losses against the square of fundamental voltage does not yield a straight line like that shown in Fig. 4.2. Instead, it yields a curve that typically takes the form shown in Fig. 4.3, owing to the to increased core losses at low modulation index [50].

Therefore, the friction and windage loss can no longer be taken simply as the intercept of the obtained curve at zero voltage.

To provide a solution to the above challenge, [50] proposed that: if a 4th order polynomial is fitted on the curve obtained by plotting the constant losses against the square of voltage, the value at the zero-voltage axis results in similar values of friction and windage losses to those obtained with a sinusoidal supply. When this approach was tested on a 55kW IM according to the previous version of the IEC 60034-2-1; 2007 standard (which does not specify the voltages needed to determine the friction and windage losses), it produced acceptable results. However, the four low-voltage setpoints specified in the IEC 60034-2-1; 2014 standard are not enough to produce a 4th order polynomial that accurately covers the constant losses. This presents challenges in the adoption of the 4th order polynomial method. Therefore, since there is no scientific reason why the friction and windage losses of the motor during operation with a converter must be different from those obtained with a sinusoidal supply, the usual approach is to use the value obtained in the latter to analyse both sinusoidal and converter supply losses.

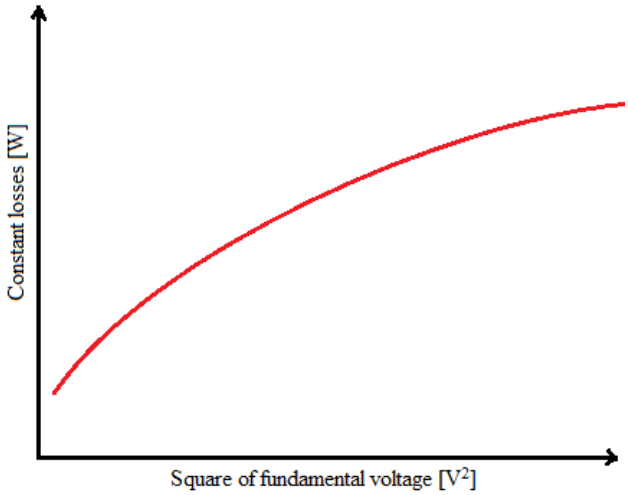

Fig.4.3 Typical graph of constant losses against square of voltage in a converter-fed induction motor

Once the stray-load losses in the converter-fed motor are determined using the procedure outlined in section 4.15, the difference in stray-load losses between converter and sinusoidal supplies gives the load-dependent component of additional harmonic losses. This is according to (4.16) as provided in the IEC/TS.

$$P_{HL\,load} = P_{SLL\,conv} - P_{SLL\,sin} \tag{4.16}$$

where $P_{SLL\,conv}$ is the converter supply stray-load loss and $P_{SLL\,sin}$ is the sinusoidal supply stray-load loss.

4.2.3 Efficiency determination

The summation of the constant and load-dependent additional harmonic loss components gives the total additional harmonic motor losses due to the converter. These losses shall then be added to the fundamental motor losses determined with a sinusoidal supply to obtain the total converter-fed motor losses according to (4.17) and (4.18).

$$P_{HL} = P_{HL\,no-load} + P_{HL\,load} \tag{4.17}$$

$$P_{T\,conv} = P_{T\,sin} + P_{HL} \tag{4.18}$$

where all the above loss components are as defined in the preceding sections.

The efficiency of the motor under converter supply is then given by:

$$\eta = \frac{P_2}{P_2 + P_{T\,conv}} \tag{4.19}$$

where P_2 is the output mechanical power with a sinusoidal supply and $P_{T\,conv}$ is the total converter supply motor losses determined according to (4.18).

Although the above determination of converter-fed induction motor efficiency is theoretically valid, there are certain considerations that must be addressed when performing these tests in the laboratory. For example, since the output power used in (4.19) is determined during the sinusoidal supply test, any slight mismatch in load torque or frequency (speed) between the sinusoidal and converter supply load tests will affect the accuracy of the converter-fed motor efficiency obtained. Moreover, the use of output mechanical power in (4.19) contradicts with the recommendation in the IEC 60034-2-1 standard, which states that this equation is preferred for generators. Furthermore, the use of output power to determine efficiency does not incorporate all the improvements introduced in the IEC 60034-2-1 standard, such as the correction of input power to a standard coolant temperature of 25°C. These considerations, although minor, will be highlighted in chapter 8 of this dissertation which presents the discussion and analysis of experimental results.

The IEC 60034-2-3 procedure for determining converter-fed induction motor efficiency can be summarized in the flow-chart shown in Fig. 4.4.

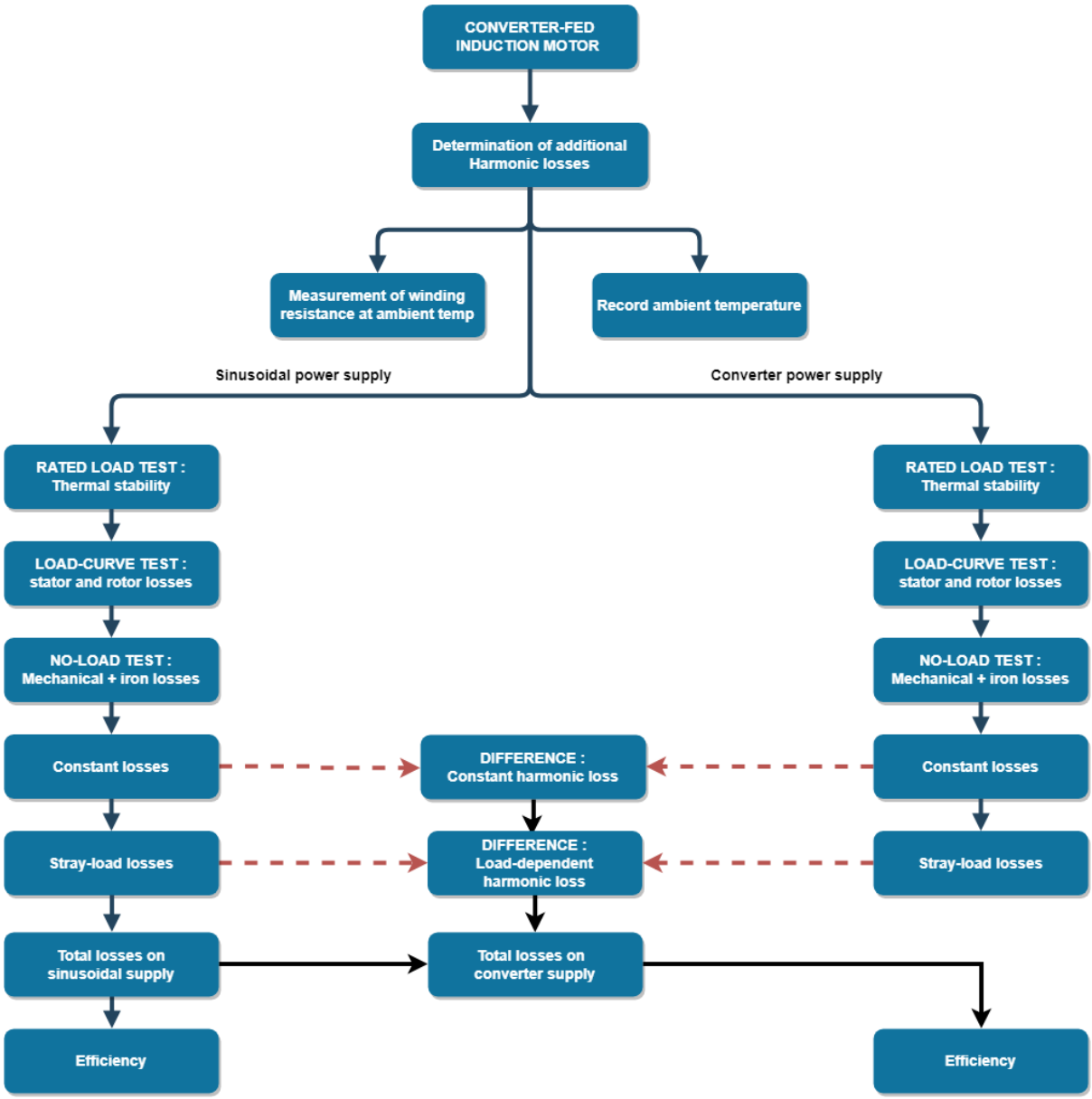

Fig.4. 4 Sequence of tests required for determination of converter-fed motor efficiency using the IEC/TS

4.3 SUMMARY

In this chapter, the experimental determination of fundamental motor losses as well as additional harmonic losses was discussed. This was done to provide a clear explanation of the test procedure as some of the statements in the standards are somewhat ambiguous. The major differences and recent improvements in the IEC 60034-2-1 standard over the more established IEEE 112 standard have also been highlighted.

The load-dependent component of additional harmonic loss, defined as the increase in stray-load losses in moving from a sinusoidal supply to a converter, is a critical issue in the proposed standard. This is because its value can be easily influenced by any errors in the determination of the other loss components. Furthermore, the ripple in the torque and other electromagnetic interference (EMI) issues due to converter supply make the accurate determination of additional harmonic losses difficult. Therefore, the development of an automated efficiency testing procedure discussed in chapter 6 is an important consideration in the determination of converter-fed motor efficiency. However, before this procedure is presented, the experimental test rig and its capability for analysing the dynamic operation of electric motors is presented in the next chapter.

5. EXPERIMENTAL TEST RIG AND DYNAMIC OPERATION OF INDUCTION MOTORS

The measurement of harmonic quantities with a converter supply is more complex than with a mains supply. As demonstrated in [14], harmonic power measurements are easily influenced by power analyser sampling rates, bandwidth and other digitization settings such as line filters. In addition, the measurement of all electrical and mechanical quantities needed to evaluate the converter-fed motor efficiency must be done in a synchronized manner to avoid instrumentation and sampling errors. Therefore, as test standards for the determination of converter-fed motor efficiency are under development, there is need for the establishment of test facilities for the research community to validate these draft standards and provide useful feedback to the relevant standards committees.

In general, efficiency tests for electric motors normally last between 4 and 7 hours. The larger part of this time is spent establishing thermal stability in the motor. Thus, the energy consumed during motor testing can be significant – especially when testing large motors. Therefore, a regenerative test rig like the one described in this chapter is certainly an attractive solution as it provides an energy efficient platform for motor testing.

The test rig also offers great flexibility, allowing different motor sizes up to 110kW to be tested using different power supply configurations. The measurement device of the test rig is the *Genesis 7i* high-speed Data Acquisition System (DAQ) which allows synchronous capture of various electromechanical quantities, with high accuracy, in both dynamic and steady-state conditions. The automated-data recording and processing capabilities of the DAQ were instrumental in realizing the automated testing procedure developed in this study.

In this chapter, the developed 110kW test rig for evaluating the steady-state and dynamic characteristics of motor-drive systems is first described. A few examples of some dynamic operations that were analysed are then presented to demonstrate the suitability of the test rig and the high-speed DAQ for transient performance studies.

5.1 DESCRIPTION OF 110kW TEST RIG

The 110kW test rig described in this section was specially developed to investigate the dynamic operation and efficiency of inverter-fed motors. It consists of an active front-end

connected to a common DC link which feeds two variable speed drives (VSDs). The two VSDs in turn feed two induction machines coupled together through an in-line torque transducer as shown in Fig.5.1. This system is capable of bi-directional power flow and recycles power between the motor drives.

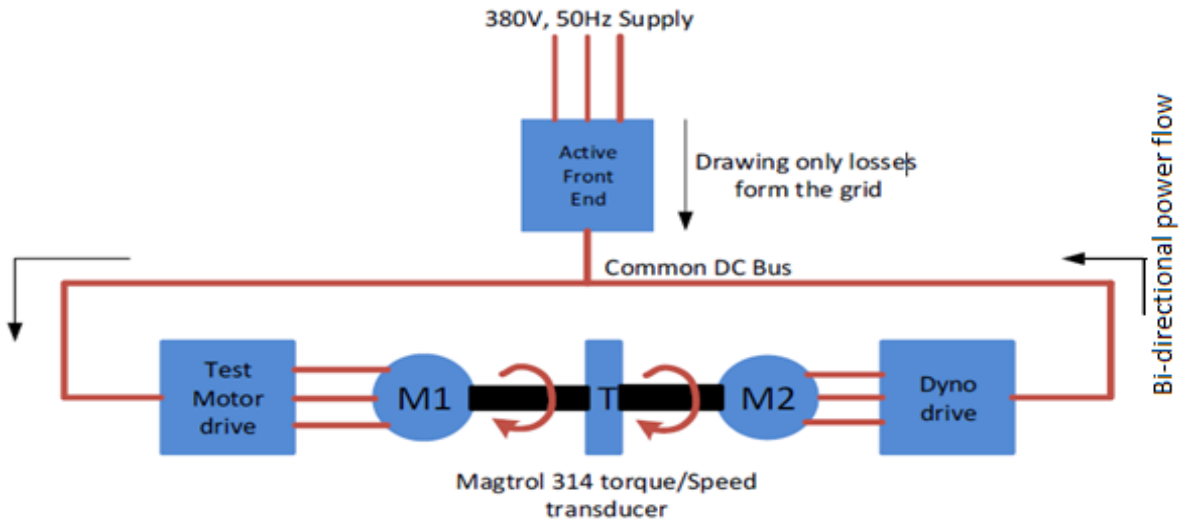

Fig.5. 1 Schematic diagram of power flow in the test rig during operation [35]

In general, an induction motor takes about 4-8 hours of operation at full load to attain thermal stability (gradient of 2K/ hour). Whereas some test rigs such as the one used in [44] dissipate all the energy generated in the dynamometer across a braking resistor, the developed 110 kW rig returns this energy to the common dc link where it is again fed to the motor under test. Thus, under steady state conditions only the losses are drawn from the grid. The common dc link also ensures power balance and minimizes the stress on the dc link capacitor.

The use of a bi-directional converter that feeds the energy generated in the dynamometer directly into the grid, like the one in [45], is another attractive configuration for back-to-back testing. However, such a configuration requires additional hardware and filtering mechanisms to mitigate harmonic injection into the grid to meet the IEEE 519 criteria. The developed 110kW test rig therefore provides an energy-efficient platform for testing converter-fed machines for emerging applications. Under dynamic operating conditions, when accelerating or decelerating the machines, power is drawn or returned to the mains, respectively, through the active front-end.

The main data recorder and storage device of the test rig is the Genesis 7i Data Acquisition System which allows synchronized recording of all electrical and mechanical quantities. The next section describes each component of the test rig.

5.2.1 Test Rig components

- **Machine Under Test (MUT)**

  The induction motor (or any motor type) under test is fed by a 2-level converter – model SPMD 1404 from Control Techniques. This converter uses IGBTs and is capable of bidirectional power flow. For the efficiency tests, the MUT inverter was operated in open-loop (V/f) speed control mode, with slip compensation turned off and a switching frequency of 4kHz as specified in [11]. Each test motor was fitted with three thermocouples for measuring the average winding temperature.

- **AC Dynamometer**

  The loading motor is a 110kW induction motor fed by the same type of converter as the MUT. However, it is operated in closed loop vector control mode, and is in torque control mode to provide the different load torques required for the tests. The load torque can be adjusted through an analogue input on the front panel or by digital means using drive programming software. Both converters of the test motor and the load motor are fitted with an output reactor. This aspect is discussed further in chapter 6.

- **Active Front-End**

  The active front end has two drive units – a thyrister rectifier (pre-charge) unit (model SPMC 1402) that charges the dc bus to 700V and an IGBT regenerative drive (model SPMD 1404). This configuration allows induction machines to be tested in motor or generator mode. The active front-end is synchronized to the mains frequency by means of a phase-locked-loop (PLL). This allows the power generated in the load motor drive to be fed directly into the grid if the motor-under-test motor is not running from the drive supply.

- **Inline torque and speed transducer**

  The torque and speed data are obtained using an inline Magtrol TM 314 torque transducer. The speed is given out as a 5V pulse while the torque is given out as a dc voltage signal. The Magtrol torque transducer meets the requirements of IEC 60034-2-1 and is rated for 1000Nm with an overload capability of 100%. Therefore, the transducer has a maximum operating torque capability of 2000Nm, and a maximum speed of up to 7000rpm, with a sensitivity of 5mV/Nm at 60 pulses per revolution.

- **Data Acquisition System (DAQ)**

  The Genesis 7i high-speed DAQ from HBM is the data recording and storage system of the test rig. All the signals from the various sensors are fed to the DAQ through four input cards (recorders), each with 6 channels. The type and range of data acquired at each of the points A, B, C, D, E, and F, shown in Fig. 5.2, are given in Table 5.1. The DAQ allows synchronous recording of raw data from all the 24 inputs, at a high sampling rate of 2MS/s, either continuously or in very fast sweeps. This feature allows the dynamic operation of inverter-fed machines to be studied with such detail and accuracy that would otherwise be almost impossible to capture with ordinary power analysers.

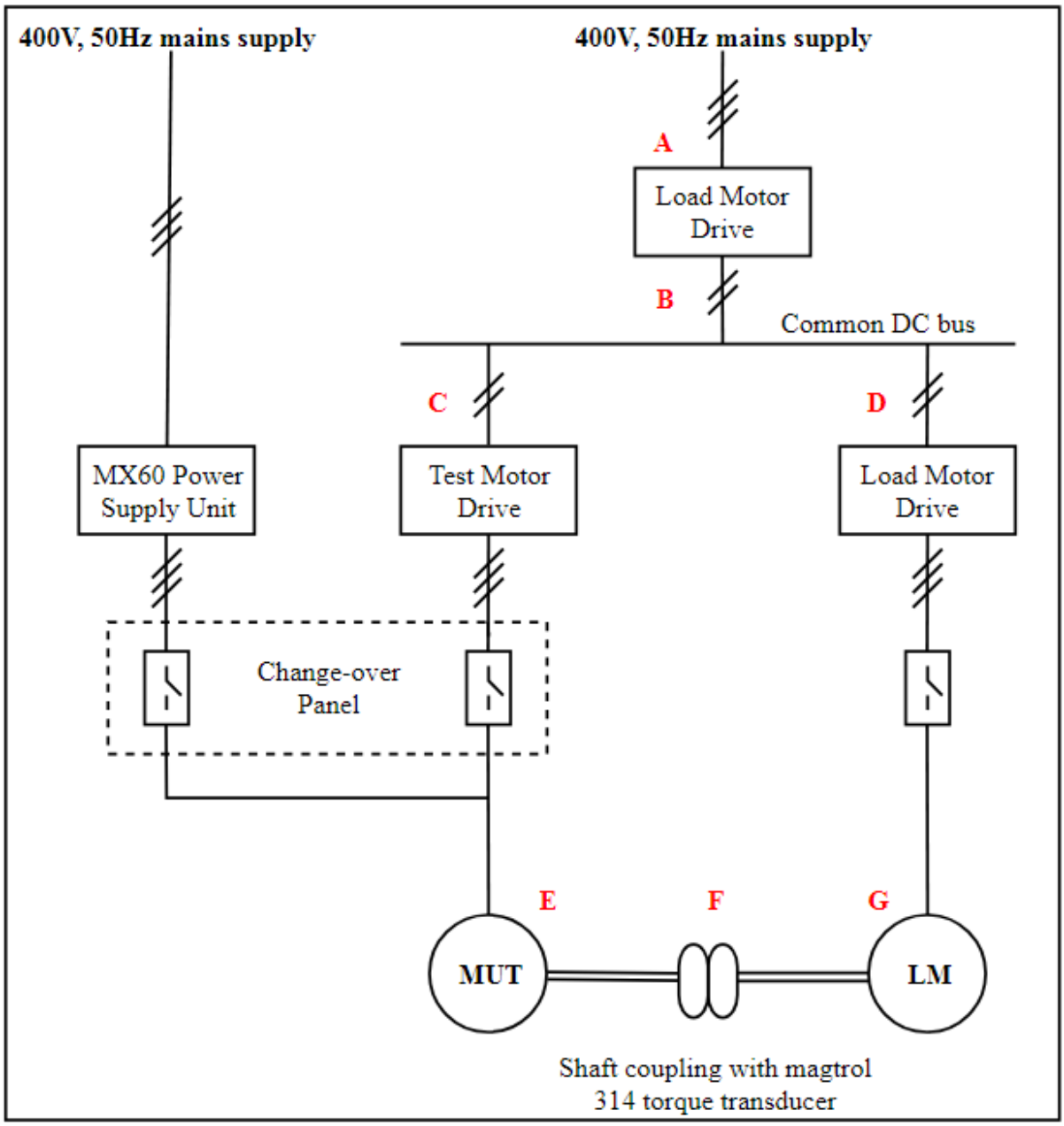

Fig.5. 2 Schematic diagram of the 110kW test rig

Fig.5.3 Laboratory test bench showing DAQ (right), Drive panel (orange) and supply change-over panel (white)

The DAQ also offers advanced digitizing features such as filtering, Fast Fourier Transform, and segregation of the fundamental components of voltage, current and power from the raw signals, without interfering with the active power measurement. This segregation feature is very attractive when dealing with PWM signals and was particularly useful when matching the fundamental voltage under PWM supply to the sinusoidal voltage during the tests described in chapter 7. The DAQ also has a formula database that allows the user to create custom formulae that can be applied on the recorded raw data for further analysis and reporting.

Table 5.1 Measured signals

Measurement point	Designation	Acquired Data
A	Active Front End	3-phase AC voltages and currents
B	DC bus	DC voltage and current
C	Test Drive Input	DC voltage and current
D	Load drive output	DC voltage and current
E	Test motor Input	3-phase AC voltages and currents
F	Shaft output	Shaft torque and speed
G	Load motor output	3-phase voltages and currents

For analogue measurements, voltages up to 2kV are fed directly into the data recorders while the phase currents are measured with high accuracy external LEM sensors, through a current conditioning unit (MCT), and fed into the data recorder via burden resistors. The temperature signals from the K-type thermocouples placed inside the motor windings are fed into the QuantumX MX1609 module and interfaced to the Gen 7i for synchronous data capture. The Gen 7i also offers an automated data recording capability that was invaluable in realizing the automated testing procedure presented in chapter 7 of this dissertation.

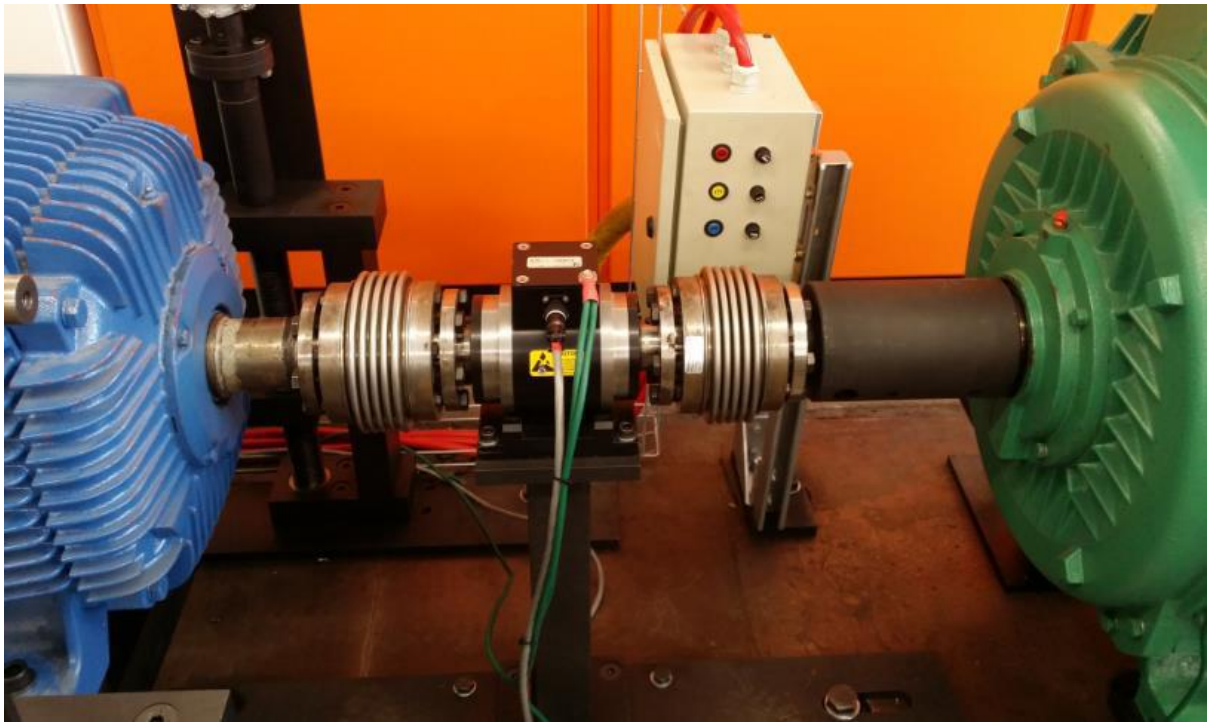

Fig.5.4 Laboratory test bench showing the motor-under-test (blue) coupled to an AC dynamometer (green) through and an in-line Magtrol 14 torque-speed transducer.

5.2 DYNAMIC OPERATION OF CONVERTER-FED MOTORS

Although VFDs bring flexibility to the otherwise ‘rigid’ induction motor, their various control features certainly increase the complexity of understanding the motor behaviour under different operating conditions. Features such as ramp rates, slip compensation, current limits, etc. often cause the motor to draw power in a very specific manner. This is usually dictated by the PI controllers of the VFD. The developed rig allows the behaviour of the different components of the power drive system (PDS) to be analysed fully under dynamic operating conditions.

Whether an induction motor is run on converter supply or sinusoidal supply, the dynamic behaviour of interest includes starting transients, accelerating/ braking transients, and changes in load torque. Therefore, the high-speed Gen 7i DAQ allows the dynamic operation and efficiency of the motor to be analysed. To demonstrate the test rig's suitability for analysis of the dynamic operation of motor-VFD systems, experimental tests were performed on a 37 kW totally enclosed fan-cooled induction motor. The name plate details of the motor are given in Table 5.2. In the next section, the starting transients of the 37kW induction motor under a controlled V/F ramp, realized by programming an MX30 power supply, and the acceleration/deceleration transients on converter supply are demonstrated.

Table 5.2 37 kW motor name plate details

Power [kW]	Speed [rpm]	Volts [V]	Amps [A]	Frequency [Hz]	P.F	Poles
55kW	1475	400	67.4	50	0.86	4

5.2.1 Starting Transients under a controlled V/F ramp on sinusoidal supply

Generally, an induction motor draws 5-8 times it's full-load current when started direct-on-line. To mitigate this high start-up current, several methods are used. These include reduced-voltage starting using autotransformers, star-delta starters and soft-starting using solid state devices. When the 110kW test rig was first commissioned in 2015 in the UCT machines lab, no mechanism was put in place to reduce the start-up current when starting the motor-under-test from mains supply. Therefore, an unconventional start-up method was devised in which any motor to be started was run to full speed using the VFD, before quickly switching off the drive and starting the sinusoidal power supply.

In order to perform the above start-up procedure, the drive mode was set such that the motor was free to coast to prevent a loss of speed. The problem with this approach was that at any given time, two people were needed to perform the switch-over. Furthermore, the magnitude of the instantaneous current spike depends on the magnitude and phase of the incoming supply with respect to the decaying induced voltage in the motor as shown in Fig. 5.5.

Looking at Fig. 5.5 (a) which shows the intantaneous line voltages, the converter (VFD) was switched off just before the 5.4s mark (portion enclosed in black). The corresponding line current plot Fig.5.5 (b) shows that the motor current suddenly drops to zero. At this instant, the induced voltage in the motor starts to decay until the incoming sinusoidal supply is switched

on 600ms later, corresponding to the 6s mark. Although the incoming supply was almost in-phase with the decaying induced voltage at the instant of switching (portion enclosed in blue), there was a current spike of about 8-10 times the no-load value. However, the advantage of this method, compared to reduced-voltage starting, is that the current spike typically lasts less than 200ms although its magnitude can be much higher if the two voltages are out of phase.

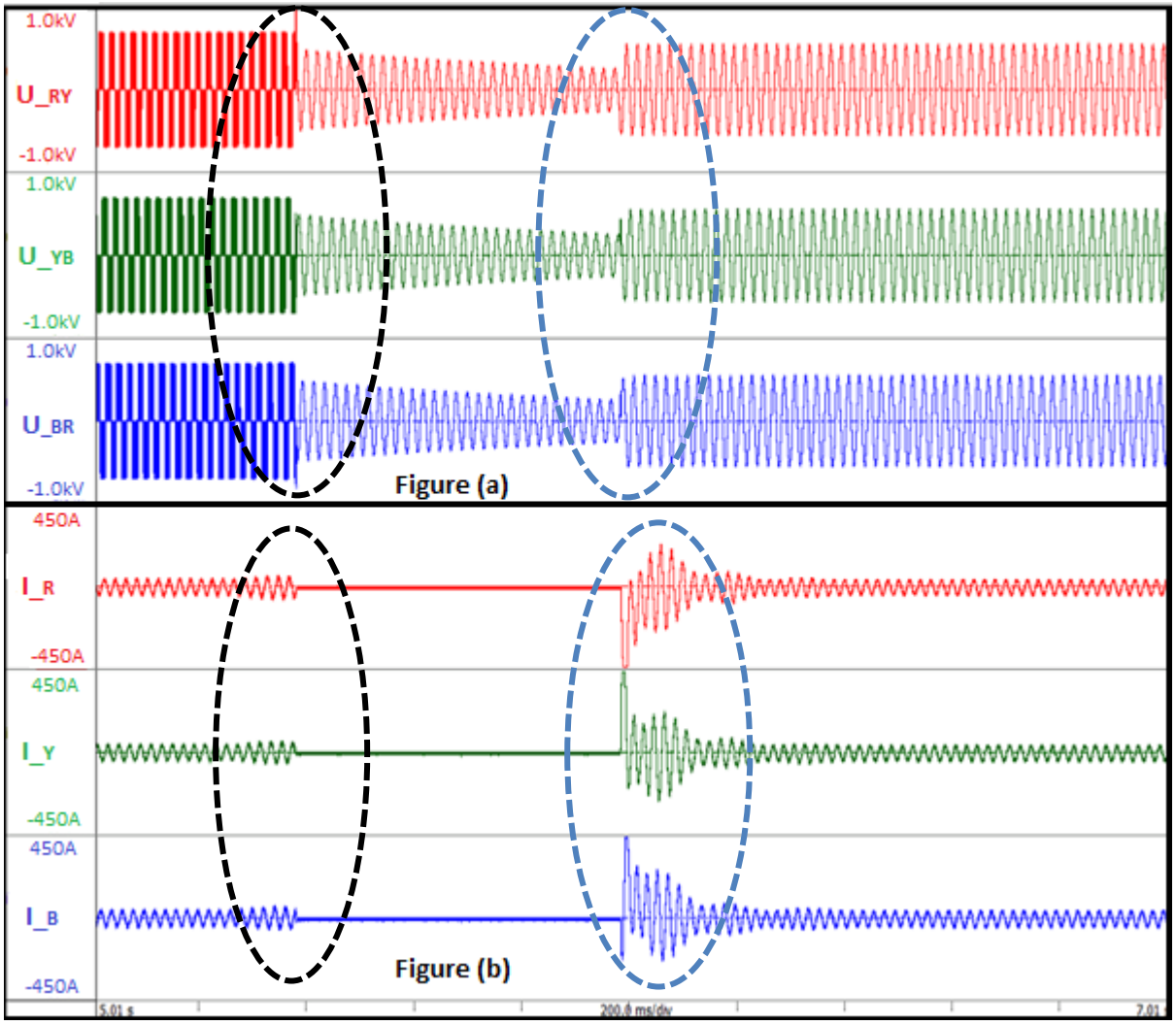

Fig.5.5 change-over of induction motor supply from VFD to mains. (a) Line-to-line voltages (b) line currents

At present, sinusoidal supply tests are performed using a programmable MX 60 California Instruments power supply. With this power supply, a controlled V/F starting-profile was programmed to limit the start-up current, in a manner similar to the soft-starting method employed in most VFDs. However, to circumvent the hardware limitations of the MX 60 power supply, the controlled V/F starting profile was customized in the following manner:

Since the minimum frequency output of the MX 60 is 17Hz, the start-up V/F ramp starts at 30Vph/ 17Hz and increases to 92Vph/ 20Hz in 3s. Setting up a ramp faster than this caused the MX 30 programmable power supply to trip on over-current, even when the delay on the current limit was set to its maximum of 5 seconds. On the high voltage range, the maximum current limit of this power supply is 150A. Once the induction motor started to turn slowly, another ramp was applied to increase the voltage and frequency to their rated values in 10s. The above values were carefully selected to meet the output capabilities of the power supply and were only arrived at after several trial runs in the lab. For this operation, the MX 60 over-current trip delay was set to 3s to ensure the unit did not trip during start-up. Fig. 5.6 shows the programmed start-up ramp.

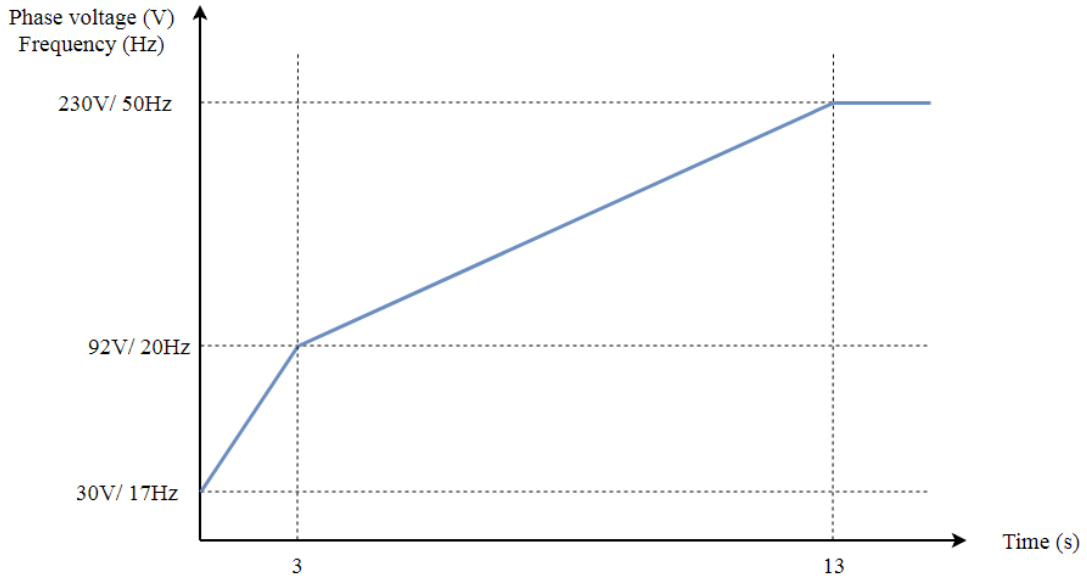

Fig.5.6 37 kW induction motor start-up profile

To demonstrate the capabilities of the DAQ for analysis of dynamic operation, the start-up profile shown above was applied to a 37kW induction motor and data was captured. The first report shown in Fig. 5.7 shows instantaneous phase quantities captured using the continuous mode of data acquisition. This mode is suitable for highlighting some overall trends in the dynamic under consideration. For instance, it can be easily observed that during the start-up operation, there was a sudden increase in current required to develop the starting torque to overcome the motor inertia and friction. Once the motor starts rotating, a constant current is then drawn which maintain a constant accelerating torque as the motor voltage and frequency are increased gradually as shown in Fig. 5.7 (a). Similarly, Fig.5.7 (b) shows the gradual increase in motor terminal voltage according to the programmed V/F ramp. As shown in Fig.

5.7 (c), the motor draws a significant amount of active power from the supply during the initial start-up phase, but it suddenly drops and then steadily increases with voltage.

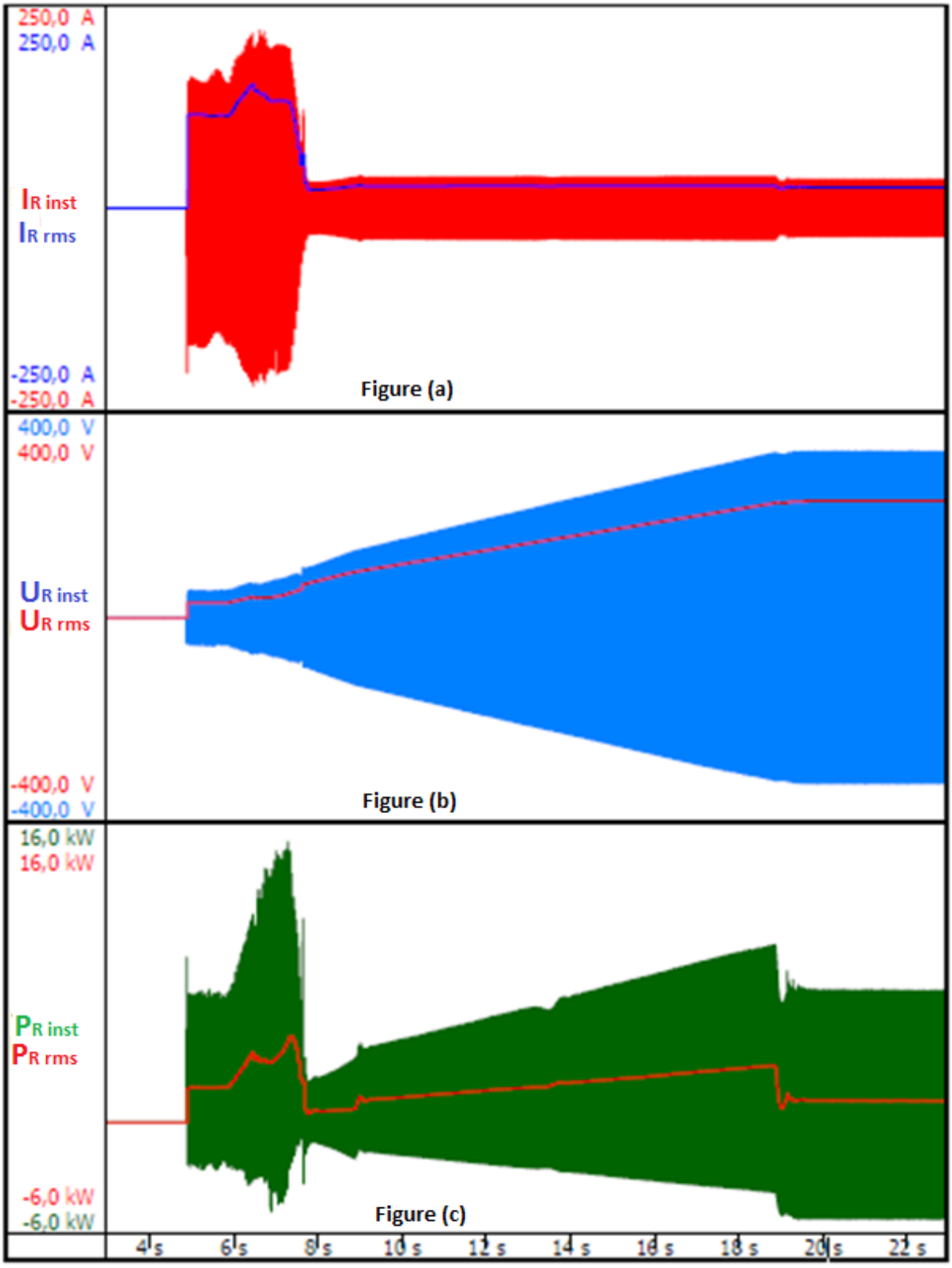

Fig.5.7 continuous mode of data acquisition: **(a)** instantaneous phase current and its rms; **(b)** instantaneous phase voltage and its rms; **(c)** instantaneous phase real power and its mean per cycle. Note that the rms and mean values are computed on a cycle basis, over each complete period of the instantaneous current waveform (reference).

The DAQ is also capable of filtering the captured data, and computing more data traces from the raw data captured at the measurement channels. This computed data is very useful and often helps to highlight specific events in the dynamic operating condition under consideration. For example, the behaviour of the motor in the presence of a current limiting circuit can be investigated by analysing the trace of the arithmetic mean of the three line-to-line rms currents.

Figure 5.8 (a) shows the filtered torque and speed traces of the motor as it accelerates from rest to no-load speed. Clearly, the motor performs the most work in the first three seconds of the profile as the torque reaches its peak values. During acceleration, the motor maintains a constant torque. As expected, maximum torque corresponds to the maximum current as shown in Fig. 5.8 (b). The magnitude of this peak current was equal to the current limit of the power supply which was 150A for the set voltage range. From the acquired voltage and current data, a trace of the total input active power to the motor was also computed as shown in Fig.5.8 (c). As expected, this trace of motor input power follows the relative current and voltage magnitudes. Similarly, the trace of mechanical output power was also computed from the speed and torque data as shown in Fig. 5.8(c).

For the computations described above to take place, the DAQ has a formula database that allows the user to set custom formulae that can be applied on data captured from the different channels or data computed from other signals. This makes the DAQ a very resourceful tool for analysis of complex dynamic processes as it saves time and provides extra data.

Sometimes, it is necessary to analyse the complete set of measured and computed data to fully analyse a given dynamic operating condition. For example, the 37kW motor experiences resonance at a speed of about 1020 rpm, corresponding to a frequency of about 35Hz. This resonance results in torque pulsations, magnetic noise and excessive vibrations in the motor. It is therefore paramount to know the frequency (speed) at which the motor exhibits reasonce in order to avoid operating in that region. However, from the graphs analysed so far, there has been nothing or very little indication of this important phenomena. The motor behaviour during resonance can only be highlighted by analysing the raw (unfiltered) torque data in Fig.5.9 (a).

From Fig 5.9 (a), the magnetic noise and excessive vibrations can be deduced from the sudden increase in noise on the torque signal at a speed of 1020 rpm, relative to other operating speeds. By plotting the frequency trace on the same time axis as the torque and speed, the resonance frequency can easily be identified by the red cursor value as shown in Fig.5.9 (b).

During resonance, there is also a slight increase in input power absorbed by the motor, indicated by the sudden ‘bump’ in the power trace at the cursor position shown in Fig.5.9 (c).

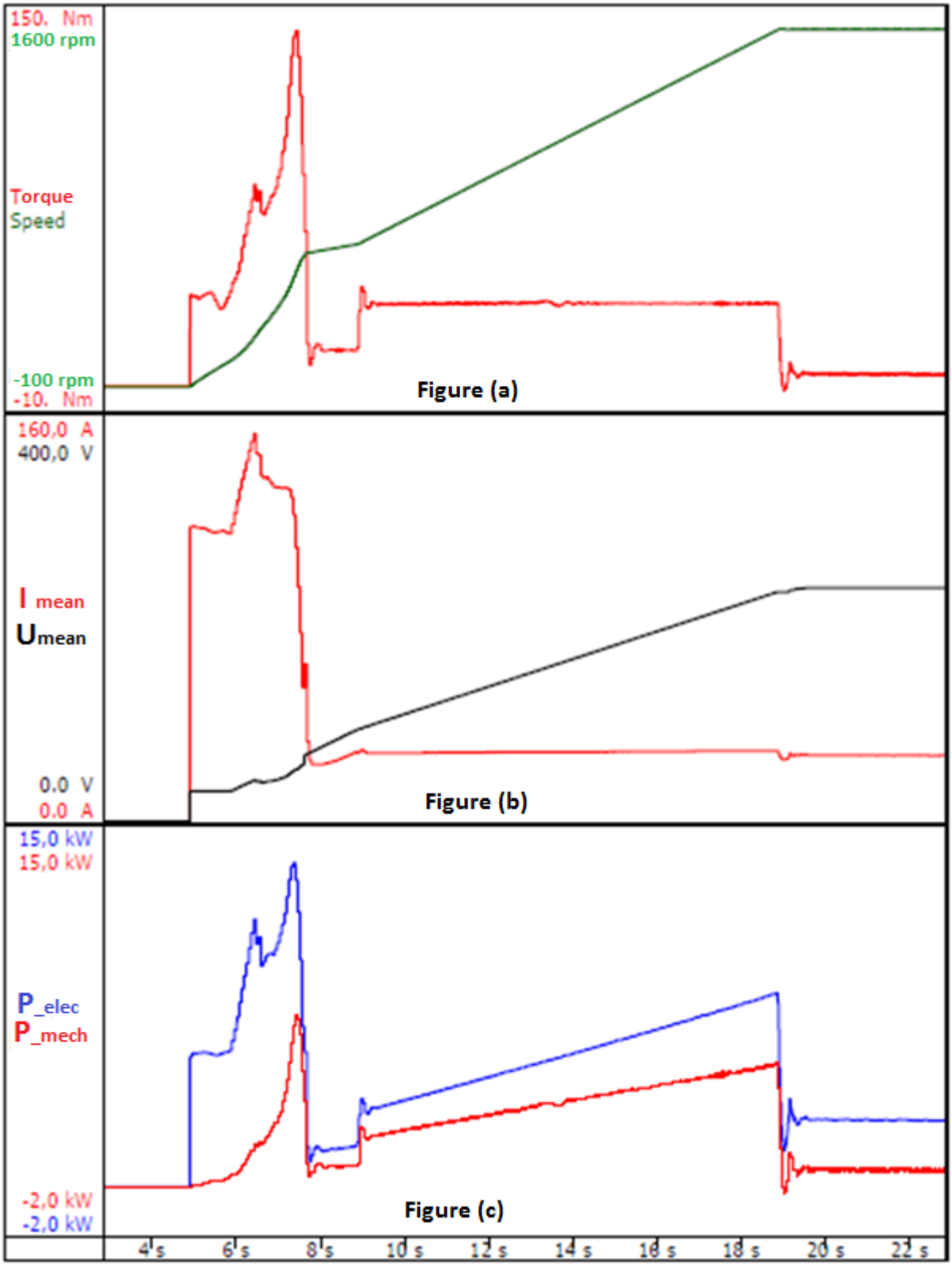

Fig.5.8 Filtered and computed quantities: **(a)** filtered instantaneous torque and speed traces; **(b)** arithmetic mean of the rms line currents and voltages; **(c)** computed traces of input power and mechanical power.

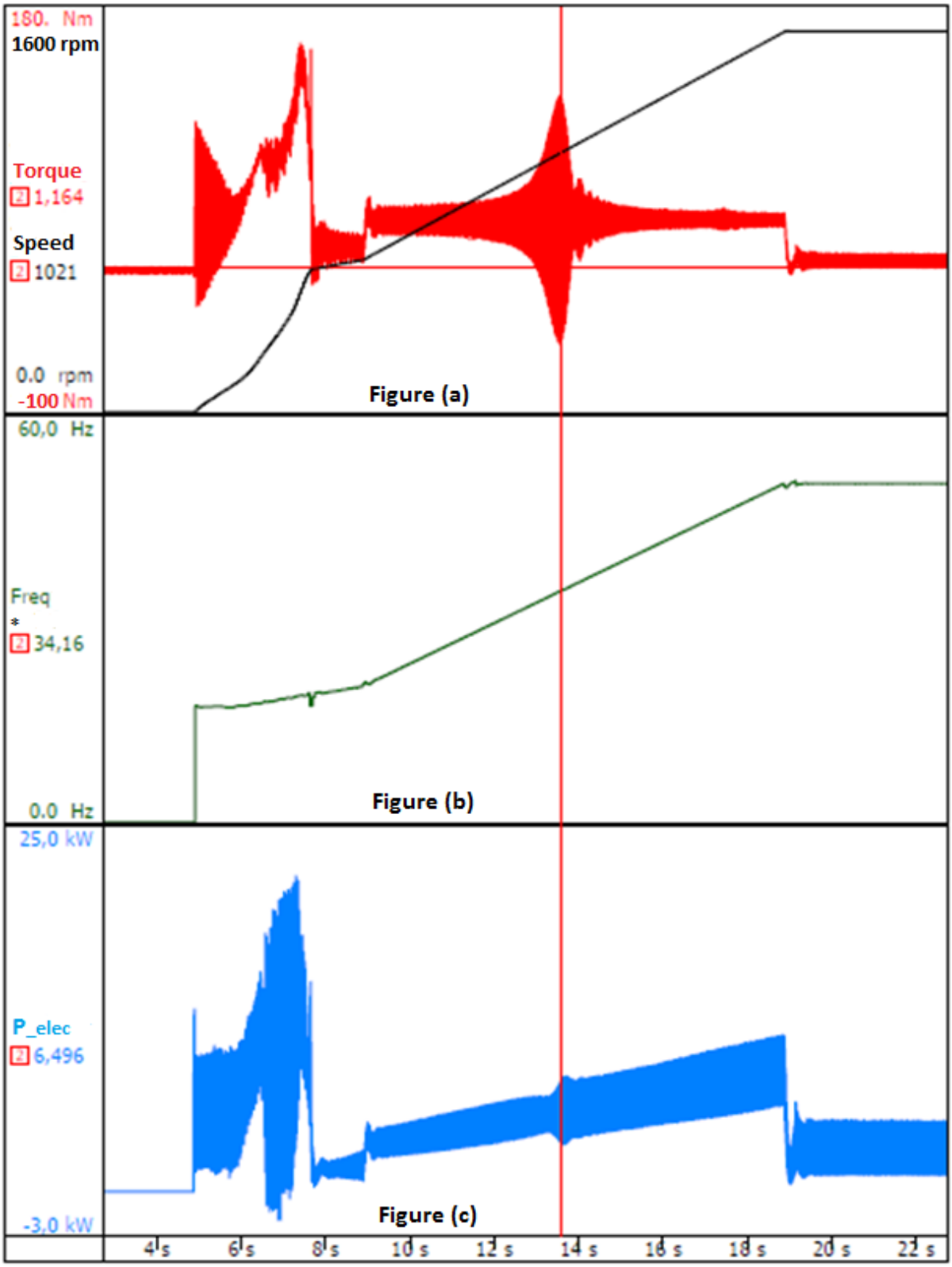

Fig.5.9 Combined analysis of raw and computed quantities: **(a)** Raw torque and filtered speed traces showing resonance at cursor position; **(b)** Trace of measured frequency; **(c)** Computed instantaneous input active power.

*Note that the values indicated by 2 on the vertical axis indicate the instantaneous value of the trace at the cursor position (red line).

5.2.2 Acceleration/ Deceleration under converter supply

In this section, we investigate the impact of the current limiting feature of Variable Frequency Drives on induction motor performance during acceleration and deceleration. To isolate this control feature from the influence of other drive controls, any current and speed feedback were disabled, as well as the slip compensation feature turned off. For this dynamic operation, a 55kW induction was accelerated from 1000 rpm to 1200 rpm on no-load. As the VFD was operating in open-loop V/F control mode, the acceleration and deceleration were achieved by applying pre-set frequency references corresponding to the initial and final speeds, at a fast ramp rate of 2s/100Hz. The filtered torque and speed traces captured by the DAQ are shown in Fig. 5.10.

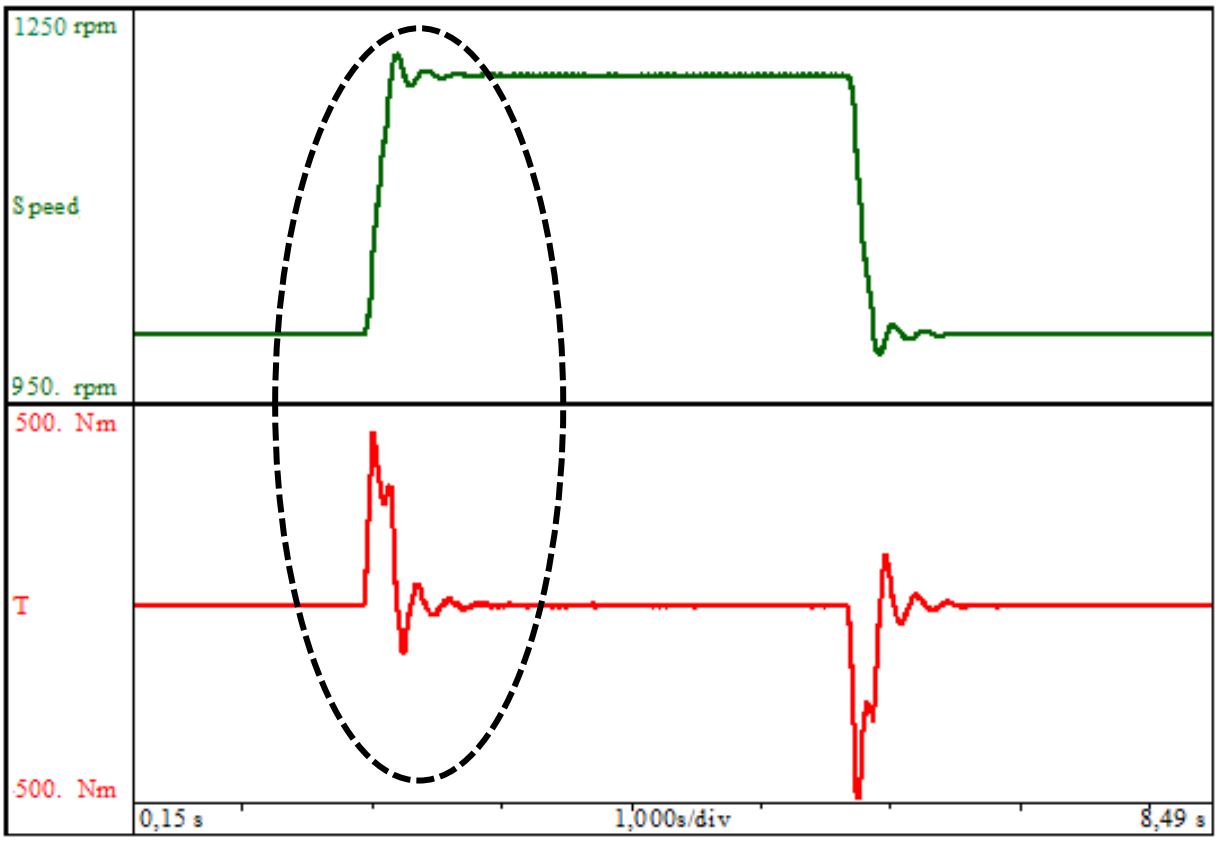

Fig.5.10 Acceleration/ Deceleration operation of converter-fed induction motor

By zooming into the acceleration region, shown dotted, and analyzing the computed traces of mean dc bus voltage, rms current, input power and frequency as shown in Fig. 5.11, the motor behaviour can be fully explained. As shown in Fig. 5.11 (b), the motor starts by drawing a high current to provide the required accelerating torque, resulting in a drop in the dc bus voltage as shown in Fig. 5.11 (d).

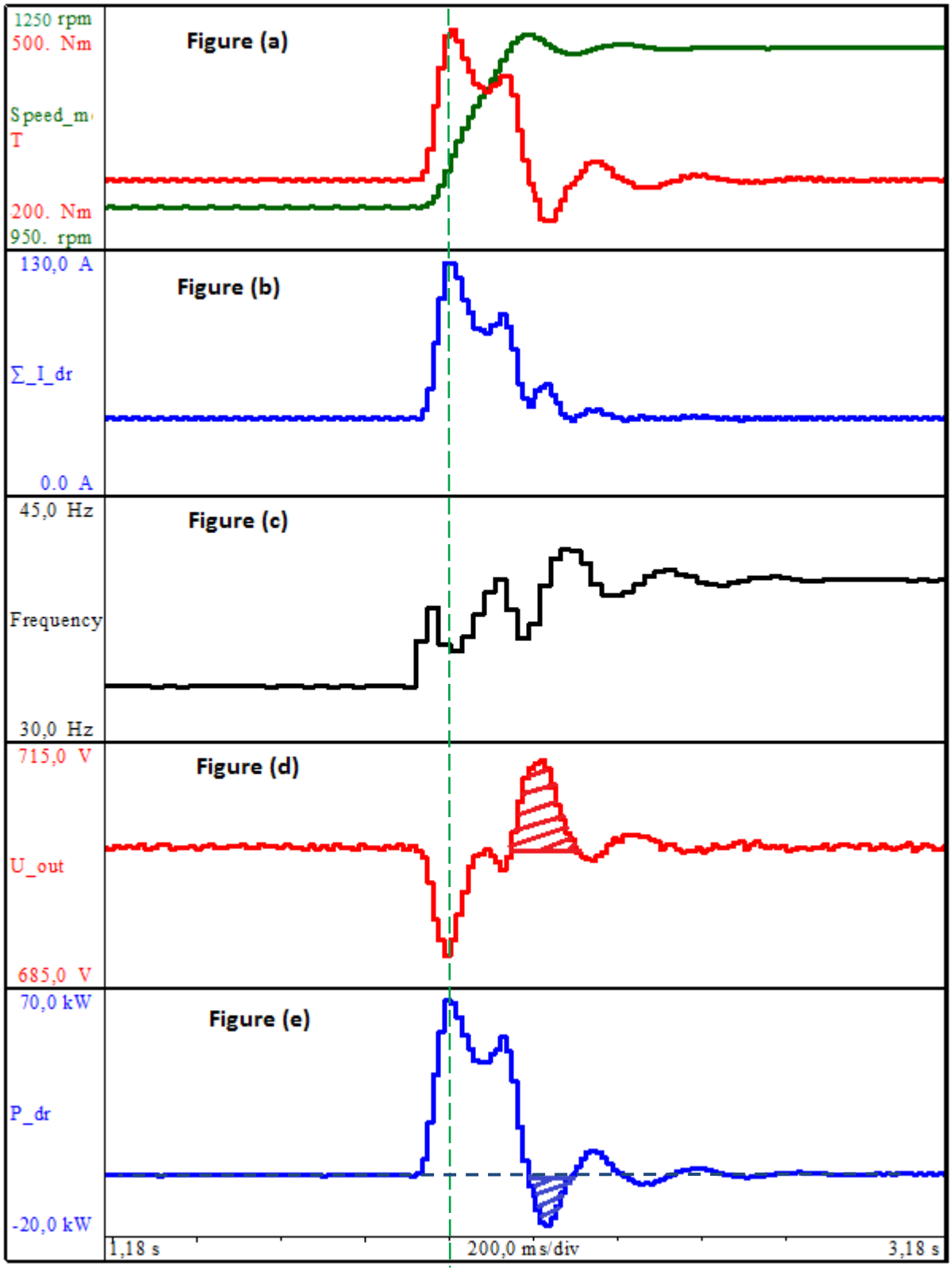

Fig.5.11 Analysis of current limiting feature of induction motor drives during acceleration*

*The Genesis 7i DAQ uses a data computation technique based on cycle math. This means the mean and rms values of all computed quantities are calculated based on the period of a selected reference signal. Therefore, computed data can be zoomed in until it begins to look stepped, especially when looking at highly dynamic data. However, this is different from raw data which consists of pixels sampled at 1MS/s.

When the current reaches the limit set in the controller, in this case 120A (shown in Fig. 5.11 (b) by a green broken line), the PI controller gives a command to reduce the frequency as shown in Fig.5.11 (c). This action produces a counter (braking) torque, thus reducing the torque producing current. It must be noted here that even when the current limit is active, the motor continues to follow the ramp and keeps accelerating. This is because the purpose of the current limit is to ensure the motor current is kept within required levels – not to stop the ramp. If this was not the case, the motor would immediately start slowing down before reaching the programmed speed. When the motor reaches its target speed, the ramp is disabled, and the motor undergoes a brief regenerative braking period. This is confirmed by the increase in the dc bus voltage and the negative power flow, represented by the shaded regions in Fig. 5.11 (d) and (e) respectively.

During deceleration or rapid braking, the current limit ensures the motor current is kept within the required levels by increasing the frequency when the regenerating current limit is exceeded. This feature ensures the dc-bus capacitor voltage is kept within the required limits. The ability to synchronously capture the above operation which lasts just under 400ms clearly demonstrates the suitability of the Gen 7i DAQ for dynamic studies of induction motor drives. The Gen 7i can therefore be used for both teaching and research purposes.

5.3 SUMMARY

In this chapter, the experimental setup used in this research has been described. The data measurement device of this test bench is the *Genesis 7i* Data Acquisition System which has high-speed data capturing and computation capabilities. To demonstrate these capabilities, some dynamic operations of induction motors were analysed. In the first application, the behaviour of the motor when it is accelerated from rest to near-synchronous speed in a controlled manner was studied to provide insight into the current, torque and power characteristics. The analysis further highlighted the torque pulsations, accompanied by a sudden increase in the absorbed active power, when the motor reached its resonance frequency. The second application highlighted the influence of the drive control features during acceleration and deceleration.

The rich data provided by the DAQ demonstrates its usefulness as a tool for both research and teaching purposes. Another interesting feature of the DAQ is the automated-data-capturing which was utilized to develop the automated testing procedure described in the next chapter.

6. AUTOMATED EFFICIENCY TESTING PROCEDURE

The determination of mains-fed IM losses, and hence efficiency, has become well-established over the years. This is demonstrated by the fact that revisions to the two most widely used international standards [9], [10] have become minor and are more related to improvements in instrumentation accuracy than testing procedure and analysis [14]. On the other hand, the determination of converter-fed motor losses is still an open research field as most of the technical documents available on the subject [11], [18], [19] are still in their infancy.

The concept of determining the additional harmonic losses introduced in the IEC/TS is still a challenge for researchers as evidenced by the conflicting reports cited in literature. While the IEC/TS asserts that additional harmonic losses increase with load and is supported by results in [13], [22], other studies [12], [29] have reported that these losses are constant. Although the reasons for such discrepancies are not clearly known, it is logical to attribute them to inconsistencies during measurement and testing from one individual to another.

This chapter discusses an automated efficiency testing procedure which was developed to mitigate the adverse effect of varying technical skill and competence levels of the human operator on efficiency test results. The advantage of using the developed automated testing procedure is that it improves the determination of stray-load losses and hence the load-dependent component of additional harmonic losses introduced in the IEC/TS.

6.1 DEVELOPMENT OF AUTOMATED EFFICIENCY TESTING PROCEDURE

To ensure that the sinusoidal and PWM supply tests are performed under identical conditions of load torque, motor terminal voltage and temperature variation, an automated efficiency testing procedure was developed. This procedure is an attractive approach to motor testing as it speeds up the entire testing process and simplifies the synchronized-recording of all electrical and mechanical quantities. The reduction in test duration results in a corresponding reduction in temperature variation between consecutive load steps as recommended in test standard [10]. Furthermore, the automated approach eliminates the need for highly technical personnel to conduct efficiency tests as it can be run by anyone with basic computer knowledge. As will be shown later in this dissertation, the developed procedure presents an improvement in the determination of additional harmonic losses.

The developed automated testing procedure is simply a program written into the drives and programmable power supply unit to control the sequence in which output test quantities such as load torque and motor voltage are fed to the machine-under-test (MUT). It also generates external trigger signals to control the systematic capture of data. Such a system eliminates the problems associated with manual testing, which include mismatch of test points and mechanical loading, unsynchronized data capture, and long test durations which often lead to significant temperature variations [16], [45], [47]. Although it is impossible to automate the entire efficiency testing process owing to mechanical tasks such as decoupling the MUT from the dynamometer, the load curve test and the no-load tests can be fully automated.

6.1.1 Automated Load curve Test

For the load curve test, a program was written into the load motor drive (Unidrive SP: Model SPMD 1404) using a Drive Programming Language (DPL) in *Syptrol* software. This DPL code applies a sequence of pre-determined torque references to the dynamometer, which provides load torques on the Motor-Under-Test (MUT). The applied load torques are in accordance with the requirements of the latest version of the IEC 60034-2-1 test standard, which was released in 2014.

The DPL program also generates external triggers in the load motor drive to control the acquisition of data in the Genesis 7i DAQ. Since the load motor drive generates digital outputs at 24V while the DAQ requires 5V TTL-compatible signals, a relay with a 24V dc coil was used to interface the external trigger signals from the load motor drive to the DAQ. The DAQ allows the user to select active HIGH or LOW trigger signals for the external start/stop condition that controls the remote acquisition of data. Setting the external start mode to active-LOW selection maintains the internal voltage of the *external start connector* at 5V. Thus, it only requires a short circuit to activate the acquisition of data. Therefore, the 24V digital outputs generated in the load motor drive were used to control the normally-open contacts of the relay, which in turn created the necessary short circuit to trigger the DAQ.

At each set point, a sufficient delay period, *d*, was allowed for the motor to attain steady-state operation before triggering the DAQ. Once steady-state operation is achieved, a continuous recording of 5 seconds, denoted by t, is taken to ensure an averaged reading that exceeds the requirements of the IEEE 590 standard for harmonic measurements. The schematic of the load test is illustrated in Fig. 6.1.

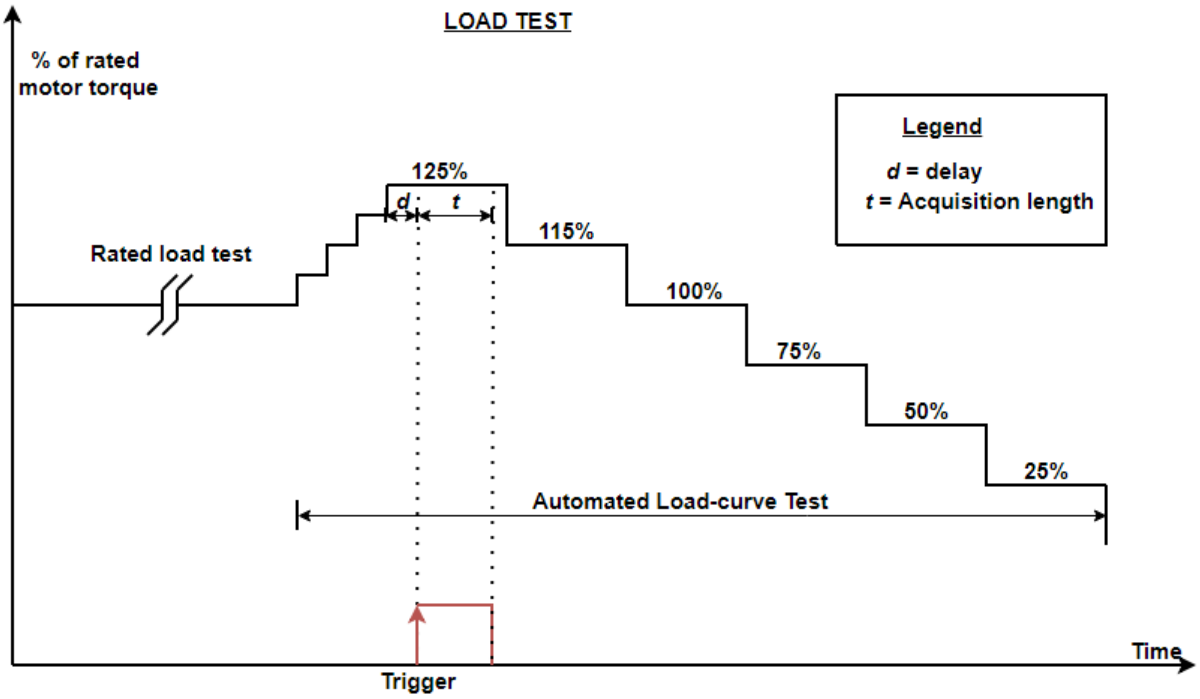

Fig.6.1. Automated Load-curve Test sequence

The required torque references for each MUT can be determined at the end of the rated load test and then input into the automated test procedure. However, since the same dynamometer was used for all tests, the determination of load torque was simplified by using an interpolation method. With the 55kW motor under thermal stability, a graph of load torque was plotted against torque reference and the relationship shown in Fig. 6.2 was then used to pre-determine the required torque references for all subsequent test motors. Although different motors attain thermal stability at different temperatures, the torque references obtained using the above procedure were adequate for the subsequent motors.

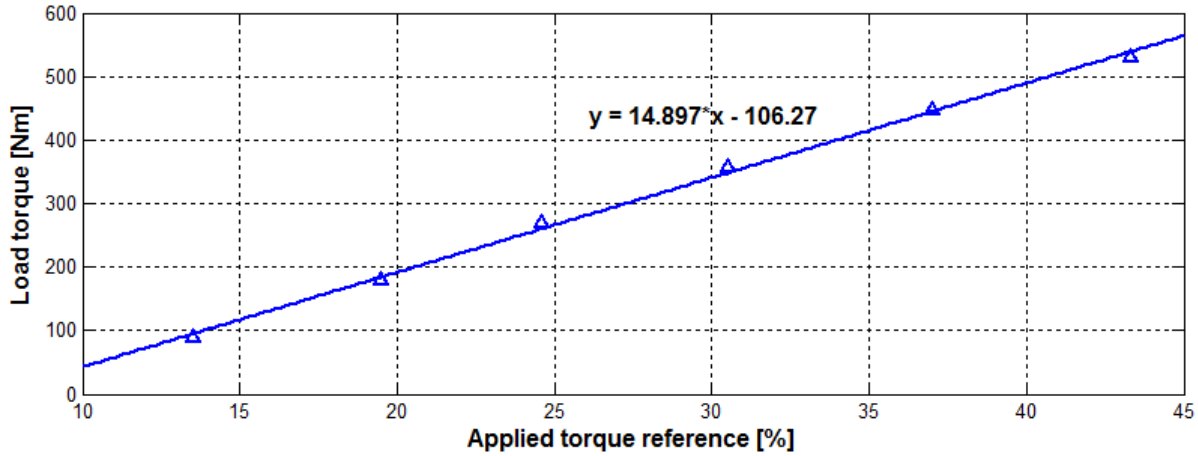

Fig.6.2 Relationship between load torque (Nm) and required torque reference (%). The relationship obtained is used to predetermine the required torque references for the automated load test.

6.1.2 Automated No-Load Test

For the no-load test, the test motor drive and the programmable power supply unit were programmed to sequentially apply a set of pre-determined voltages to the MUT. To achieve this, the MUT drive was programmed using DPL while the California Instruments MX 60 Power Supply was programmed using a '*Transient Lists*' function in the *Virtual Panels* software. It was easy to generate external triggers for the DAQ with the MX 60 power supply because it has a dedicated TTL trigger channel that generates, 400 microsecond pulses at 5V. The MX 60 was used for the no-load tests with a sinusoidal supply.

The no-load voltages were selected according to the requirements of IEC 60034-2-1 as shown in Fig. 6.3. Again, a sufficient delay was allowed between voltage steps to ensure measurements were taken after the motor voltage had stabilized.

The main challenge encountered during the implementation of the automated testing procedure was the frequent erroneous triggers due to signal interference from the high-frequency switching action of the IGBT switches in the drives. Even with a shielded cable, the signal interference from the load motor side was difficult to contain. To mitigate this issue, the 24V DC relay and all cables were routed as far away from the motor power cables as possible.

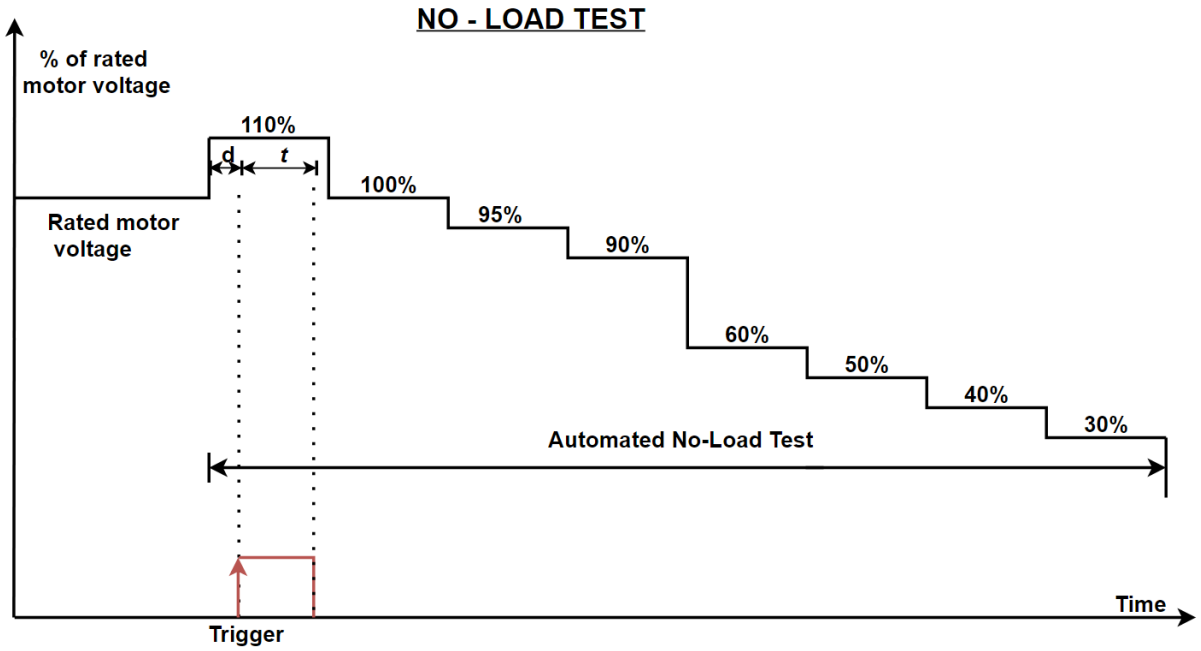

Fig.6.3 Automated No-Load Test sequence

The system interface diagram showing generation points and flow of trigger signals for the DAQ is shown in Fig. 6.4. In the load and test motor drives, the signal cables are connected to terminals 12 and 9 (GND) on the SM plus applications module. This module is the one that allows user-programming of the drives and generates the 24V digital outputs that control the normally-open contacts of the 24V DC relay. Since the MX60 power supply generates 600ms external trigger pulses at 5V, it does not require a relay as shown in Fig. 6.4.

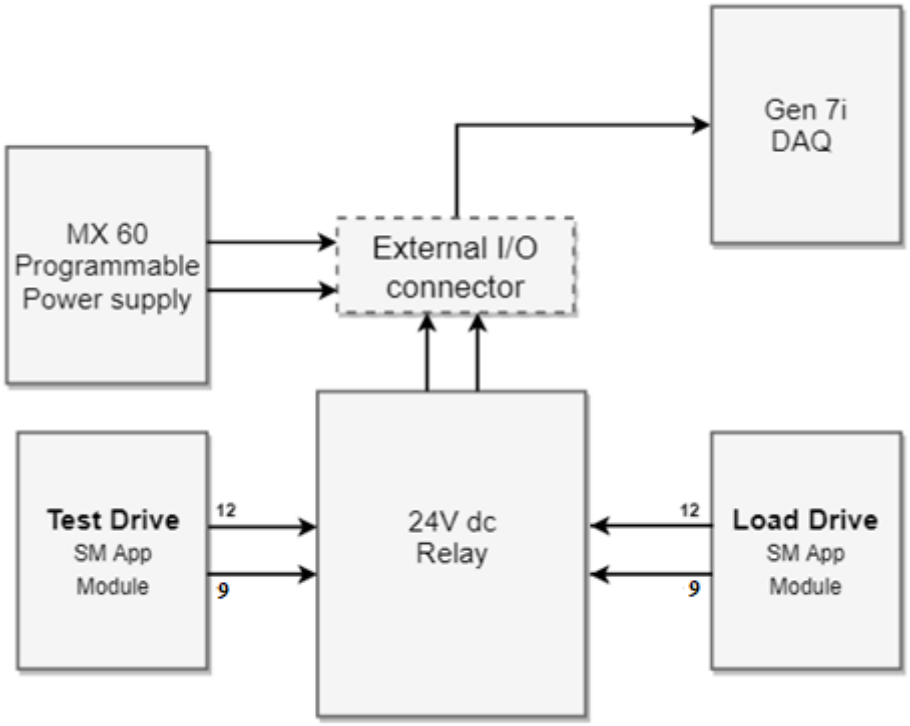

Fig.6.4 System interface diagram showing the flow of control signals for the implementation of Automated-testing procedure.

6.1.3 Complete Efficiency Testing sequence

The complete testing sequence is illustrated in the form of a flow chart shown in Fig. 6.5. As certain tasks in the efficiency estimation process are mechanical, such as decoupling the MUT and dynamometer or measuring the winding resistance, not all aspects of the efficiency test can be automated. Therefore, the automated sections of the test procedure are highlighted in dashed rectangular portions. The actual DPL codes for the load-curve test and no-load tests, including instructions for running the code, are provided in appendix C of this dissertation.

In the determination of additional harmonic losses according to the IEC/TS, the automated tests are first performed with a sinusoidal power supply, and then repeated with a converter supply as shown in the flow chart in Fig. 6.5.

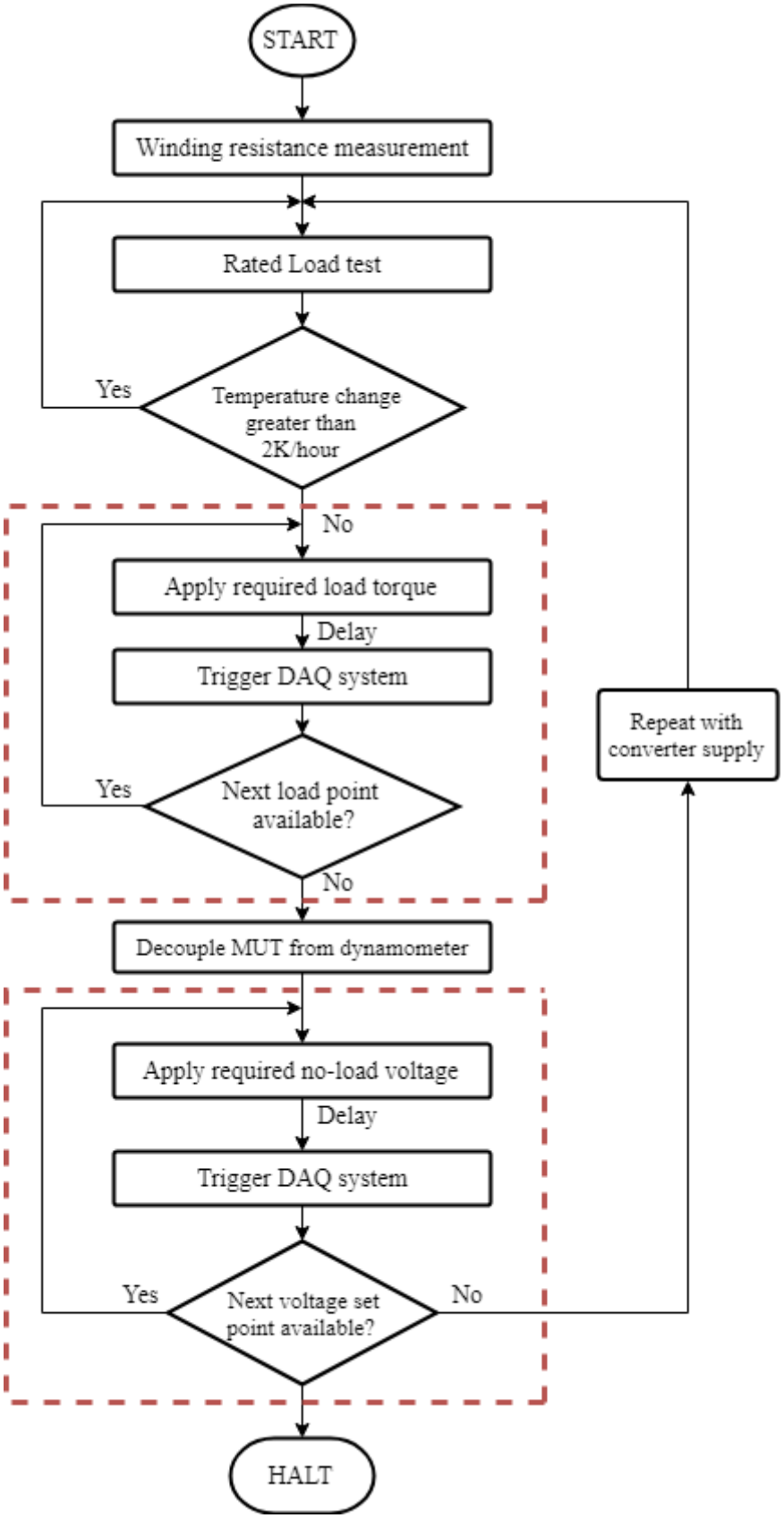

Fig.6.5 Flow chart for efficiency testing of converter-fed induction motors: The sections enclosed in dashed rectangular portions represent the automated sections of the test

6.2 SUMMARY

The determination of additional harmonic losses proposed in the IEC/TS depends on the accurate determination of induction motor losses on both sinusoidal and PWM supply. Any mismatch in test parameters between the two sets of tests introduces an error in the load-dependent component of harmonic losses. Therefore, the automated test procedure presented in this chapter was developed to minimize any errors due to the human operator. As will be shown in the results and discussions chapter, the automated procedure presents an overall improvement in the quality and repeatability of test results.

The developed automated procedure is easy to carry out and allows non-specialists to perform efficiency testing. It also speeds up the testing procedure, thus minimizing temperature variations during the load-curve test.

7. EXPERIMENTAL RESULTS AND CONSIDERATIONS

This chapter presents experimental results that were obtained by testing three induction motors whose name plate details are given in Table 7.1. The aims of these experimental tests were to:

1. Investigate the relationship between voltage, current and power in a sinusoidal mains supply and the fundamental components of a PWM supply in a converter-fed induction motor. The objective was to ascertain whether the afore-mentioned components of power can be used interchangeably, and to assess the impact of such a development on the efficiency estimation process.
2. Test the practical applicability of the IEC/TS 60034-2-3 and comment on the additional harmonic losses obtained.
3. Validate the developed automated efficiency testing procedure.

To perform the segregation of induction motor losses, certain motor parameters must be known. Depending on the test method being used, the parameters of interest include: winding resistance, magnetizing and leakage reactance, rated motor torque, and winding temperature. Some of these parameters can be easily calculated using name plate details while others require direct measurements or locked-rotor and no-load tests. However, for the loss-segregation method B of the IEC 60034-2-1 and IEEE 112 standards, only the stator winding resistance at ambient or test temperature is required.

In this chapter, measured data is reported for the various tests that were performed. For each set of tests, the technical considerations and the methodology adopted are fully explained. The analysis and discussion of these experimental results will then be presented in chapter 8 of this dissertation.

Table 7.1 Motor Name Plate details

Parameter	37kW Motor	45kW Motor	55kW Motor
Number of Poles	4	4	4
Rated Frequency (Hz)	50	50	50
Rated Line Voltage (V)	400	400	400
Rated Line current (A)	67.4	81.6	99.6
Rated Speed (rpm)	1475	1475	1475
Rated Power factor	0.86	0.86	0.90
Insulation Class	F	F	F
Connection	Δ	Δ	Δ

7.1 MOTOR PARAMETERS

When using the indirect (loss-segregation) method to estimate the motor efficiency, the only equivalent circuit parameter needed in the analysis of results is the stator winding resistance. For this study, the resistance values were measured when the motor was at ambient temperature and then corrected to the temperature of the test as discussed in section 4.1.1. Table 7.2 shows the average of several measurements of the three line-to-line cold winding resistance values for the three induction motors, measured with a Wheatstone bridge.

Table 7.2 Cold winding resistance measurements

Motor	Winding Resistance [Ω]	Winding temperature [°C]
37 kW	0.1335	18.68
45 kW	0.1035	20.26
55 kW	0.0881	23.26

7.2 MEASUREMENT OF FUNDAMENTAL POWER QUANTITIES

The measurement of non-sinusoidal power quantities is more complex than sinusoidal ones. This is because they require more sophisticated equipment with higher sampling and bandwidth capabilities than the latter. Furthermore, even with the right equipment in place, the measured rms values of voltage can be confusing because they are generally much higher than expected. For example, the screenshot in Fig. 7.1 was captured when the VFD was programmed to deliver 400V rms (approximately 231V/ phase). Looking at the set of meter readings on the drive inverter output section (dotted region), the first reading, which indicates the rms value of the PWM phase voltage, shows a much higher value of 284V while the fundamental voltage value of 231V (shown in the bottom right corner) is as expected.

Obviously, the scenario demonstrated here is a basic concept that is well-understood. However, it must be stressed that the measured fundamental value of voltage is the one required in the determination of converter-fed motor core losses – not the ‘total’ rms value. This means that the power analyser used in the determination of converter-fed motor losses must be capable of extracting the fundamental voltage value, without affecting the total active power measured. Whereas older power analyser models generally allow the user to estimate fundamental quantities by applying digital line filters, modern DAQs like the Gen 7i have sophisticated algorithms to achieve this.

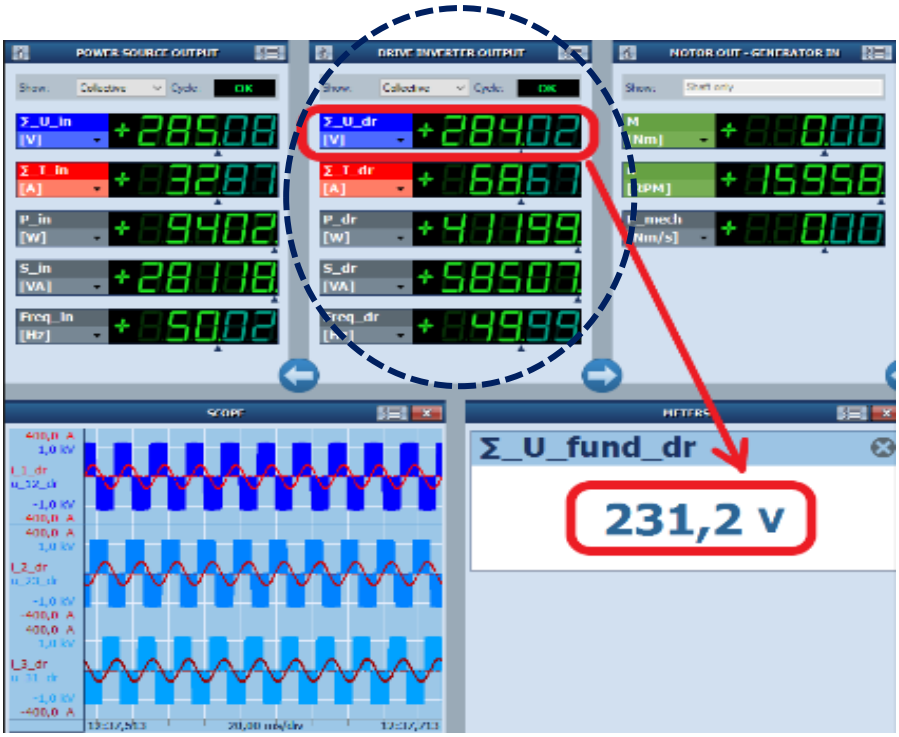

Fig.7.1 Measured RMS and Fundamental values of non-sinusoidal power quantities

For a given load torque at rated voltage, a motor will draw more power when connected to a PWM supply than it will on sinusoidal supply, due to additional harmonic losses. Since the instantaneous real power drawn by a system is obtained from the product of instantaneous values of voltage and current according to (7.1), the total active power under PWM supply is expected to be higher due to the high instantaneous voltage as shown in Fig 7.1.

$$p(t) = v(t).i(t) \tag{7.1}$$

The difference between the total measured active power and the power due to the fundamental components of voltage and current is generally referred to as the harmonic power. According to [3], "*the current components at harmonic frequencies do not contribute to the average power drawn from the power electronic converter.*" In other words, the harmonic power drawn from the drive supply is generally dissipated as heat in the core of the motor and constitutes a large part of the iron losses. The harmonic currents also produce harmonic torques which lead to torque pulsations in the motor.

Taking the above discussion into consideration, one would expect to obtain very similar efficiency values when testing a motor using a sinusoidal supply or by using the fundamental measurements from a PWM supply test, provided the load torque is kept constant. To test this hypothesis, the three induction motors were tested according to the IEC 60034-2-1 standard loss segregation procedure outlined in section 4.1. The no-load and load test measurements

from a sinusoidal supply test and fundamental quantities under a PWM supply for the 55kW motor are provided in Tables 7.3 to 7.5 while data for other motors is provided in appendix A.

Table 7.3 55 kW motor No-load test results: comparison of sinusoidal and fundamental pwm measurements

Temperature * [°C]		**Fund Input Power [W]**		**Fund Voltage [V]**		**Fund Current [A]**	
sine	pwm	sine	pwm	Sine	pwm	sine	pwm
102.98	93.80	1485.56	1428.63	429.42	429.36	30.87	30.92
101.86	93.30	1263.52	1210.13	390.90	390.37	26.01	25.88
100.78	92.18	1184.25	1127.06	370.42	370.00	23.97	24.01
99.82	91.77	1105.51	1056.80	351.18	351.24	22.38	22.40
98.44	91.34	749.58	717.29	234.74	234.08	14.41	14.34
97.56	90.76	650.56	637.48	195.42	195.65	12.06	12.02
96.70	90.31	575.75	562.80	156.24	156.54	9.84	9.82
95.43	89.58	513.46	510.06	117.96	117.84	7.89	7.79

Table 7.4 55 kW motor Load-curve test results obtained from Sinusoidal supply measurements

Temp [°C]	**Torque [Nm]**	**Speed [rpm]**	**Voltage [V]**	**Current [A]**	**Power [W]**	**Freq [Hz]**
126.82	531.26	1445.50	389.50	152.63	91512.95	49.94
129.58	443.45	1456.44	390.35	125.20	75745.66	49.94
129.32	356.58	1465.30	391.33	100.18	60588.35	49.91
126.86	264.27	1473.82	391.57	75.94	45033.44	49.89
123.46	177.27	1486.03	393.46	54.98	30825.98	50.03
118.63	88.58	1491.48	393.45	36.67	16466.25	49.97

Table 7.5 55 kW motor Load-curve test results obtained from Fundamental PWM supply measurements

Temp [°C]	**Torque [Nm]**	**Speed [rpm]**	**Voltage [V]**	**Current [A]**	**Power [W]**	**Freq [Hz]**
126.98	530.50	1446.99	389.45	152.49	91433.84	49.99
130.75	443.26	1458.11	391.05	124.98	75776.77	49.99
130.29	356.30	1467.71	391.58	100.16	60661.22	49.99
127.64	265.89	1476.97	393.13	76.13	45350.66	49.99
123.97	176.88	1484.82	393.91	54.73	30709.75	49.99
117.90	88.64	1492.11	393.87	36.57	16451.43	49.99

*Since the average winding temperature is a function of the current flowing in the windings [50], there is always a significant loss of temperature when decoupling the test motor from the dynamometer at the end of the load tests. Furthermore, as the current drawn on no-load is much lower than that drawn during the load test, there is a continuous loss of temperature between the no-load test performed first with a sinusoidal supply, and then with a PWM supply as reported in Table 7.3.

7.3 DETERMINATION OF HARMONIC LOSSES

To estimate the efficiency of converter-fed induction motors in accordance with IEC/TS, certain aspects of the procedure must be well-understood to avoid erroneous results. Since this procedure is relatively new and is undergoing validation, the discussion presented in this section is meant to provide guidance to other researchers and individuals performing the test. The results that will be presented in chapter 8 of this dissertation show some interesting observations regarding the proposed methodology and will serve as good feedback to the relevant IEC standards committee.

The fundamental motor terminal voltage is a critical parameter in the determination of converter-fed motor efficiency. Since additional harmonic losses are evaluated as the increase in motor losses when fed from a PWM supply, taking sinusoidal supply losses as a reference, it is crucial to match the motor parameters in the two tests. This is why the IEC/TS states as a reference condition that: *for rated voltages up to 1kV, the fundamental motor voltage must be equal to motor rated voltage at 50Hz or 60Hz, and that no additional components influencing output voltage or current shall be installed between the test converter and motor except those required for measuring instruments*. Although the required value of fundamental motor voltage can generally be programmed into the VFD, some VFDs incorporate an output choke, which can influence the output voltage waveform and magnitude as discussed in the next section.

7.3.1 Output choke and fundamental motor voltage

As explained in chapter three of this dissertation, output chokes (or reactors) reduce the harmonic distortion of line current, nuisance drive over-voltage trips caused by transient voltage spikes, and minimize motor insulation failure. The major drawbacks of using an output choke are the associated voltage drop across it and the power loss due to its resistance and eddy currents in the iron core [43]. This is in addition to the extra cost, weight, and space requirements that it imposes on the system. The rating of a reactor is usually specified by its percentage impedance, which is defined as the voltage drop across the reactor at rated current, expressed as a percentage of rated voltage. It is given by:

$$\%_{impedance} = \frac{I_{rms} \times 2\pi f_{50/60Hz} \times L_{reactor}}{V_{ph}} \times 100 \qquad (7.2)$$

where I_{rms} is the motor current at a given load, f is the fundamental frequency, $L_{reactor}$ is the inductance of the reactor, and V_{ph} is the line-to-neutral motor voltage.

When testing a unique combination of motor and converter (VFD) which has an output reactor, the motor terminal voltage will be lower than that specified in the drive parameters owing to the voltage drop across the reactor. From (7.2), this voltage drop increases with loading on the motor. Therefore, the usual industrial practice of merely entering the rated motor voltage into the drive parameters does not suffice when testing according to the IEC/TS.

Although the IEC/TS states that there must be no additional components between the converter output and the motor, it is the author's view that if the converter for the motor has an output reactor, the reactor must be considered part of the VFD and its voltage drop be treated as an internal drop. Therefore, to match the PWM supply fundamental terminal voltage to the sinusoidal value, as required by the IEC/TS, the drive voltage must be continuously adjusted during testing. To demonstrate the implication of a mismatch in terminal voltage between the sinusoidal and PWM tests, three efficiency tests described below were performed on a 55kW:

7.3.2 Load-curve tests at variable fundamental voltage

The first load curve test, whose results were presented in Table 7.4, was a standard IEC 60034-2-1 procedure on sinusoidal supply with load torque up to a maximum torque of 150% of rated value. Note that the new IEC 60034-2-1; 2014 only specifies load torques up to 125% of rated value, but the motor was loaded to 150% for this test to amplify the impact of the voltage drop across the reactor. At each load point, the motor terminal voltage was recorded to take note of any voltage fluctuations due to loading. In the second test, whose results are presented in Table 7.6, the fundamental PWM motor voltage was constantly adjusted to match the value of the corresponding sinusoidal supply test and is hereafter referred to as the *matched PWM test.* The final load-curve test, whose results are presented in Table 7.7, was performed by simply setting the motor terminal voltage drive parameter to the nominal sinusoidal voltage at rated load torque and is hereafter referred to as the *unmatched PWM test*.

The analysis of test results presented in Tables 7.5 to 7.7, to highlight the impact of the voltage mismatch between sinusoidal and converter supply efficiency tests on the 55kW motor, are presented in chapter 8 of this dissertation. The experimental test results for the 37kW and 45kW motors are also included in Appendix A of this dissertation and are also analysed in chapter 8. However, for these two motors, the fundamental motor voltage was matched to the sinusoidal supply value by carefully considering the voltage drop across the reactor.

Table 7.6 Load-curve test data for the "matched PWM" test

Temp [°C]	Torque [Nm]	Speed [rpm]	Fund Voltage* [V]	Current [A]	Power [W]	Freq [Hz]
126.98	530.50	1446.99	389.45	152.62	91812.79	49.99
130.75	443.26	1458.11	391.05	125.12	76152.51	49.99
130.29	356.30	1467.71	391.58	100.32	61034.93	49.99
127.64	265.89	1476.97	393.13	76.32	45722.29	49.99
123.97	176.88	1484.82	393.91	54.94	31078.56	49.99
117.90	88.64	1492.11	393.87	36.82	16823.70	49.99

Table 7.7 Load-curve test data for the "unmatched PWM" test

Temp ** [°C]	Torque [Nm]	Speed [rpm]	Fund Voltage * [V]	Current [A]	Power [W]	Freq [Hz]
130.62	530.49	1445.26	386.38	154.23	91989.74	49.99
133.31	443.48	1456.62	387.02	126.67	76316.71	49.99
130.19	357.28	1466.67	387.57	101.58	61245.02	49.99
128.53	264.97	1476.13	388.28	76.79	45612.85	49.99
126.03	176.67	1484.31	388.90	55.17	31051.61	49.99
123.55	88.53	1491.86	389.83	36.60	16791.93	49.99

* Since the 55kW motor could not be powered by the MX 60 power supply, the sinusoidal supply load-curve test was performed on direct grid supply which was around 390V. The drive supply was then adjusted as described above to match the values on sinusoidal supply.

** The higher winding temperatures recorded during the unmatched PWM test were due to the higher line currents caused by a reduction in motor terminal voltage.

7.4 VALIDATION OF AUTOMATED EFFICIENCY TESTING PROCEDURE

The developed automated testing procedure was validated by performing efficiency tests on the three induction motors. In order to check the consistency of the procedure and the repeatability of results, two sets of manual and automated tests were performed with a sinusoidal supply, and with a PWM supply. However, only the first and repeat automated test results for the 55kW motor on PWM supply are presented in tables 7.8 and 7.9. Test data for the sinusoidal supply tests and other motors can be found in appendix A of this dissertation. For these tests, the motor was loaded to the recommended maximum torque, equal to 125% of rated load torque, as discussed in section 4.1.

Table 7.8 Load-curve test data for the first PWM supply automated test

Temp [°C]	Torque [Nm]	Speed [rpm]	Voltage [V]	Current [A]	Power [W]	Freq [Hz]
131.7	445.8	1456.6	389.4	128.1	77542.4	49.99
132.5	409.0	1460.8	389.6	117.2	71064.0	49.99
132.8	358.0	1466.5	390.0	102.6	62178.1	49.99
132.4	265.6	1475.9	390.6	77.9	46493.1	49.99
131.1	175.7	1484.1	391.2	55.9	31595.1	49.99
129.5	88.6	1491.5	392.1	37.6	17541.6	49.99

Table 7.9 Load-curve test data for the repeat PWM supply automated test

Temp [°C]	Torque [Nm]	Speed [rpm]	Voltage [V]	Current [A]	Power [W]	Freq [Hz]
132.5	445.9	1456.2	389.5	128.1	77625.3	49.99
133.5	409.1	1460.5	389.7	117.1	71082.3	49.99
134.0	357.8	1466.2	390.0	102.6	62194.3	49.99
133.6	265.5	1475.6	390.6	77.9	46505.1	49.99
132.5	175.4	1484.0	391.3	55.8	31559.2	49.99
130.9	88.4	1491.5	392.0	37.6	17503.6	49.99

7.5 SUMMARY

This chapter presented the experimental results obtained from efficiency tests performed on three induction motors. The first set of tests were aimed at investigating the relationship between the measured fundamental voltage, current and power in a PWM supply and the measurements with a sinusoidal supply. The second set of tests were aimed at testing the practical applicability of the IEC/TS procedure for determining harmonic losses. This was also done to identify any technical considerations and areas that need to be well understood by stakeholders to ensure accurate results. Finally, the last set of tests was performed to validate the developed automated testing procedure. The analysis and discussion of the data obtained from the tests is presented in the next chapter.

8. ANALYSIS OF RESULTS

The analysis and discussions presented in this chapter are based on experimental results presented in the previous chapter and appendix A. The analysis is divided into three sections, according to the three key objectives presented in chapter 7.

The first part of the analysis demonstrates the feasibility of using a PWM supply to estimate the sinusoidal supply efficiency of an induction motor. The second part of the analysis deals with the determination of harmonic losses in a converter-fed induction motor. In this section, comparisons are drawn between the motor losses obtained with a sinusoidal supply and with a PWM supply in accordance with the requirements of the IEC/TS 60034-2-3. The section also highlights the technical considerations regarding the fundamental motor terminal voltage. The final section of the analysis demonstrates some of the technical improvements that were realized by adopting the automated efficiency testing procedure.

8.1 ESTIMATION OF SINUSOIDAL-SUPPLY EFFICIENCY USING PWM SUPPLY

8.1.1 Fundamental motor losses on no-load

Although the load test is normally performed first, the no-load test results are generally analysed first to determine the constant losses which consist of mechanical and conventional iron losses. From the no-load test results presented in Table 7.3, obtained according to the methodology presented in section 4.1.4, the rms value of the fundamental component of current in the PWM supply test was found to closely match the rms current drawn during the sinusoidal supply no-load test. A similar trend of results has been reported in [6]. The slight increase reported in the rms value of the unfiltered PWM current, compared to the rms current in the sinusoidal supply no-load test, can be attributed to temperature variations between the two tests. As expected, this increase in current was highest at the lowest voltage point (117V), which corresponds to the lowest modulation index, due to the decrease in flux and hence torque capability of the motor. In addition, the motor must overcome the increased iron losses under PWM supply, which constitute a large portion of the no-load losses. Fig 8.1 compares the no-load currents for the sinusoidal and PWM supply tests, as a function of line voltage.

From Fig. 8.1, it can be established that voltage harmonics due to the VFD have very little impact on the induction motor current. Therefore, an induction motor draws practically the same current – whether it is fed from a sinusoidal supply or a PWM supply – provided the load torque and fundamental terminal voltage in the two supplies are well-matched.

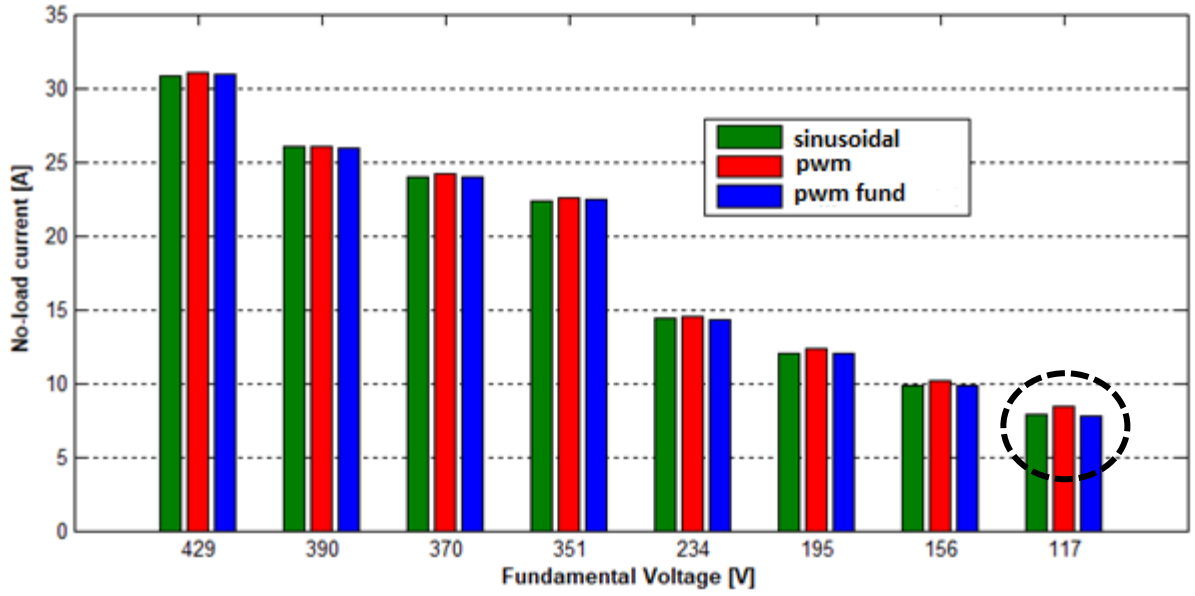

Fig.8.1. Comparison of 55kW motor No-Load current between sinusoidal supply and PWM supply

By subtracting the no-load stator copper losses from the no-load input power, the resulting constant losses (iron + mechanical losses) were plotted against the square of fundamental voltage to obtain the friction and windage losses at near-synchronous speed. As reported in Fig. 8.2, the value of friction and windage losses obtained from the fundamental measurements in a PWM supply no-load test on the 55kW motor were very similar to the value obtained with a sinusoidal supply. The same trend was observed in the other two motors.

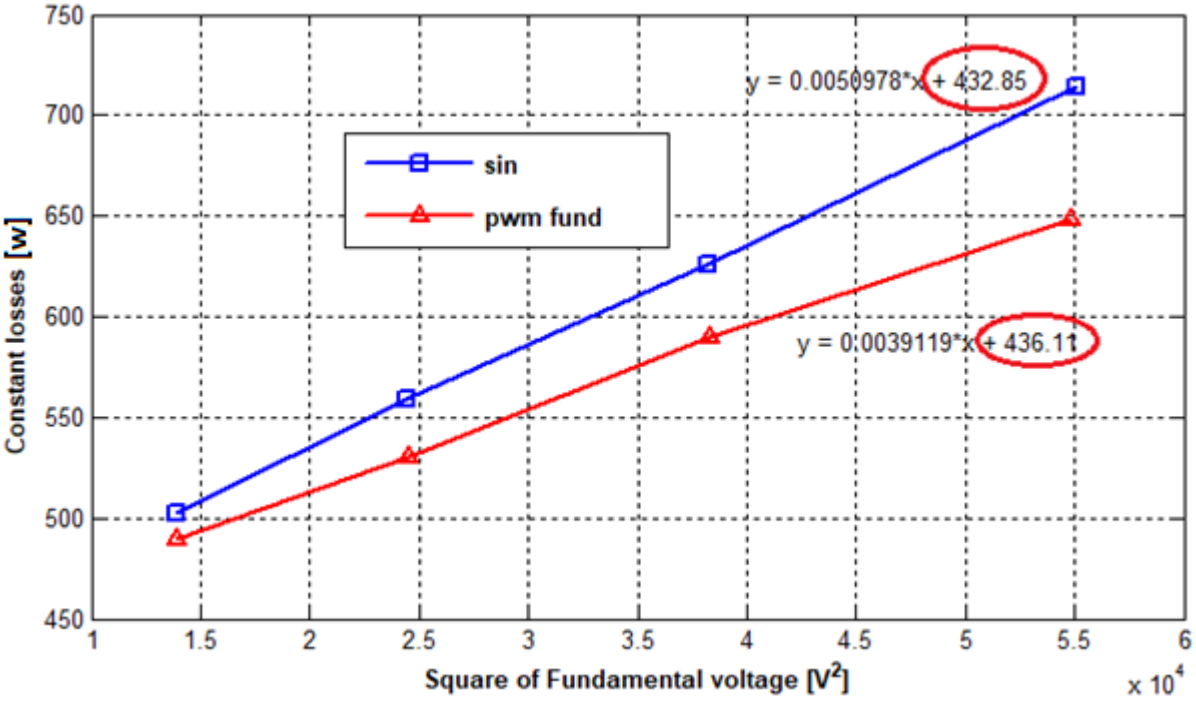

Fig.8.2 Determination of mechanical losses from sinusoidal and PWM supply fundamental measurements

8.1.2 Fundamental motor losses on load

The conventional iron losses were obtained by subtracting the mechanical losses reported in Fig. 8.2 from the constant losses. To account for the effects of loading, the corrected iron losses were evaluated by plotting the conventional iron losses against voltage (from 110% to 90% of rated value) as discussed in section 4.1.4. Using an interpolation technique in MATLAB, the iron losses corresponding to the magnetizing branch voltage at each load point in the sinusoidal supply and the fundamental measurements in a PWM supply test are reported in Table 8.1. Although the magnetizing branch voltages obtained using the two supplies were equal, the iron losses obtained using the fundamental measurements in the PWM supply test were about 6 to 7 percent lower due to the lower value of the measured fundamental input power with respect to the sinusoidal supply. This was reported earlier in Table 7.3 (footnote).

Table 8.1 55kW motor iron losses obtained from sinusoidal and fundamental pwm supply test data

%Load	$P_{iron,\ sine}$ [W]	$P_{iron,\ fund}$ [W]	Δ [%]
150	661.98	622.02	-6.0
125	673.12	633.86	-5.8
100	685.07	642.24	-6.3
75	694.99	653.43	-6.0
50	710.50	662.02	-6.8
25	719.03	668.13	-7.1

Considering the rating of the motor (55kW), the differences in the values of the corrected iron losses obtained with the two supplies were generally inconsequential in the final determination of motor efficiency as only a minor difference was observed at the lowest load point. This will be highlighted later in this section when the efficiency plots are presented. Interestingly, the 37kW and 45kW motors produced practically equal values of iron losses.

Analysis of the load test results presented in Table 7.4 - 7.5 revealed that the stator current in the sinusoidal supply test and the fundamental component in the PWM supply test were practically equal. Therefore, similar values of corrected stator copper losses were obtained – save for negligible differences due to temperature effects. Similarly, the rotor copper losses in the two sets of tests were also found to be in agreement. Fig. 8.3 reports the corrected stator and rotor copper losses in the 55kW motor obtained from sinusoidal supply and fundamental measurements in the PWM supply load tests as a function of load torque. Note how the graphs from the two supplies overlap. Similar results were also reported in the other two motors.

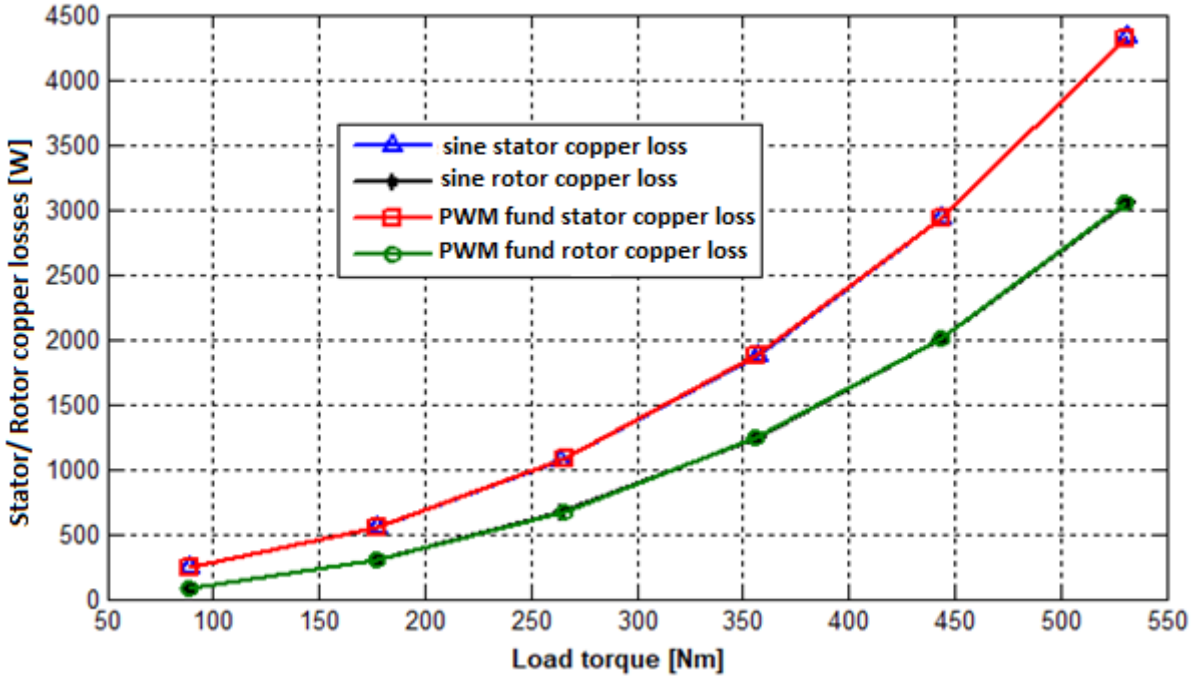

Fig.8. 3 corrected stator and rotor copper losses from sinusoidal and fundamental PWM measurements

As discussed in section 4.1.5, the residual losses were obtained by subtracting the conventional losses from the difference between the input and mechanical power. Here, the uncorrected stator and rotor losses were used while the mechanical losses were corrected to the operating slip. The residual losses obtained were then plotted against the square of load torque and smoothed by linear regression to obtain the slope constants. The stray load losses (SLL) were obtained for each load point by multiplying the slope constant by the square of load torque. Fig 8.4 reports the obtained SLL against the square of load torque for the two supplies.

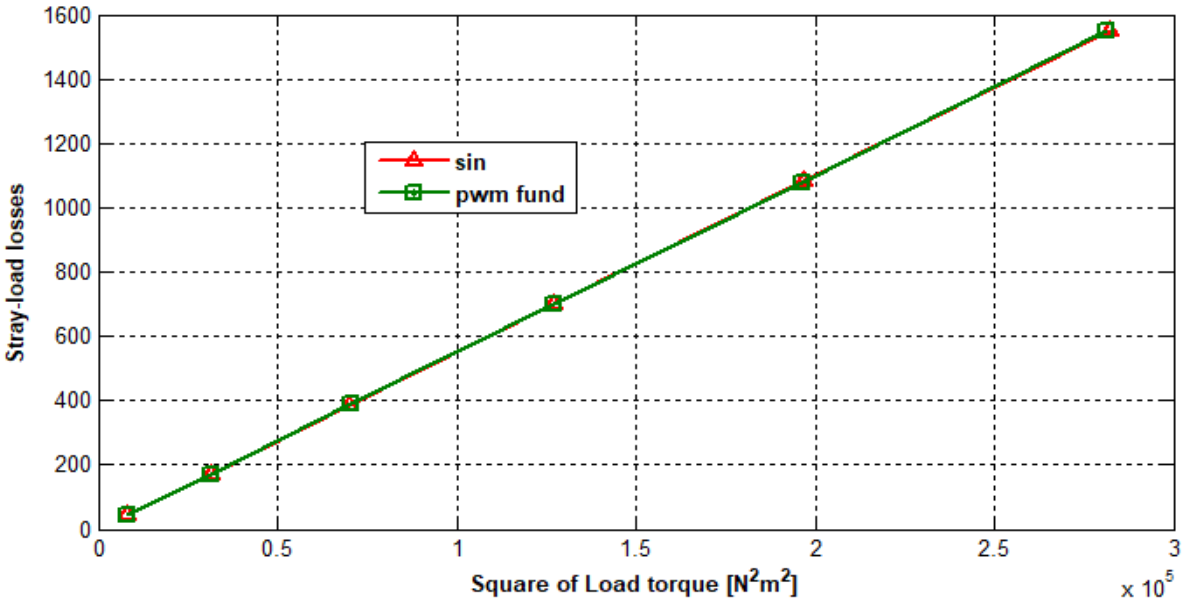

Fig.8.4 Stray load losses on sinusoidal and fundamental pwm supply measurements

As shown in Fig. 8.4, the stray-load losses obtained using test data from the sinusoidal supply and the fundamental measurements in the pwm supply were equal. The same trend was also reported in the 37kW and 45kW motors – any differences obtained were insignificant and can generally be attributed to tolerances in the measurement of various test quantities. Collating all the motor losses from the sinusoidal and fundamental PWM supply measurement data, it was found that their magnitudes were approximately equal for the two supplies used. Therefore, the pie-chart in Fig. 8.5 reports the distribution of losses in the 55kW motor at rated load on sinusoidal supply. As expected, these loss contributions are within the expected allocations discussed in Table 3.1.

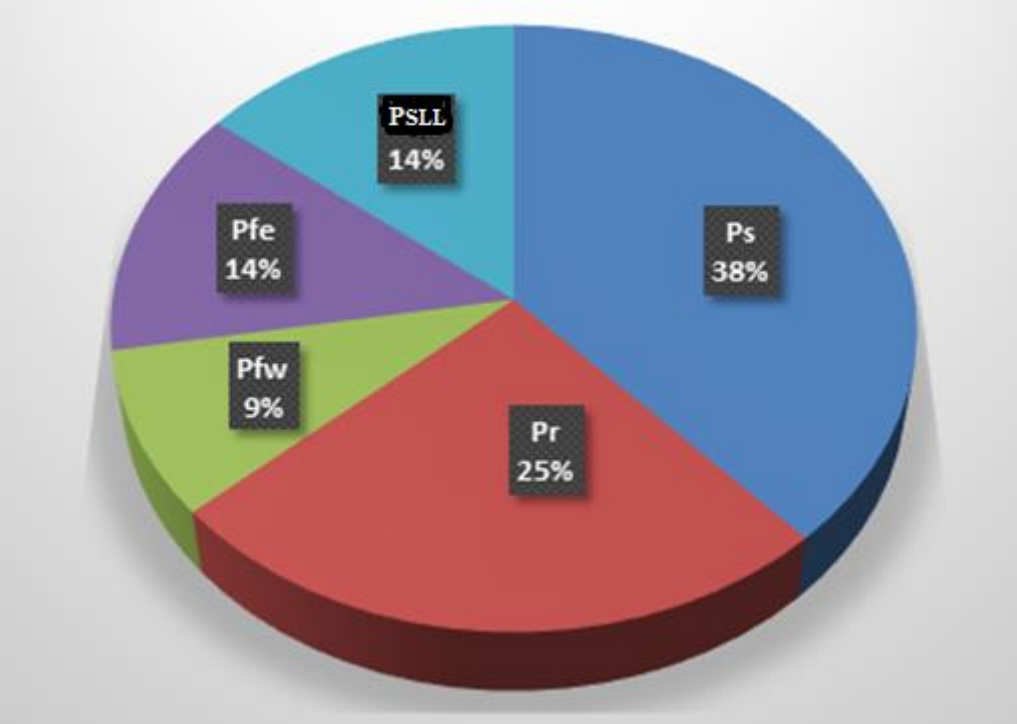

Fig.8.5 Distribution of sinusoidal supply losses in the 55kW motor at rated load

The efficiency results obtained from sinusoidal supply and PWM supply tests – taking only the measured fundamental quantities in the loss segregation analysis – are reported in Fig. 8.6 – 8.8. It is interesting to observe that both the direct and indirect efficiency results obtained from the fundamental quantities measured during a PWM supply test are very close to the sinusoidal supply values. For the 55kW motor, the minor difference in the indirect efficiency at the lowest load point, reported in Fig. 8.6, can be attributed to the difference in the obtained iron losses which was discussed in Table 8.1. This is because the contribution of the iron losses to the total motor losses is highest at the lowest load point, when stator and rotor losses are

minimum. Similar trends were obtained in the 45kW and 37kW motor efficiencies as reported in Fig 8.8 and 8.9, respectively. These results lead to the conclusion that a VFD can be used to estimate, with sufficient accuracy, the sinusoidal supply induction motor efficiency.

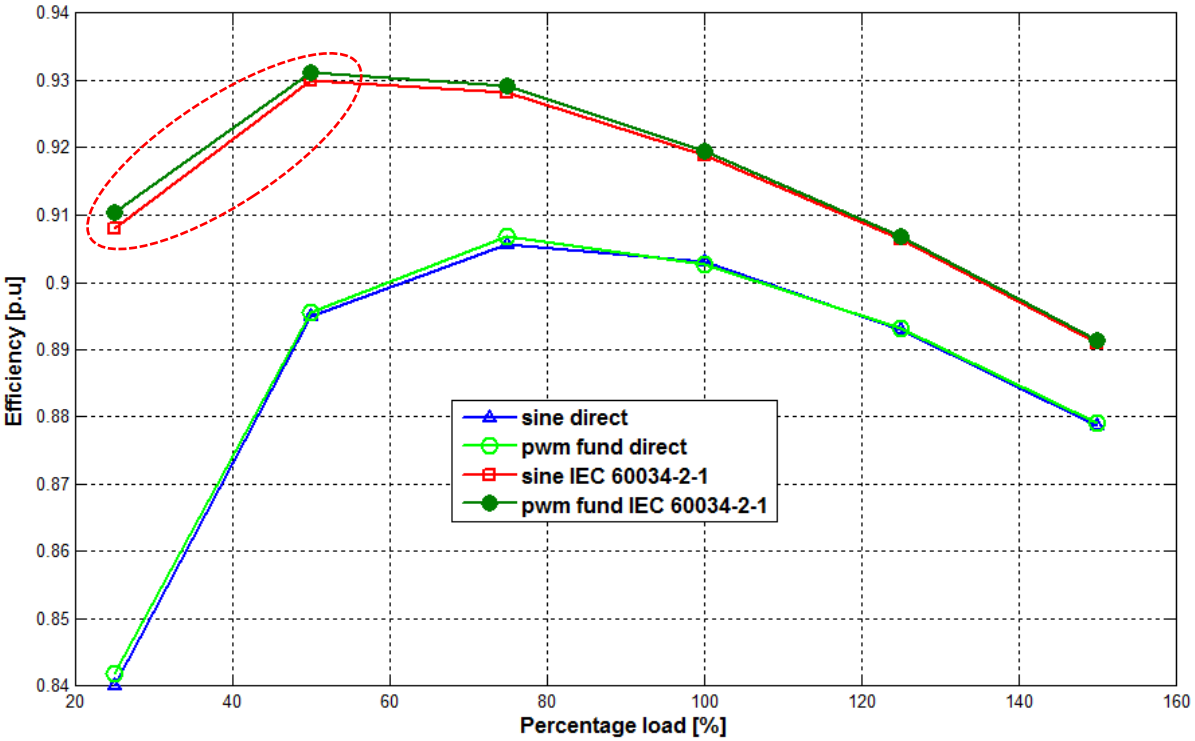

Fig.8.6 55kW motor efficiency determined from PWM supply fundamental measurements

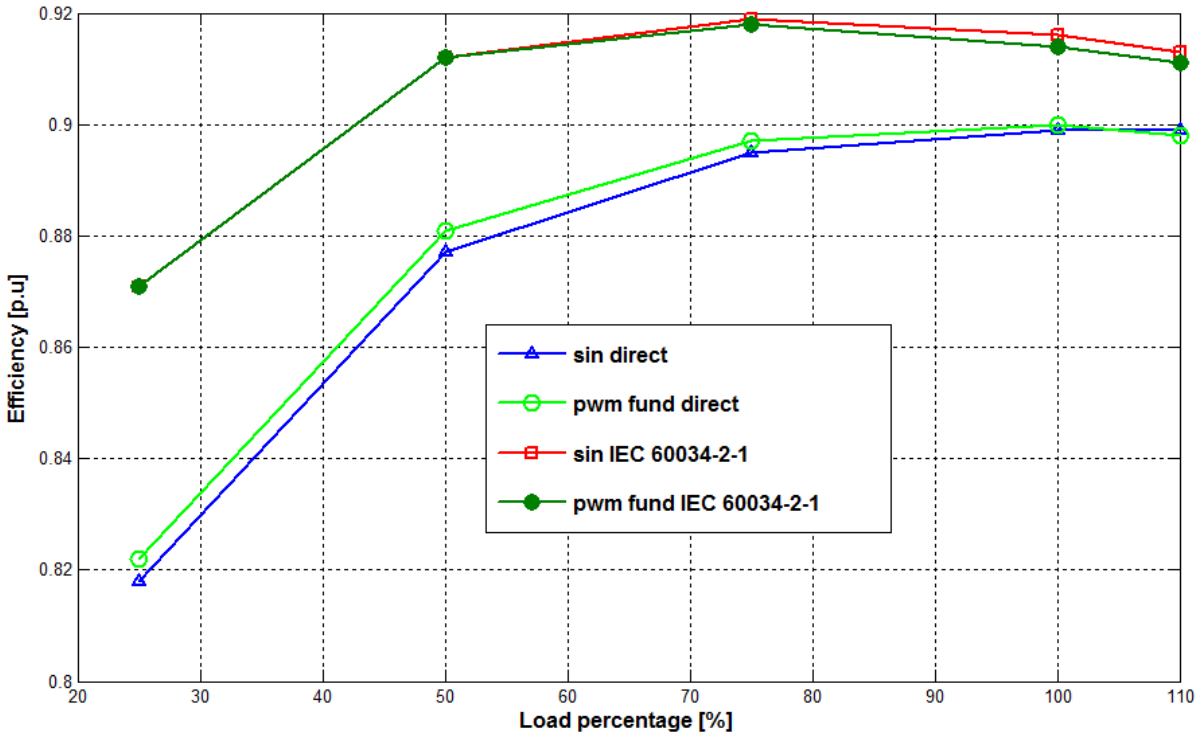

Fig.8.7 45kW motor efficiency determined from PWM supply fundamental measurements

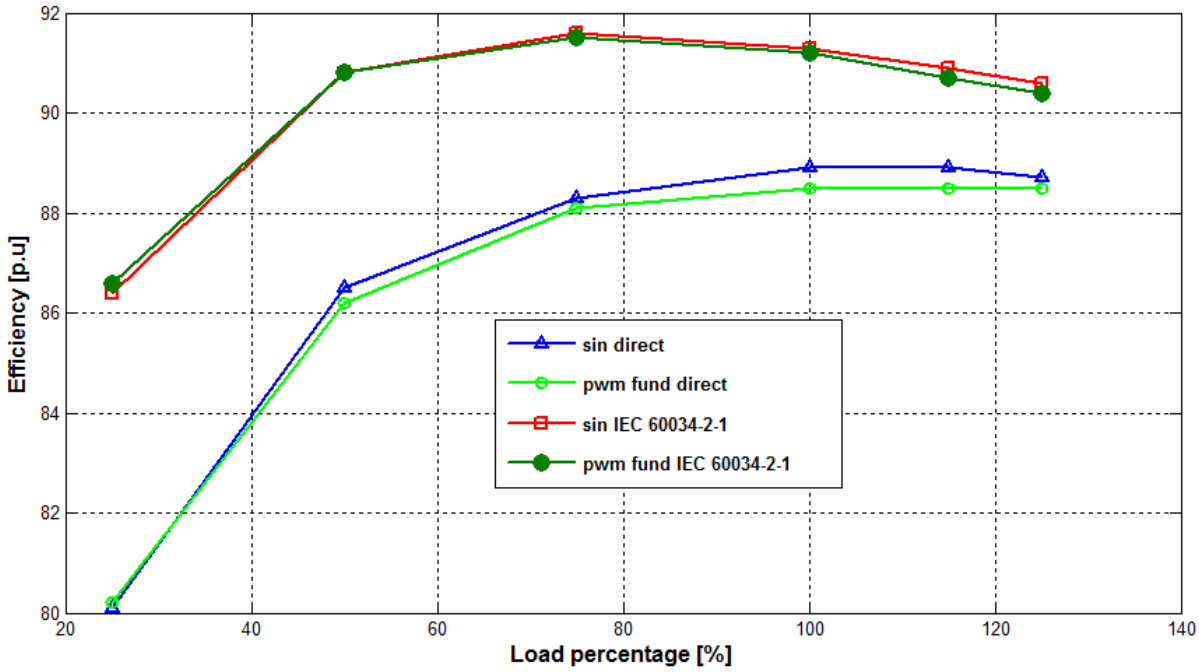

Fig.8.8 37kW motor efficiency determined from PWM supply fundamental measurements

The above set of results is interesting as it corroborates the assertion that harmonic components do not contribute to the average (useful) power in the machine [3]. The results also highlight an improvement on the work presented in [14] in which the author proposed an approximate method for determining the sinusoidal supply efficiency of an induction motor by applying a 500Hz line filter to PWM supply power measurements, taking the sinusoidal supply current as a reference. The problem with the proposed procedure was that it introduced a huge error at the low load points owing to the mismatch in load torque, despite the sinusoidal and PWM currents being well-matched. The challenge in using the load current as a reference is that the converter-fed motor's torque capability is significantly reduced at the lowest load owing to the huge contribution of the harmonic losses. Therefore, as shown above, the use of load torque is a more accurate approach.

The determination of sinusoidal supply efficiency using a VFD is a very interesting development. Whereas conventional motor testing requires a variable-voltage sinusoidal supply for the no-load test, the use of a PWM supply adds flexibility to the efficiency testing process. This can also be utilized in field testing applications where there is likely to be a VFD than a variac. Furthermore, since the proposed IEC/TS procedure for determining converter-fed efficiency first requires a sinusoidal supply test, the above development can potentially eliminate the need to physically perform a sinusoidal supply test. This is because both the fundamental and additional harmonic motor losses can now be estimated by performing one

set of tests with a PWM supply. This can potentially eliminate possible mismatches in loading as well as voltage and frequency variations between the required sinusoidal and PWM supply load tests.

8.2 CONSIDERATIONS IN THE DETERMINATION OF HARMONIC LOSSES

The difficulty in the accurate measurement of voltages under PWM supply, and the relative newness of the IEC/TS procedure makes the determination of harmonic losses a dauting task. While the method itself may be valid, some guidance must be provided to various stakeholders on some of the incorrect testing practices. This section demonstrates some of the technical issues encountered when testing the practical applicability of the IEC/TS.

8.2.1 Converter-fed motor losses on no-load

As was discussed in section 2.1.1, the plot of constant losses against the square of voltage, obtained by performing a PWM supply no-load test at a constant modulation index (varying the DC bus), results in a linear relationship like the one that was reported in Fig 8.2 with a sinusoidal supply. As reported in [15], this approach yields mechanical losses comparable to those obtained from a sinusoidal supply test. However, the plot of constant losses at variable modulation index (constant DC bus) is non-linear as reported in Fig. 8.9. This is due to increased iron losses at lower modulation indices, caused by higher voltage distortion (THD) at the lower voltages. This scenario presents challenges in the separation of constant losses into iron and mechanical losses.

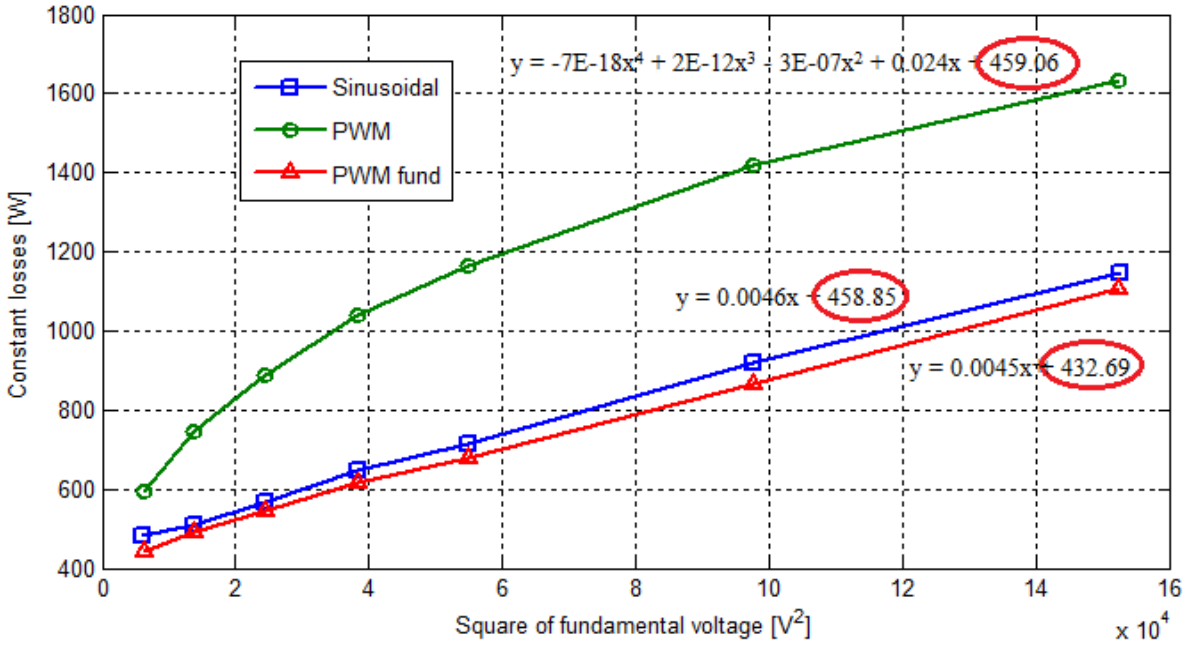

Fig.8.9 Determination of mechanical losses on PWM supply using 4th order polynomial fitting method

Although [49] proposes a 4th order polynomial fitting method to obtain mechanical losses at the zero-voltage intercept, this approach cannot be used with the IEC 60034-2-1; 2014 standard which strictly specifies four voltages between 30% and 60% of rated motor voltage. These four voltages are insufficient to produce a polynomial that accurately covers the non-linear plot of constant losses. Therefore, since there is no mechanical evidence or any scientific explanation why the mechanical losses would vary with the power supply, the only logical approach was to use the same value of mechanical losses obtained from the sinusoidal supply test. However, it must be reported here that the 4th order polynomial fitting method produced expected results when it was applied to a set of PWM no-load test data for the same 55kW motor, obtained using the older IEC 60034-2-1; 2008 standard test voltages. This was after discarding the highest no-load voltage from the curve, before fitting with the polynomial as shown in Fig. 8.9. Therefore, the approach seems feasible, albeit with some minor tweaks.

By subtracting the mechanical losses from the constant losses on PWM supply, the resulting conventional iron losses were plotted against fundamental voltage as reported in Fig.8.10. As shown in this figure, the increase in conventional iron losses between the sinusoidal and PWM supply is due to the harmonic losses and is the main reason for the degradation in motor efficiency under PWM supply. To accurately quantify these harmonic losses, the IEC/TS provides a method that accounts for the temperature variation between the sinusoidal and PWM no-load tests as discussed below:

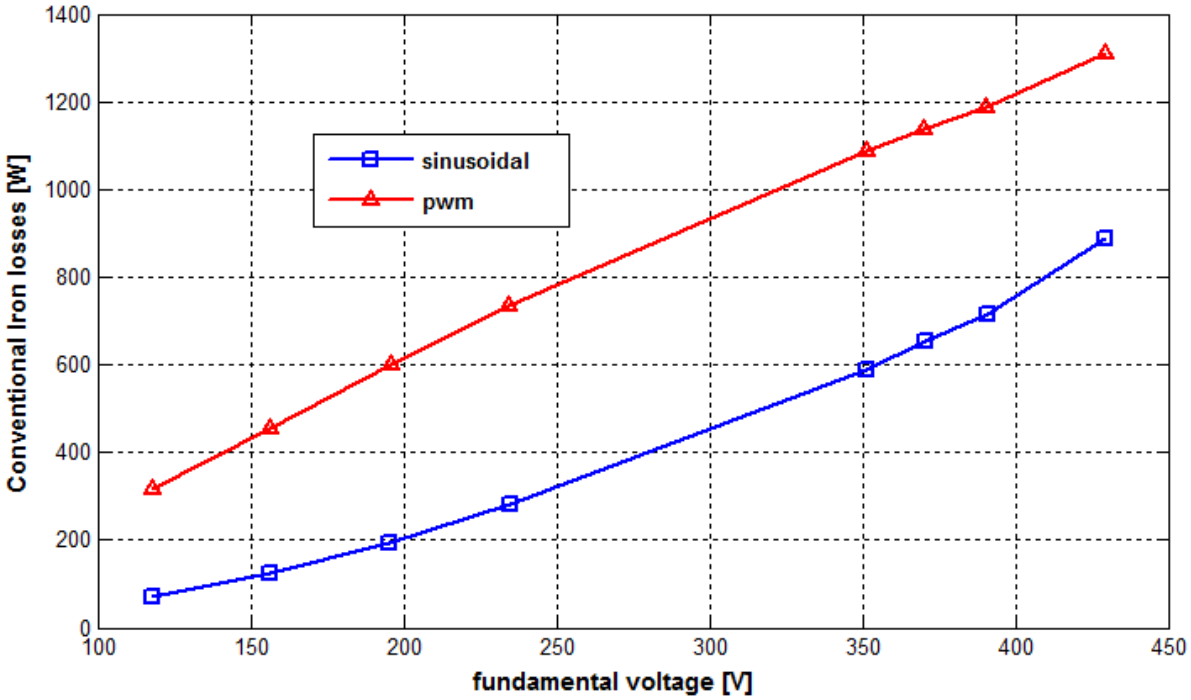

Fig.8.10 55kW motor no-load iron losses on sinusoidal and PWM supply

As discussed in section 4.2.1, the constant (load-independent) harmonic loss component is determined by subtracting the constant losses obtained with a sinusoidal supply from the constant losses obtained with a PWM supply at the rated voltage. Removing the stator copper loss from the determination of the harmonic losses ensures any temperature differences during the two no-load tests are taken care of. Obviously, this approach assumes the same value of mechanical losses between the sinusoidal and PWM supply tests.

Using modern power analysers, like the Genesis 7i used in this study, the harmonic loss can also be directly estimated by subtracting the measured fundamental input power from the 'total' (unfiltered) input power measured during a PWM supply no-load test at rated fundamental voltage. Using these two approaches described above, the constant harmonic losses were evaluated. The measured experimental data at rated fundamental voltage used in the calculation of the constant additional harmonic losses is reported in Table 8.2.

Table 8.2 Measured no-load operating parameters of 55kW motor at rated fundamental voltage

Supply	Temp [°C]	Voltage [V]	Current [A]	Power [W]	Fund Power [W]
Sine	101.9	390.9	26.01	1263.5	1262.9
PWM	93.3	390.4	26.00	1734.5	1210.1

IEC determination of constant harmonic losses:

$$P_{HL\,no-load} = P_{k\,pwm} - P_{k\,sin}$$

$$P_{HL\,no-load} = (P_{1\,pwm} - P_{s\,pwm}) - (P_{1\,sin} - P_{s\,sin})$$

$$P_{HL\,no-load} = (1734.5 - 3 \times 26.00^2 \times 0.1119) - (1263.5 - 3 \times 26.01^2 \times 0.1148)$$

$$P_{HL\,no-load} = 1507.6 - 1030.5$$

$$\boldsymbol{P_{HL\,no-load} = 477.1\mathbf{W}}$$

Estimated constant harmonic losses using power analyser:

$$P_{HL\,no-load} = P_{k\,pwm} - P_{k\,sin}$$

$$P_{HL\,no-load} = 1734.5 - 1210.1$$

$$\boldsymbol{P_{HL\,no-load} = 524.1\mathbf{W}}$$

From the above calculations, it was found that the harmonic losses 'measured' using the power analyser were 47W higher than the value obtained using the IEC/TS recommended method. However, this difference which translates into a loss 9% increment, is small as it is only about 2% of the absorbed no-load power. Moreover, there was a 10°C loss of temperature between the sinusoidal and pwm supply no-load tests (reported in Table 7.3), which might have slightly impacted the results. Therefore, the use of the power analyser to provide a first approximation of the constant harmonic losses is feasible as it allows for a quick assessment of the additional motor losses due to non-sinusoidal supply. It is important to note that only the value obtained at the nominal voltage is used in the final determination of efficiency since the load-curve test is performed at rated motor voltage.

8.2.2 Converter-fed motor losses on load

In addition to the sinusoidal supply load test, two load tests were performed with a PWM supply as described in section 7.3.2. The first PWM supply test was performed with the fundamental motor voltage closely matching the value obtained during the sinusoidal supply test, to account for the reactor voltage drop. This is hereafter referred to as the *matched PWM* test. The other test was performed with the voltage parameter in the VFD set to the nominal sinusoidal voltage value, which is usually the case in industrial VFD operations, and is hereafter referred to as the *unmatched PWM*. This means that the voltage drop across the reactor was not accounted for, hence the motor terminal voltage was slightly lower than the value used in the sinusoidal and matched PWM supply tests. As more stakeholders are getting involved in converter-fed motor efficiency estimation, this failure to regulate the converter-fed motor terminal voltage is one potential mistake that testing personnel must avoid.

As expected, analysis of the load test results presented in Table 7.6 – 7.7 revealed that the stator current during the sinusoidal and matched PWM tests was approximately equal. However, the unmatched PWM test recorded slightly higher currents owing to its lower terminal voltage. This is because the lower motor terminal voltage due to the reactor voltage drop results in reduced voltage at the magnetizing branch. This effectively reduces the airgap flux and hence the motor's torque capability. Therefore, for a given load torque, the motor draws more power from the PWM supply to overcome the increased stator and rotor copper losses reported in Fig. 8.11. As the loading is reduced, the reactor voltage drop becomes less, increasing the airgap flux. Therefore, as the required motor torque becomes small, the stator current and hence copper losses begin to match the sinusoidal and matched PWM supply tests.

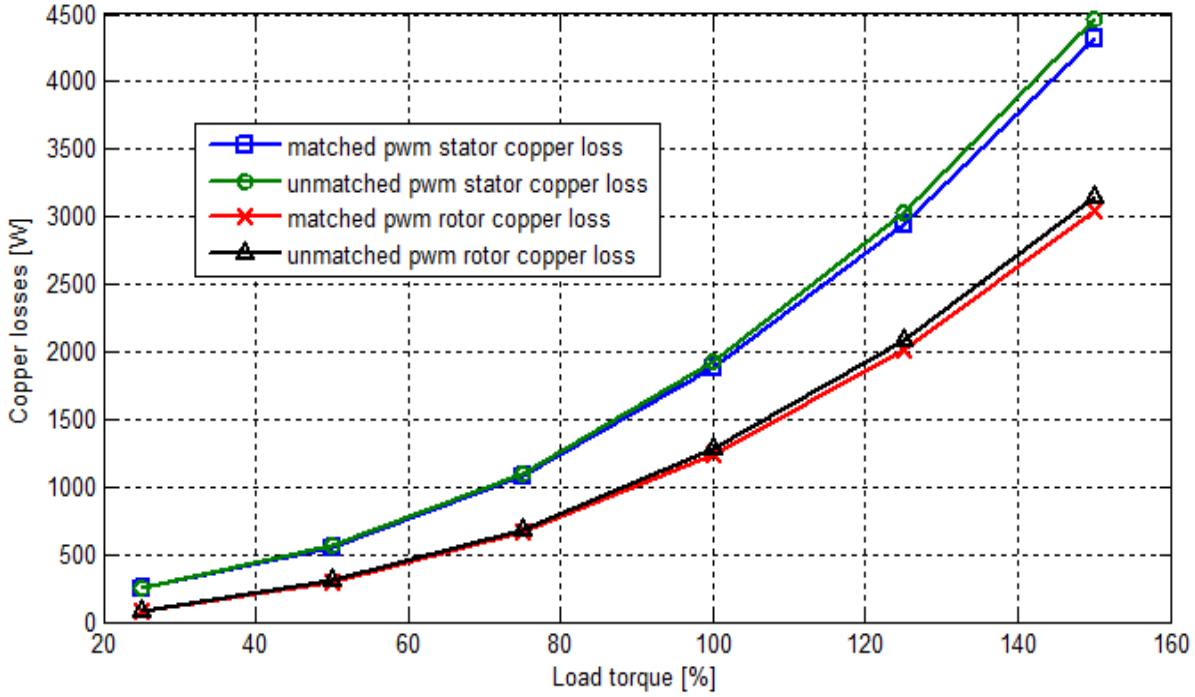

Fig.8.11. Increase in stator and rotor copper loss due to lower fundamental motor voltage

Whereas the sinusoidal and matched PWM tests yielded similar values of stator copper losses, there was a 2.5 to 3 percent increment in the unmatched PWM stator losses between full-load and 150 percent load. Since the slip values in the three cases under consideration, were consistent, a similar trend was reported in the rotor copper losses, also shown in Fig. 8.11. Note that the stator and rotor copper losses on sinusoidal supply have not been included in Fig. 8.11 since they perfectly overlapped with the matched PWM.

Although the above results demonstrate how the voltage drop across output reactors can lead to an increase in stator and rotor copper losses, it is important to realize that output reactors generally lead to reduced harmonic losses in the motor. However, the discussion presented here focusses on their impact on the proposed IEC/TS efficiency testing procedure – not on their overall harmonic loss reduction capability on an induction motor.

From the graph of no-load iron losses presented in Fig. 8.10, the iron losses on load were evaluated by fitting the four higher voltage points with a suitable polynomial, and interpolating the value corresponding to the magnetizing branch voltage at each load point. Since the iron losses increase with magnetizing voltage, the matched PWM load test reports slightly higher iron losses, about 1% more, than the unmatched PWM test owing to the lower magnetizing branch voltage in the later. Although iron losses are generally considered constant, Fig. 8.12 highlights their slight variation with load torque as was discussed in section 4.1.4.

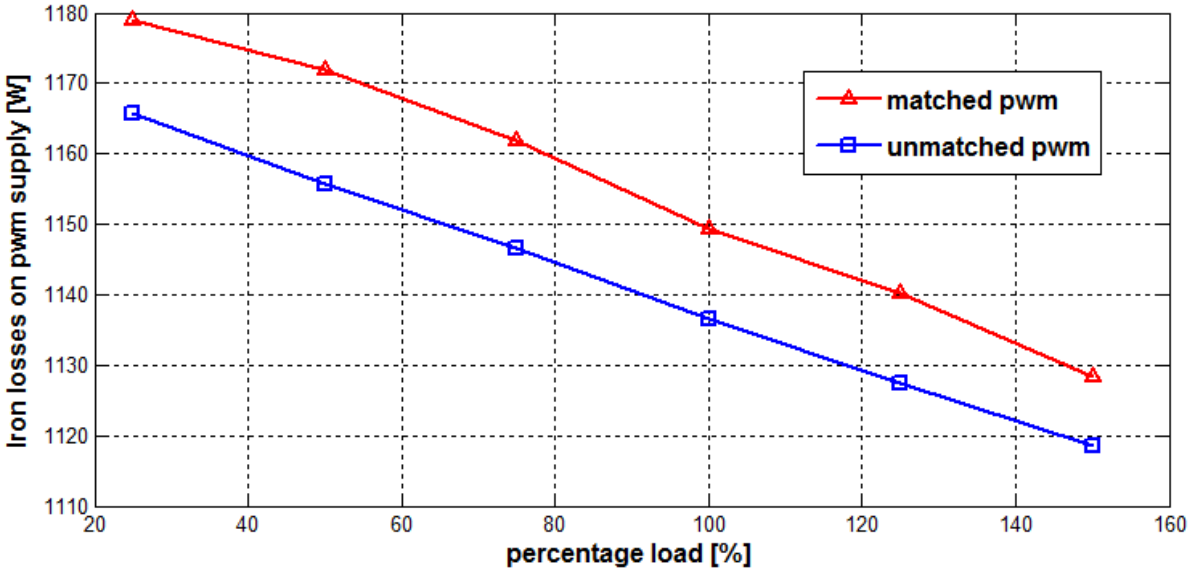

Fig.8.12 Variation of iron losses with load on PWM supply using IEC 60034-2-1 methodology

In the IEC/TS, the determination of stray-load losses is a very important stage in the analysis. This is because the increase in these losses from their sinusoidal supply value gives the load-dependent additional harmonic losses. While this procedure is theoretically valid, the accurate determination of stray-load losses can never be guaranteed as these losses are not measured directly. For the three sets of load tests under consideration, the obtained stray-load losses are reported in Fig. 8.13.

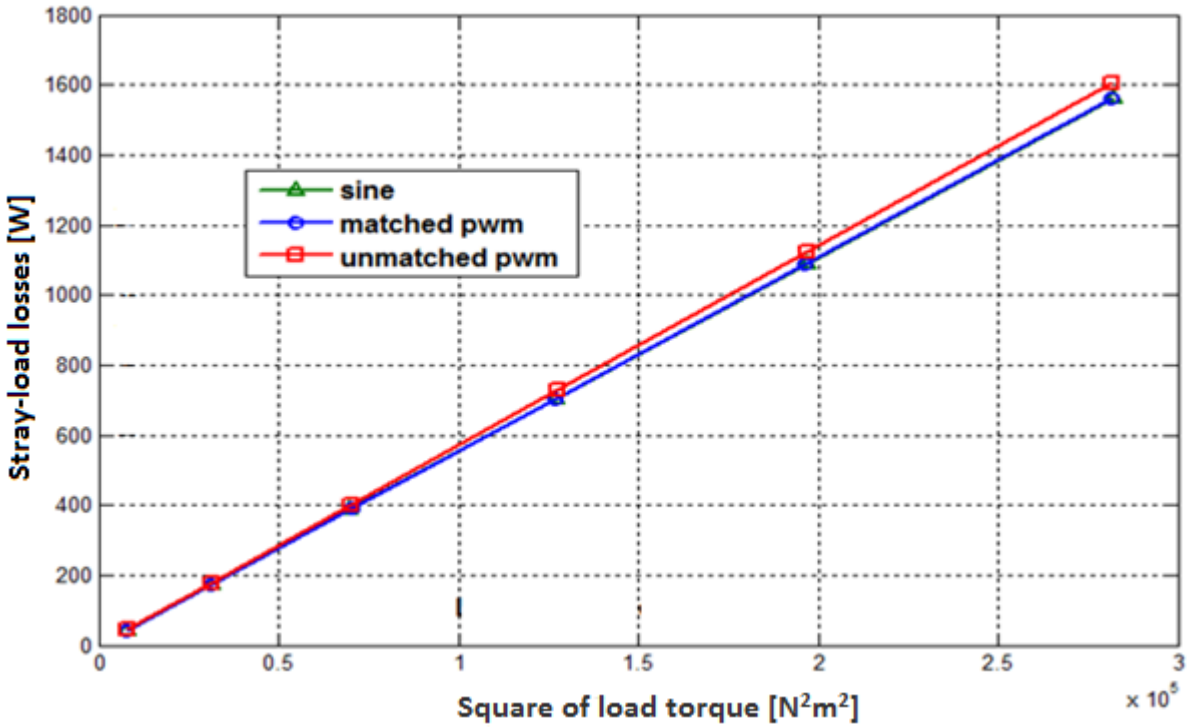

Fig.8.13 Stray load losses on sinusoidal and pwm supply

From Fig. 8.13, It is interesting to observe that the stray-load losses obtained in the sinusoidal and the matched PWM supply tests were approximately equal (shown overlapped on the graph). Only the unmatched PWM supply test resulted in an increase of about 2 to 3 percent from the sinusoidal supply value at each load point. Since these load-dependent additional harmonic losses are evaluated by subtracting the stray-load losses on sinusoidal supply from those on PWM supply, the above results lead to two contrasting conclusions:

Since there is no change in stray-load losses between the sinusoidal and matched PWM tests, the results suggest that there is no load-dependent component of harmonic losses. Thus, the harmonic losses considered in the determination of efficiency are only those obtained from the no-load test at rated voltage. On the other hand, the unmatched PWM test shows an increase in stray-load losses over the sinusoidal supply value, suggesting finite values of load-dependent additional harmonic losses at each load point. However, as discussed already, this increase in stray-load losses is due to the higher input power caused by a mismatch in fundamental voltage between the sinusoidal and PWM supply tests. Moreover, given the size of motor, these loss values are so small that they can be considered well within the measurement tolerances.

Based on the above two sets of results, it is clear that the adopted testing methodology, in particular regarding fundamental motor voltage, can easily influence the obtained harmonic loss values. Moreover, any measurement errors or mismatch in test conditions can also influence the stray-load losses. Nevertheless, in all three motors tested, the difference in stray-load losses was minimal. Therefore, the obtained load-dependent harmonic losses were very small and generally accounted for about 1% of the total motor losses. In fact, neglecting them was inconsequential in the three motors tested. Perhaps a first-hand approximation or a rule-of thumb for determining the converter-fed motor efficiency is to simply add the constant harmonic losses determined on no-load to the sinusoidal supply losses at each load point.

The above discussion has demonstrated how different motor losses can be obtained based on the adopted testing methodology. However, despite these clear differences in the obtained losses, the final efficiency values obtained using the IEC/TS proposed methodology were similar, as reported in Fig. 8.14. This is because the proposed method uses the mechanical power and fundamental losses determined from the sinusoidal supply test – not the actual losses obtained in the PWM test. Therefore, the final efficiency obtained may not be a true reflection of the actual losses in the PWM supply test, if not well-performed. Perhaps this is why the IEC/TS procedure avoids such complications by taking sinusoidal supply losses as a reference.

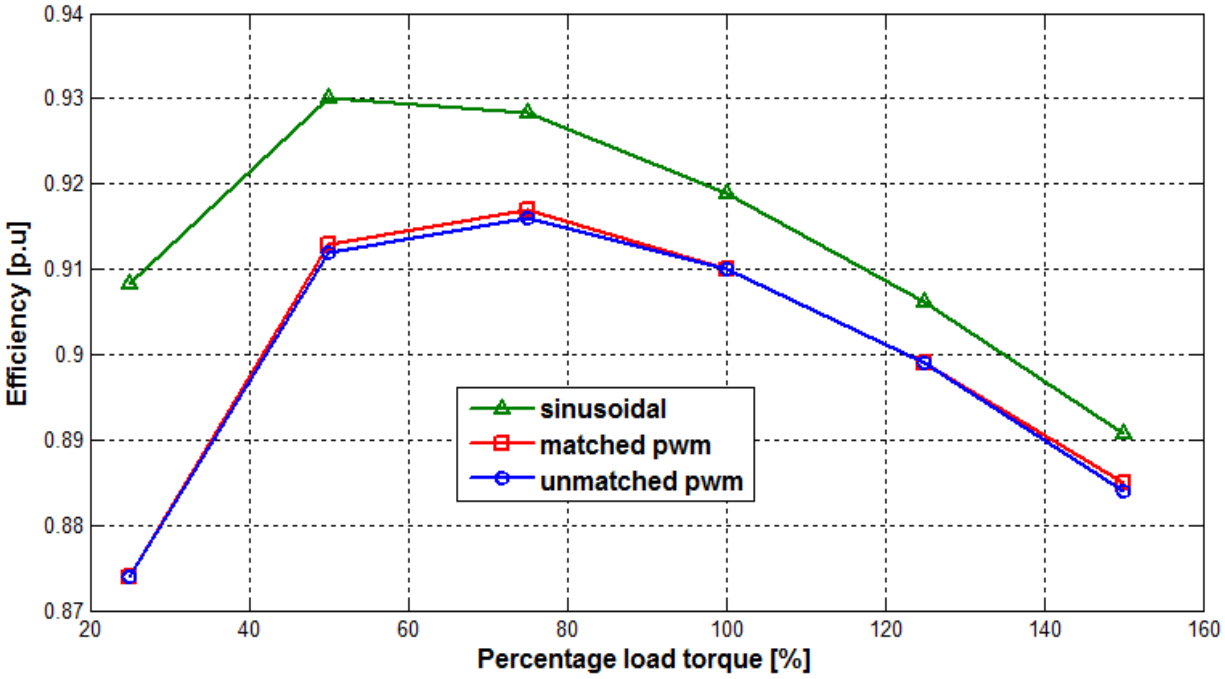

Fig.8.14 55kW motor PWM supply efficiency obtained using IEC/TS 60034-2-3 procedure

For the converter-fed motor efficiency determined according to IEC/TS to be considered accurate, the sinusoidal and PWM supply tests must be performed strictly under identical conditions of fundamental voltage, frequency, and load torque. However, given the complexities of practical testing and measurement of non-sinusoidal power quantities, the above conditions may be difficult to achieve, especially by a human operator.

For the three induction motors tested in this study, it was found that the converter-fed motor efficiency obtained using the already established IEC 60034-2-1 standard loss segregation was comparable to that obtained using the IEC/TS. The only major difference is that the harmonic losses are included in the iron losses. This is in agreement with [6] which demonstrated that the IEC 60034-2-1 standard is sufficient for estimating converter-fed motor efficiency. The advantage of using this standard is that it accurately captures the actual losses of the motor on converter operation, regardless of any mismatch between the sinusoidal and PWM supply tests. Furthermore, it allows the incorporation of all recent improvements in the IEC testing methodology such as the correction of input power to a standard temperature of 25°C, which allows comparison of efficiency results performed at different ambient temperatures.

Using the IEC 60034-2-1 standard, the difference in converter-fed motor efficiency due to the mismatch in fundamental motor voltage is clearly reported in Fig. 8.15. As shown, the unmatched PWM efficiency was lower due to increased stator and rotor copper losses.

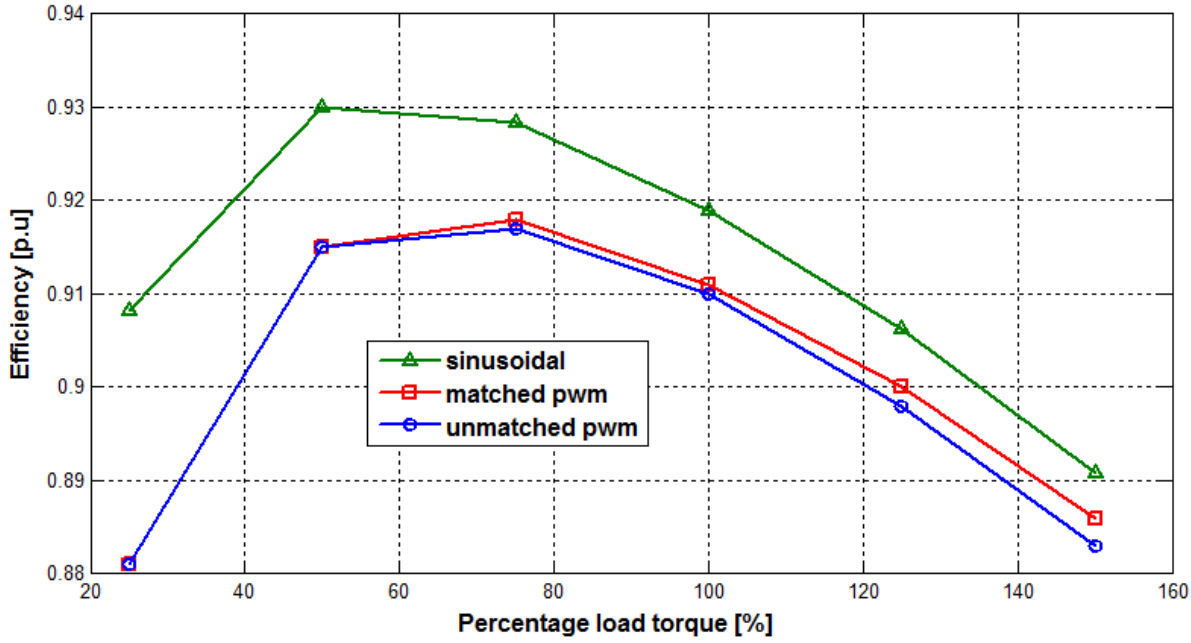

Fig.8.15 55kW motor PWM supply efficiency determined using IEC 60034-2-1 to highlight higher losses in unmatched pwm

8.2.3 Distribution of converter-fed induction motor losses and harmonic loss ratio

Despite the challenges highlighted in the previous section, the determination of converter-fed induction motor efficiency using the IEC/TS is feasible. Since the 37kW and 45kW motors showed a very small increment in stray-load losses between sinusoidal and PWM supply, the results generally suggest that the converter harmonics have very little or no impact on the stray-load losses. Therefore, the decrease in motor efficiency due to PWM supply is mainly caused by the constant harmonic losses, or simply the increase in iron losses.

Converter-fed induction motors can be ranked in terms of their harmonic loss ratios. The harmonic loss ratio, according to the IEC/TS, is the ratio of the total harmonic losses to the total sinusoidal supply losses, expressed to the nearest whole number. Therefore, motors optimized for operation with a converter supply are expected to have a low harmonic loss ratio.

The distribution of motor losses on converter supply is slightly different from the corresponding sinusoidal supply loss distribution. While actual magnitudes of the mechanical losses, stator and rotor copper losses normally remain unchanged between sinusoidal and converter supply, their relative percentages generally become lower owing to the increase in the total motor losses. The converter-fed motor efficiency, corresponding loss distributions and harmonic loss ratios of the 37kW and 45kW motors are presented in Fig. 8.16 to 8.19.

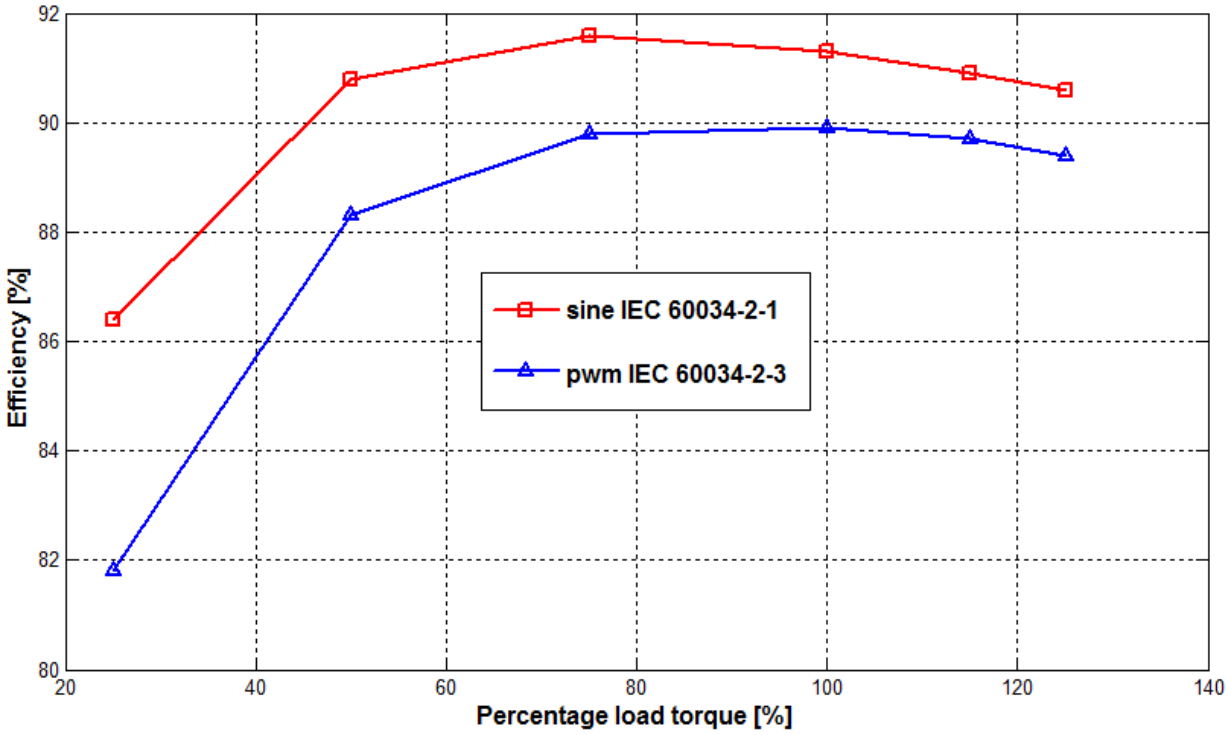

Fig.8.16 37kW Motor efficiency on PWM supply obtained using IEC 60034-2-3

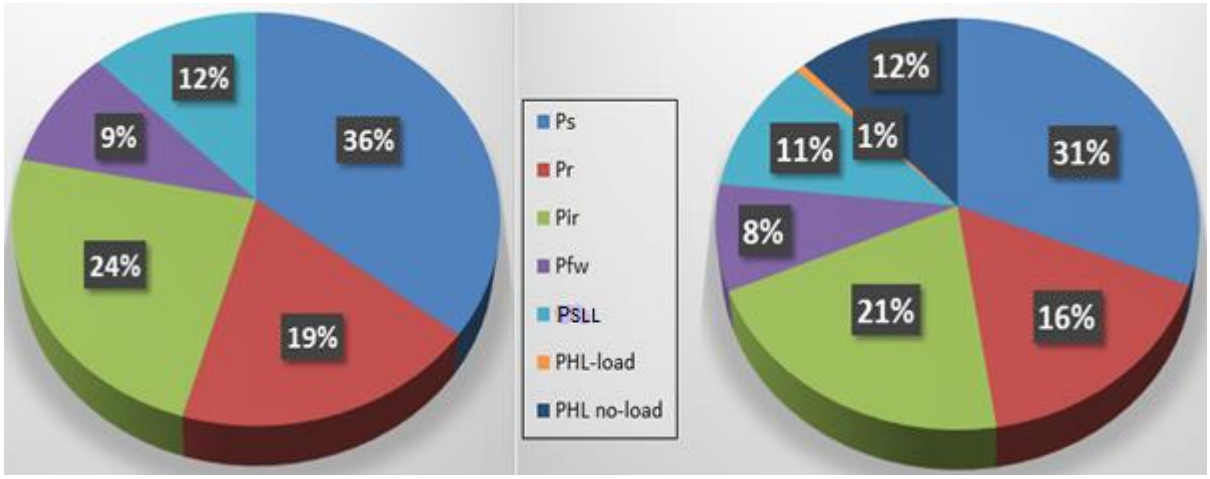

Fig.8.17 comparison of 37kW motor loss distribution on sinusoidal (left) and PWM supply (right)

$$Harmonic\ loss\ ratio, r_{HL} = \frac{P_{HL}}{P_{T\,sin}} \times 100 = \frac{(494.35+27,27)}{3641.48} \times 100 = \mathbf{14}\%$$

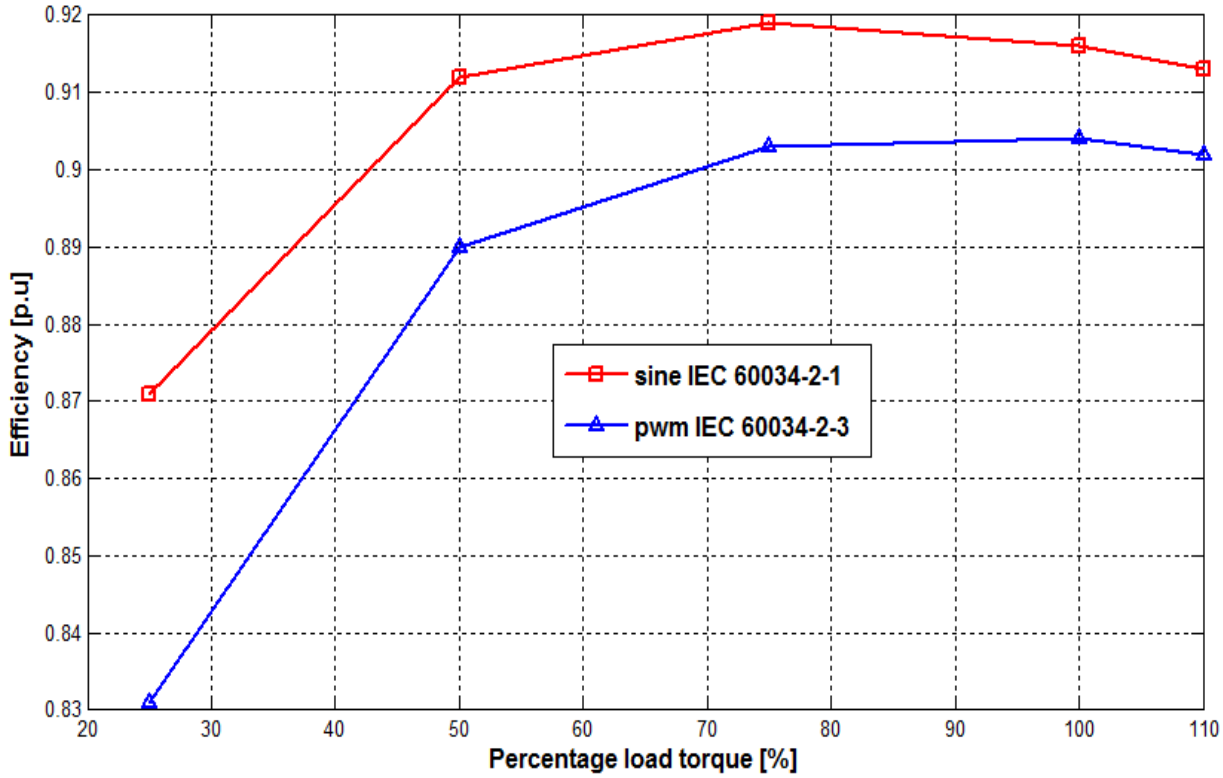

Fig.8.18 45kW Motor efficiency on PWM supply obtained using IEC 60034-2-3

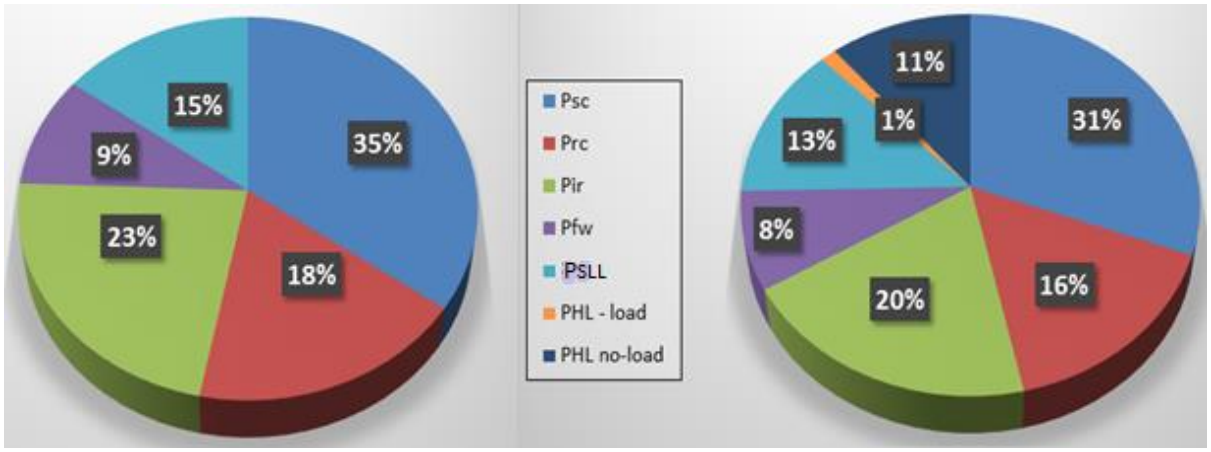

Fig.8.19 comparison of 45kW motor loss distribution on sinusoidal (left) and PWM supply (right)

$$Harmonic\ loss\ ratio, r_{HL} = \frac{P_{HL}}{P_{T\ sin}} \times 100 = \frac{(529.39+59.65)}{4224.29} \times 100 = \mathbf{14}\%$$

8.3 IMPROVEMENTS DUE TO AUTOMATED EFFICIENCY TESTING

The previous section has demonstrated some of the challenges in the determination of additional harmonic losses from a methodological point of view. It is therefore important for individuals performing the tests to fully understand the IEC/TS procedure. Obviously, one of the critical issues is the determination of stray-load losses. Since these losses are not directly measured but are simply obtained by smoothing the unaccounted-for losses, it is important to provide a method of testing that ensures the sinusoidal and PWM supply tests are performed identically, without any errors due to the human operator. In this section, the automated efficiency testing procedure discussed in chapter 6 was validated by comparing the results obtained with those from a manually performed test.

Experimental results obtained by testing a 55kW induction motor reveal some of the improvements that can be realized from the automated testing procedure over the manual approach. Although both testing methods produced similar efficiency results, the following discussion highlights some improvements in the overall quality of the test. As the motor losses and efficiency of the 55kW motor have already been covered in previous sections, they will not be repeated in this section.

8.3.1 Variation of winding temperature

One parameter that has a significant impact on the copper losses as well as the friction and windage losses is temperature. Although the load test is performed when the motor has attained thermal stability, different load torques demand different currents in the motor. Since the motor current is directly related to the temperature rise, as illustrated using short-time thermal models [50], the duration of the load test becomes an important consideration. Whereas the IEC 60034-2-1 standard stipulates that the load test must be performed as quickly as possible to minimize temperature changes, there is no specific guidance on what constitutes an acceptable temperature variation. Moreover, enough time must also be allowed for the system to achieve steady-state operation before measurements are taken.

The adjustment of load torque by hand (using some analogue means) often takes several seconds and may require some fine-tuning to get the required torque. The process can take even longer if the objective is to match torque values during tests performed with different supplies, resulting in significant temperature variations. The automated procedure on the other hand allows a quicker and consistent load torque adjustment, resulting in minimal temperature variation. As reported in Fig 8.20, the variation in winding temperature during the automated

load test with a PWM supply was only 3.3 ºC, compared to the 9.4 ºC reported in the manual test. Note that the initial (steady-state) winding temperature was 130ºC in both cases.

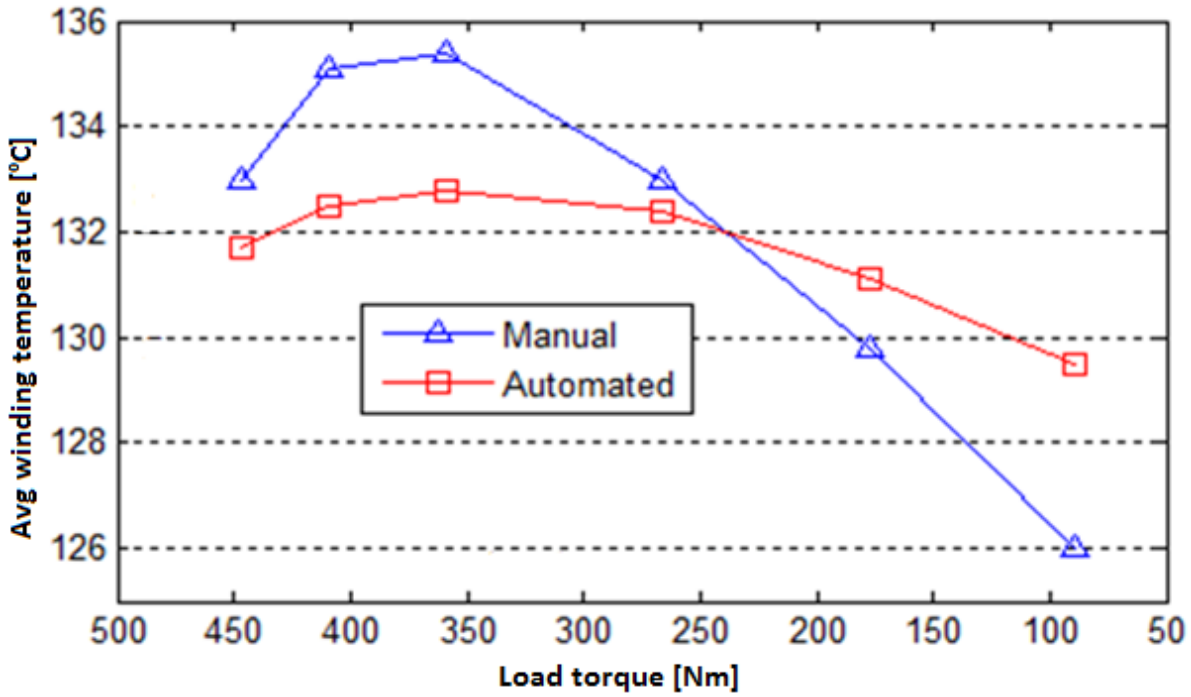

Fig.8.20 Comparison of temperature variation between manual and automated PWM supply load tests.

The reduction in temperature variation owing to the shorter duration of tests and a more uniform loading achieved with the automated testing procedure results in an improvement in the repeatability of test results. As reported in Table 8.3, the standard deviation in the corrected stator copper losses, expressed as a percentage of the mean, obtained from two consecutive manual load tests performed with a PWM supply was much higher than that obtained from two automated load tests on the same PWM supply. The lower value of standard deviation obtained from the automated tests highlights an improvement in the overall repeatability of test results. A similar trend was observed in other measured quantities such as winding temperature, motor current and load torque on both sinusoidal and PWM supply.

The results presented in Table 8.3 also show that the copper losses from the manual load tests are generally higher than those obtained from the automated test. This is more prominent at the higher load points and can be attributed to the higher temperatures associated with the manual loading process as highlighted in Fig. 8.20. Since the duration of the load test mainly depends on the technical skill and competence levels of the operator, the automated testing procedure clearly has an advantage over the manual approach. On the 110kW test rig used for this study, the manual loading process was particularly challenging because the analogue

torque control port is positioned far from the DAQ (as was shown in Fig.5.3). Thus, the operator constantly moves between the analogue torque port and the DAQ during the entire testing process. Therefore, the temperature variation during manual test reported in Fig. 8.20 could have been worse with an inexperienced operator. This is why the automated testing procedure can be a very useful tool for future research.

Given the size of motor under consideration, the difference in the stator and rotor copper losses between the automated and manual tests was minor and does not significantly affect the efficiency results. However, it has the potential to affect the stray-load losses and hence the load-dependent harmonic losses.

Table 8.3 Standard deviation in corrected stator copper losses during PWM supply load tests

Load [%]	Manual test			Automated test		
	Test 1 Ps [w]	Test 2 Ps [w]	Std. dev [%]	Test 1 Ps [w]	Test 2 Ps [w]	Std. dev [%]
125	3038.2	3014.1	0.4	3010.3	3021.2	0.2
115	2555.9	2539.6	0.3	2525.6	2531.5	0.1
100	1962.3	1935.6	0.7	1938.0	1943.4	0.1
75	1122.1	1138.0	0.7	1115.5	1118.9	0.2
50	579.7	587.7	0.7	572.4	572.8	0.0
25	257.8	258.0	0.0	258.5	258.5	0.0

8.3.2 Coefficient of correlation

As discussed in section 4.1.5, one indicator of how well an efficiency test was performed is the correlation coefficient, obtained from the graph of residual losses against the square of load torque. The higher this value is, the more reliable the test results are considered, and hence the stray-load load losses obtained. In fact, [11] requires a correlation coefficient (R^2 value) of 0.95 or better for a test to be considered satisfactory, adding that anything less than this value could be indicative of errors in the instrumentation or test readings, or both. When the correlation coefficient is less than 0.95, the worst point is deleted, and the regression is repeated. If this new correlation coefficient is still less than 0.95, then the test is unsatisfactory, and the source of error must be investigated and corrected before repeating the test.

From several tests performed in this study, higher values of correlation coefficient were reported in the automated tests over the manual tests as shown in Fig 8.21 – 8.22. Although the difference is minor in the cases presented, the higher correlation coefficient in the automated procedure still highlights an improvement in the overall quality of the test results. Nonetheless,

the high values of correlation coefficient obtained in the two sets of tests confirm that both were performed in a very satisfactory manner. Therefore, the development of the automated testing procedure is not meant to discredit the manual approach, but rather to mitigate the adverse effect of varying competence levels of the operator on efficiency results.

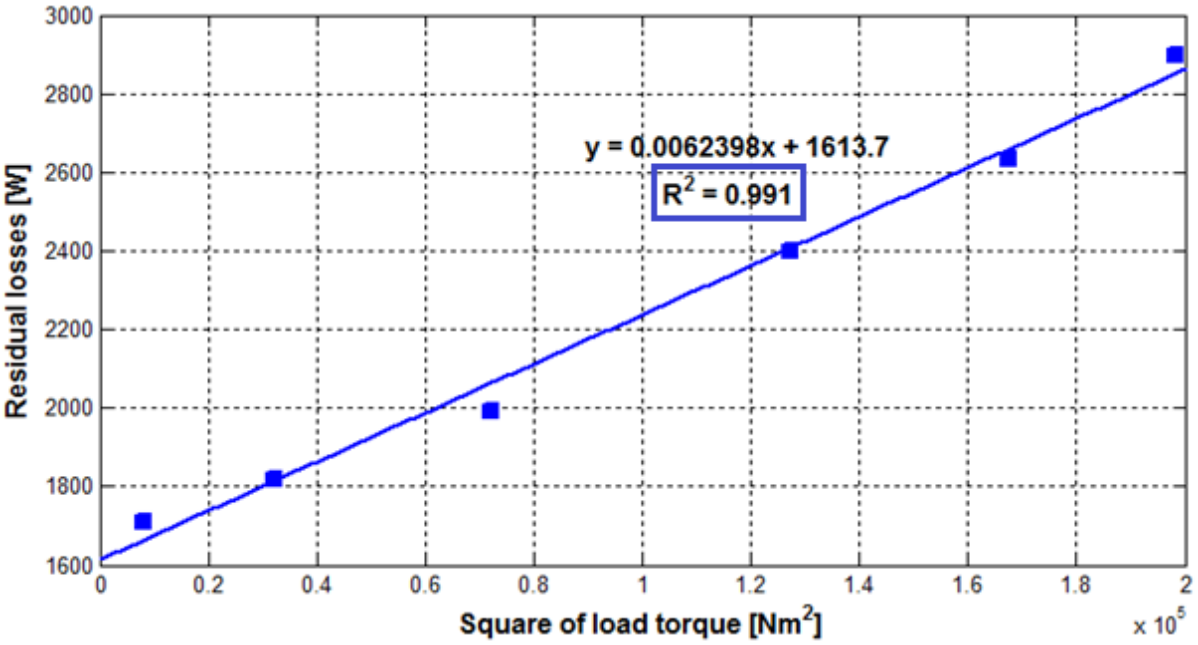

Fig.8.21 Correlation coefficient in the PWM supply manual efficiency test.

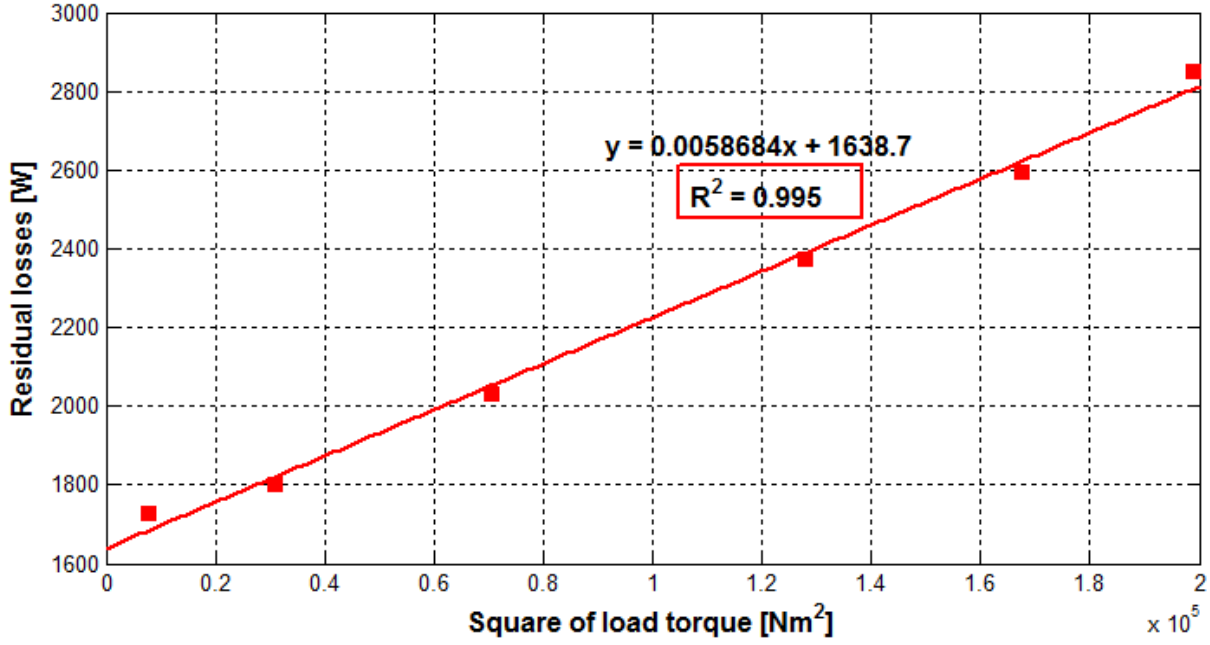

Fig.8.22 Correlation coefficient in the PWM supply automated efficiency test.

As shown in previous sections, manual tests are never ideal. Any mismatches in load torque or temperature variation between the sinusoidal and converter supply tests translates into a variation in stator and rotor copper losses, which later influence the stray-load losses. The same can be said about mismatches in fundamental frequency and motor terminal voltage. Thus, although the stray-load losses are smoothed by linear regression, any of the above factors may still influence the stray-load losses obtained and hence the load-dependent component of harmonic losses. The automated test therefore minimizes such influences by ensuring the test conditions are as closely matched as possible. From the plots in Fig. 8.21 and 8.22, the stray-load losses obtained with sinusoidal and converter supplies are reported in Table 8.4.

Table 8.4 Obtained harmonic losses from stray-load losses

Load [%]	**Manual load tests**			**Automated load tests**		
	$P_{SLL\ conv}$ [w]	**$P_{SLL\ sin}$ [w]**	**$P_{HL\ Load}$ [w]**	**$P_{SLL\ conv}$ [w]**	**$P_{SLL\ sin}$ [w]**	**$P_{HL\ Load}$ [w]**
125	1172.9	1094.2	78.8	1129.9	1129.8	0.1
115	986.5	928.4	58.0	951.0	948.9	2.1
100	756.9	703.5	53.4	728.5	726.9	1.7
75	416.8	397.3	19.5	401.1	395.4	5.7
50	184.9	173.5	11.4	175.5	170.3	5.2
25	47.0	44.7	2.3	44.6	43.7	0.9

The results presented in Table 8.4 illustrate how experimental results can lead to different conclusions about the nature of additional harmonic losses. In the manual tests, the stray-load losses on converter supply ($P_{SLL\ conv}$) were higher than the corresponding sinusoidal supply stray-load losses ($P_{SLL\ sin}$). This suggests a tendency for the harmonic losses to increase with load as asserted in the IEC/TS. On the contrary, the automated test results indicate that these losses are generally independent of load since the stray-load losses obtained with the two supplies were practically equal. Nevertheless, considering rating of the motor (55kW), these load-dependent harmonic losses obtained in the manual test are minimal and can be considered well within the tolerances of the measurement devices. At each load point, these losses were found to be less than 1% of the total losses as shown in section 8.2.3. Therefore, the obtained load-dependent harmonic losses in the manual test could be attributed to measurement errors and other practical testing considerations.

Although similar efficiencies were obtained from the manual and automated testing approaches, the above discussion regarding the stray-load losses obtained stresses the need for adopting automated testing in the determination of additional harmonic losses.

8.4 SUMMARY

In this chapter, the experimental determination of additional harmonic losses according to the proposed IEC/TS procedure has been investigated. The results obtained have highlighted three key findings: The first is that a VFD can be used to estimate the sinusoidal supply efficiency of an induction motor. This development is very important as it allows individuals and testing centres to perform efficiency tests without a conventional variable voltage source. The second key finding is that converter harmonics generally do not impact the stray-load losses. This results in no significant change in the induction motor stray-load losses between sinusoidal and PWM supplies. If any minor differences are obtained, they can generally be attributed to incorrect testing methodology or measurement errors. Therefore, the degradation in motor efficiency due to a PWM supply is mainly due to the increase in no-load iron losses.

The experimental results analysed in this chapter also highlighted the impact of not strictly meeting the voltage requirements of the IEC/TS. By applying a lower voltage to the motor owing to the voltage drop across the reactor, the stator and rotor losses were found to increase. However, this loss increment was not reflected in the final efficiency obtained using the IEC/TS formula as it considers sinusoidal supply output power and losses. Therefore, while the proposed IEC/TS methodology is valid, the more established IEC 60034-2-3 methodology offers a more cautious and reliable approach amid load torque and voltage mismatches.

Lastly, the automated testing procedure was validated with experimental results. The results reported in section 8.3 highlighted several improvements that were realized by adopting the automated efficiency testing procedure. These include the improved repeatability of test results, lower temperature variation and improved correlation coefficient. The automated testing procedure therefore improves the determination of stray-load losses, which are required in the determination of the load-depended harmonic losses according to the IEC/TS.

9. CONCLUSIONS

The estimation of induction motor efficiency under converter supply has continued to generate interest from various stake holders owing to the rapid penetration of VFDs on the market in the last two decades. Whereas a degradation in motor efficiency is generally expected between a sinusoidal supply and a PWM supply, the correct determination of this efficiency drop is of great importance. Although the recently introduced IEC 60034-2-3 Technical Specification provides a feasible method of estimating the converter-fed induction motor losses, some concepts still need to be refined. Among the contentious issues raised in this study are the standard's limitation to induction motors operating at rated fundamental voltage and frequency, and its applicability only to 2-level Voltage Source Inverters. However, since the procedure is still undergoing validation, the work presented in this dissertation provides some positive feedback to the relevant IEC standards committee.

As shown in this dissertation, the methodology adopted during testing has the potential to influence the additional harmonic losses obtained. It is therefore important that stakeholders fully understand the testing requirements regarding the fundamental motor voltage in the presence of other drive components like output reactors. Since the additional harmonic losses are largely independent of load, as shown in this study, the efficiency degradation in an induction motor due to the harmonic voltages and currents can be roughly estimated by simply adding the constant component of the additional harmonic losses at rated motor voltage to the total losses determined with a sinusoidal supply. Nowadays, this can easily be achieved using modern Data Acquisition Systems that allow the segregation of fundamental voltage, current and power from the unfiltered measurements with a PWM supply.

Using the aforementioned segregation feature of modern Data Acquisition Systems, this research further demonstrated the feasibility of determining the sinusoidal supply efficiency of an induction motor using a PWM supply. This is an interesting development to the motor-efficiency testing process as it not only increases the choice of variable-voltage power supplies but also avoids the risk of voltage and frequency fluctuations which are a common problem on mains supply. It also has the potential to eliminate the sinusoidal supply tests required for the IEC/TS procedure since the same PWM supply test can be used to estimate both fundamental motor losses and additional harmonic losses. This will then eliminate possible errors due to mismatch in loading between sinusoidal and PWM supply tests.

In research and design, it is sometimes required to analyse the dynamic response of various systems. As VFDs are fast becoming the core of industrial process control, it is important to fully understand their influence on the dynamic operation of induction motors. Therefore, this dissertation dedicated a section to the analysis of some starting and acceleration/deceleration operations to some provide insight as well as to demonstrate the capabilities of the recently developed 110kW test rig in the UCT machines lab. The rich data provided by the *Genesis 7i* high-speed DAQ demonstrates its usefulness as a tool for both research and teaching purposes.

Another interesting feature of the DAQ is its automated-data-capturing capability which was utilized to develop an automated testing procedure. Since the determination of additional harmonic losses depends on the accurate determination of induction motor losses on both sinusoidal and PWM supply, the developed automated testing procedure ensures the two tests are performed in an identical manner. Compared to the manual approach, the automated testing method resulted in an improvement in the repeatability of results and the correlation coefficient, which is a benchmark for quality assurance in efficiency tests. Automated testing also minimizes temperature variations during the load test and allows non-experts to perform efficiency testing.

Future work should include the analysis of converter-fed induction motor losses during operation above and below the base speed. In addition, other topologies of electric motors and converters should also be investigated. At present, the recently developed IEC 60034-2-3 as Technical Specification is a welcome development and its maturity into a full international standard will be of great importance to manufacturers, end-users and policy makers.

REFERENCES

[1]. P. Waide, and C. Brunner. "Energy-efficiency policy opportunities for electric motor-driven systems," IEA, paris, 2011.

[2]. A. de Almeida, F. Ferreira, and A. Quintino Duarte, “Technical and economical considerations on super high efficiency three-phase motors,” IEEE Trans. Ind. Appl., vol. 50, no. 2, pp. 1274–1285, Mar. 2014.

[3]. N. Mohan, T.M. Undeland, and W. P. Robbins, *Power electronics: converters, applications, and design*, John Wiley & Sons, third edition, 2007.

[4]. M.J. Melfi, “Quantifying the Energy Efficiency of Motors on Inverters”, IEEE Industry Applications Magazine, Vol.17, No.6, 2011, pp. 37-43.

[5]. Commission Regulation (EC) No 640/2009, “Implementing Directive 2005/32/EC of the European Parliament and of the Council with regard to ecodesign requirements for electric motors”, Official Journal of the European Union, L 191, 23.7.2009, pp. 26-34, [Online]. Available: http://eurlex.europa.eu/en/index.htm.

[6]. A. Boglietti, A. Cavagnino, M. Cossale, A. Tenconi and S. Vaschetto, "Efficiency determination of converter-fed induction motors: Waiting for the IEC 60034–2–3 standard," 2013 IEEE Energy Conversion Congress and Exposition, Denver, CO, 2013, pp. 230-237.

[7]. IEC Std 60034-30, "Rotating electrical machines—Part 30: Efficiency classes of single-speed, three-phase, cage-induction motors (IE-code), 1st Ed", 2008.

[8]. Eskom – Demand Side Management, “DSM Energy Efficient Motors,” [Online]. Available: http://www.eskom.co.za/sites/idm/Documents/117102ESKD_DSM_EE_Motors [Accessed Mar. 25, 2018]

[9]. IEEE Std 112-2004, “IEEE Standard Test Procedure for Polyphase Induction Motors and Generators," (Revision of IEEE Std 112-1996), vol., no., pp.1-83, 4 Nov. 2004.

[10]. IEC Std 60034-2-1, “Rotating Electrical Machines Part 2-1: Standard Methods for Determining Losses and Efficiency from Tests,” 2014.

[11]. IEC-TS 60034-2-3, “Rotating electrical machines - part 2-3: Specific test methods for determining losses and efficiency of converter-fed ac induction motors,” ed. 1.0, Nov. 2013.

[12]. K. Yamazaki and S. Kuramochi, "Additional harmonic losses of induction motors by PWM inverters: Comparison between result of finite element method and IEC/TS 60034," 2012 XXth International Conference on Electrical Machines, Marseille, 2012, pp. 1552-1558.

[13]. H. Kärkkäinen, L. Aarniovuori, M. Niemelä and J. Pyrhönen, "Converter-fed induction motor losses in different operating points," 2016 18th European Conference on Power Electronics and Applications (EPE'16 ECCE Europe), Karlsruhe, 2016, pp. 1-8.

[14]. E. B. Agamloh, "Power and Efficiency Measurement of Motor-Variable-Frequency Drive Systems," in IEEE Transactions on Industry Applications, vol. 53, no. 1, pp. 766-773, Jan.-Feb. 2017.

[15]. F. Tinazzi, M. Zigliotto, A. Boglietti, A. Cavagnino and M. Cossale, "Energy efficiency assessment for inverter-fed induction motors," 8th IET International Conference on Power Electronics, Machines and Drives (PEMD 2016), Glasgow, 2016, pp. 1-6.

[16]. R. Antonello, F. Tinazzi, and M. Zigliotto, “Energy efficiency measurements in IM: The non-trivial application of the norm IEC 60034- 2-3:2013,” in Proc. 2015 IEEE Workshop on Electrical Machines Design, Control and Diagnosis, Torino, Italy, 2015, pp. 248–253.

[17]. IEEE Std 995, “IEEE Recommended Practice for Efficiency Determination of AC Adjustable Speed Drives, Part 1: Load Commutated Inverter Synchronous Motor Drives,” 1987.

[18]. CSA C838-13, “Energy Efficiency Test Methods for Three-Phase Variable Frequency Drives Systems,” 2013.

[19]. EN 50598-2, “Ecodesign for Power Drive Systems, Motor Starters, Power Electronics and Their Driven Applications, Part 2: Energy Efficiency Indicators for Power Drive Systems And Motor Starters,” Dec. 2014.

[20]. P.C Sen, *Principles of Electrical Machines and Power Electronics*, 2nd ed., Kingston: John Wiley and Sons, Inc, 1997.

[21]. G. Bucci, F. Ciancetta, E. Fiorucci and A. Ometto, "Uncertainty Issues in Direct and Indirect Efficiency Determination for Three-Phase Induction Motors: Remarks About the IEC 60034-2-1 Standard," in IEEE Transactions on Instrumentation and Measurement, vol. 65, no. 12, pp. 2701-2716, Dec. 2016.

[22]. H. Karkkainen, L. Aarniovuori, M. Niemela and J. Pyrhonen, "Converter-Fed Induction Motor Efficiency: Practical Applicability of IEC Methods," in IEEE Industrial Electronics Magazine, vol. 11, no. 2, pp. 45-57, June 2017.

[23]. J. M. Kinyua, M. A. Khan and P. Barendse, "Development and efficiency estimation of a regenerative test rig for induction motor testing," 2016 IEEE Energy Conversion Congress and Exposition (ECCE), Milwaukee, WI, 2016, pp. 1-6.

[24]. A. Boglietti, P. Ferraris, M. Lazzari and M. Pastorelli, "Influence of the inverter characteristics on the iron losses in PWM inverter-fed induction motors," in IEEE Transactions on Industry Applications, vol. 32, no. 5, pp. 1190-1194, Sept.-Oct. 1996.

[25]. A. Boglietti, A. Cavagnino, D. M. Ionel, M. Popescu, D. A. Staton and S. Vaschetto, "A General Model to Predict the Iron Losses in PWM Inverter-Fed Induction Motors," in IEEE Transactions on Industry Applications, vol. 46, no. 5, pp. 1882-1890, Sept.-Oct. 2010.

[26]. L. Aarniovuori, A. Kosonen, M. Niemelä and J. Pyrhönen, "Frequency converter driven induction motor losses," IECON 2013 - 39th Annual Conference of the IEEE Industrial Electronics Society, Vienna, 2013, pp. 2881-2886.

[27]. M. Benhaddadi, F. Landry, R. Houde and G. Olivier, "Energy efficiency electric Premium motor-driven systems," International Symposium on Power Electronics Power Electronics, Electrical Drives, Automation and Motion, Sorrento, 2012, pp. 1235-1239.

[28]. C. Burt, X. Piao, F. Gaudi, B. Busch, and N. Taufik, “Electric motor efficiency under variable frequencies and loads,” Journal of irrigation and drainage engineering, 134(2), pp.129-136, 2008.

[29]. Z. Gmyrek, A. Boglietti and A. Cavagnino, "No-load loss separation in induction motors operated by PWM inverters: Numerical and experimental approaches," IECON 2011 - 37th Annual Conference of the IEEE Industrial Electronics Society, Melbourne, VIC, 2011, pp. 1941-1947.

[30]. L. Aarniovuori, P. Rasilo, M. Niemelä and J. J. Pyrhönen, "Analysis of 37-kW Converter-Fed Induction Motor Losses," in IEEE Transactions on Industrial Electronics, vol. 63, no. 9, pp. 5357-5365, Sept. 2016.

[31]. A. Boglietti, A. Cavagnino, M. Lazzari and M. Pastorelli, "International standards for the induction motor efficiency evaluation: a critical analysis of the stray-load loss determination," in IEEE Transactions on Industry Applications, vol. 40, no. 5, pp. 1294-1301, Sept.-Oct. 2004

[32]. E. B. Agamloh, "An Evaluation of Induction Machine Stray Load Loss From Collated Test Results," in IEEE Transactions on Industry Applications, vol. 46, no. 6, pp. 2311-2318, Nov.-Dec. 2010.

[33]. A. T. de Almeida, F. T. E. Ferreira, J. F. Busch and P. Angers, "Comparative analysis of IEEE 112-B and IEC 34-2 efficiency testing standards using stray load losses in low voltage three-phase, cage induction motors," 2001 IEEE Industrial and Commercial Power Systems Technical Conference. Conference Record (Cat. No.01CH37226), New Orleans, LA, 2001, pp. 13-19.

[34]. P. Pillay, M. Al-Badri, P. Angers and C. Desai, "A New Stray-Load Loss Formula for Small and Medium-Sized Induction Motors," in IEEE Transactions on Energy Conversion, vol. 31, no. 3, pp. 1221-1227, Sept. 2016.

[35]. J. Murimi, "Development of a Specialised Test Rig for Assessing the Efficiency of Large Industrial Induction Machines," Master's Thesis, University of Cape Town, Department of Electrical Engineering, 2016.

[36]. S. Corino E. Romero L. F. Mantilla, "How the efficiency of induction machine is measured," Proceedings of the International Conference of Renewable Energies and power Quality (ICREPQ '08), 2008.

[37]. A. Sheikh, "Magnetization curve," [Online]. Available: http://electricalacademia.com/electromagnetism/hysteresis-loop-magnetization-curve.

[38]. A. Boglietti, A. Cavagnino, A. M. Knight and Y. Zhan, "Factors Affecting Losses in Induction Motors with Non-Sinusoidal Supply," 2007 IEEE Industry Applications Annual Meeting, New Orleans, LA, 2007, pp. 1193-1199.

[39]. S. Williamson, A.C. Smith "Influence of interbar currents on the harmonic losses and skew in cage induction machines." Power Electronics Machines and Drives Conference April 2002 No. 487 pp. 369-374.

[40]. L. Serrano-Iribarnegaray J. Martinez-Roman "Critical review of the analytical approaches accounting for interbar currents and experimental study of ageing in two-speed asynchronous motors for elevator drives. "IEE Proc. on Electric Power Applications January 2005 Vol. 152 No. 1 pp. 72-80.

[41]. P.J. Holik D.G. Dorrell P. Lombard H.J. Thougaard F.A. Jensen "Multi-Sliced Finite Element Model for Induction Machines Incorporating Inter-bar Current." IEEE IAS Annual Meeting Tampa FL 2006.

[42]. IEEE Std 519-2014, "IEEE Recommended Practice and Requirements for Harmonic Control in Electric Power Systems," (Revision of IEEE Std 519-1992), vol., no., pp.1-29, June 11 2014.

[43]. "Output Filters (Chokes) for Optidrives Installation Guide IP20 & IP66," issue 2.10, [Online]. Available: http://www.invertekdrives.com, [Accessed Sep. 20, 2017]

[44]. E. Armando, A. Boglietti, R. Bojoi, A. Cavagnino and A. Tenconi, "Test rig for induction motor quasi-static electromechanical characteristic determination," IECON 2014 - 40th Annual Conference of the IEEE Industrial Electronics Society, Dallas, TX, 2014, pp. 919-924.

[45]. R. Bojoi, E. Armando, M. Pastorelli and K. Lang, "Efficiency and loss mapping of AC motors using advanced testing tools," 2016 XXII International Conference on Electrical Machines (ICEM), Lausanne, 2016, pp. 1043-1049.

[46]. “Effect of harmonics on induction motor,” [Online]. Available: http://www.acdrive.org/effect-of-harmonics-on-induction-motor.html, [Accessed Nov. 7, 2018].

[47]. W. Cao, "Comparison of IEEE 112 and New IEC Standard 60034-2-1," in IEEE Transactions on Energy Conversion, vol. 24, no. 3, pp. 802-808, Sept. 2009.

[48]. A. Boglietti, R. Bojoi, A. Cavagnino and L. Ferraris, "No-load operations of induction motors under PWM supply," 2010 IEEE International Symposium on Industrial Electronics, Bari, 2010, pp. 1383-1388.

[49]. A. Boglietti, R. Bojoi, A. Cavagnino and M. Lazzari, "Core loss estimation method for PWM inverter fed induction motors," IECON 2010 - 36th Annual Conference on IEEE Industrial Electronics Society, Glendale, AZ, 2010, pp. 811-816.

[50]. A. Boglietti, E. Carpaneto, M. Cossale, S. Vaschetto, “Stator Winding Thermal Models for Short-Time Thermal Transients: Definition and Validation”, IEEE Trans. Ind. Electron., vol.63, no.5,2016, pp.2713-2721.

[51]. World Energy Council, “CountryCaseStudies-ElectricMotors-SouthAfrica,” Energy Efficiency Policies and Measures, [Online]. Available: https://wec-policies.enerdata.net/Documents/cases-studies/Country CaseStudies-ElectricMotors-SouthAfrica.pdf, [Accessed Jul. 20, 2018]

[52]. Eskom Demand Side Management, “Tax allowance to grow your business (12L Tax Allowance),” [Online] Available: http://www.eskom.co.za/sites/idm/Business/Documents/Alternativefundingsolution Factsheet12L.pdf, [Accessed Jul. 20, 2018].

APPENDIX

APPENDIX A: MEASURED TEST DATA

A.1 No-load tests on PWM supply

Table A1.1 37kW Motor No-load test results on PWM supply

Temp [°C]	Voltage [V]	Current [A]	Power [W]
73.1	440.5	34.2	2439.2
73.1	400.2	25.1	1941.9
73.0	380.4	22.1	1810.1
72.9	360.2	19.8	1702.1
72.7	240.9	12.3	1196.6
72.5	200.6	10.4	1030.0
72.3	160.5	8.5	862.9
72.1	120.7	7.1	699.3

Table A1.2 45kW Motor No-load test results on PWM supply

Temp [°C]	Voltage [V]	Current [A]	Power [W]
84.3	441.2	43.9	2788.1
84.3	400.9	32.1	2171.7
84.2	381.1	28.3	2013.4
84.0	360.7	25.3	1888.1
83.9	241.4	15.5	1348.4
83.6	200.9	13.0	1163.2
83.4	160.7	10.6	978.2
83.1	120.9	8.6	795.5

Table A1.3 55kW Motor No-load test on PWM supply

Temp [°C]	Voltage [V]	Current [A]	Power [W]
93.8	429.4	31.0	1902.8
93.3	390.4	26.0	1734.5
92.2	370.0	24.1	1665.7
91.8	351.2	22.5	1605.3
91.3	234.1	14.6	1201.3
90.8	195.7	12.3	1057.3
90.3	156.5	10.2	903.5
89.6	117.8	8.4	759.8

A.2 No-load tests: Comparison of sinusoidal and fundamental PWM

Table A2.1 37 kW motor no-load test: comparison of sinusoidal and fundamental PWM

Temperature [°C]		Input Power [W]		Voltage [V]		Current [A]	
sine	pwm	sine	pwm	sine	pwm	sine	pwm
75.7	73.1	2027.3	2004.8	440.3	440.5	34.0	34.1
75.6	73.1	1446.7	1421.6	400.6	400.2	24.9	25.0
75.5	73.0	1270.0	1249.2	380.5	380.4	21.9	22.0
75.3	72.9	1137.9	1113.8	360.5	360.2	19.7	19.7
75.0	72.7	674.1	661.2	239.9	240.9	11.9	12.1
74.7	72.5	580.3	565.8	200.4	200.6	10.1	10.1
74.5	72.3	502.7	489.6	160.3	160.5	8.1	8.1
74.1	72.1	442.5	431.7	120.2	120.7	6.4	6.4

Table A2.2 45kW motor no-load test: comparison of sinusoidal and fundamental PWM

Temperature [°C]		Input Power [W]		Voltage [V]		Current [A]	
sine	pwm	sine	pwm	sine	pwm	sine	pwm
87.2	84.3	2329.1	2315.4	440.6	441.2	43.5	43.7
87.4	84.3	1639.9	1616.1	400.5	400.9	31.8	31.9
87.4	84.2	1435.8	1413.9	380.4	381.1	28.0	28.1
87.3	84.0	1285.9	1256.4	360.5	360.7	25.1	25.2
87.2	83.9	762.9	743.3	240.4	241.4	15.1	15.3
87.0	83.6	659.8	637.2	200.3	200.9	12.6	12.8
86.9	83.4	571.9	554.9	160.3	160.7	10.2	10.2
86.7	83.1	504.2	491.7	120.2	120.9	7.9	8.0

Table A2.3 55kW motor no-load test: comparison of sinusoidal and fundamental PWM

Temperature [°C]		Input Power [W]		Voltage [V]		Current [A]	
sine	pwm	sine	pwm	sine	pwm	sine	pwm
102.98	93.80	1485.56	1428.63	429.42	429.36	30.87	30.92
101.86	93.30	1263.52	1210.13	390.90	390.37	26.01	25.88
100.78	92.18	1184.25	1127.06	370.42	370.00	23.97	24.01
99.82	91.77	1105.51	1056.80	351.18	351.24	22.38	22.40
98.44	91.34	749.58	717.29	234.74	234.08	14.41	14.34
97.56	90.76	650.56	637.48	195.42	195.65	12.06	12.02
96.70	90.31	575.75	562.80	156.24	156.54	9.84	9.82
95.43	89.58	513.46	510.06	117.96	117.84	7.89	7.79

A.3 Load curve tests on sinusoidal supply

Table A3.1 37 kW motor load-curve test on sinusoidal supply

Temp [°C]	Torque [Nm]	Speed [rpm]	Voltage [V]	Current [A]	Power [W]	Freq [Hz]
97.8	300.8	1466.9	400.8	85.8	52113.9	50.0
98.3	277.8	1469.8	400.9	79.5	48080.6	50.0
98.3	240.8	1474.3	400.9	69.9	41803.7	50.0
97.8	179.8	1481.2	401.0	55.1	31578.6	50.0
96.6	120.5	1487.5	401.1	41.9	21709.8	50.0
95.2	60.3	1493.6	401.2	31.0	11774.2	50.0

Table A3.2 45 kW motor load-curve test on sinusoidal supply

Temp [°C]	Torque [Nm]	Speed [rpm]	Voltage [V]	Current [A]	Power [W]	Freq [Hz]
110.4	321.9	1473.2	400.6	91.5	55263.9	50.0
110.3	291.9	1475.9	400.7	84.0	50214.8	50.0
108.6	219.4	1482.3	400.8	66.7	38057.6	50.0
106.4	146.6	1488.2	400.9	51.0	26057.5	50.0
104.7	73.9	1493.9	401.0	38.5	14137.4	50.0

Table A3.3 55kW motor load-curve test on sinusoidal supply

Temp [°C]	Torque [Nm]	Speed [rpm]	Voltage [V]	Current [A]	Power [W]	Freq [Hz]
126.82	531.26	1445.50	389.50	152.63	91512.95	49.94
129.58	443.45	1456.44	390.35	125.20	75745.66	49.94
129.32	356.58	1465.30	391.33	100.18	60588.35	49.91
126.86	264.27	1473.82	391.57	75.94	45033.44	49.89
123.46	177.27	1486.03	393.46	54.98	30825.98	50.03
118.63	88.58	1491.48	393.45	36.67	16466.25	49.97

A.4 Load-curve tests on PWM supply

Table A4.1 37 kW motor load-curve test on PWM supply

Temp [°C]	Torque [Nm]	Speed [rpm]	Voltage [V]	Current [A]	Power [W]	Freq [Hz]
99.3	301.0	1466.2	400.9	86.0	52534.8	50.0
100.0	277.0	1469.2	401.1	79.6	48455.3	50.0
100.2	240.4	1473.5	400.4	70.2	42227.2	50.0
99.8	179.7	1480.6	400.8	55.2	31963.9	50.0
98.9	120.1	1487.0	400.7	42.0	22031.2	50.0
97.6	60.4	1493.2	401.1	31.1	12138.3	50.0

Table A4.2 45 kW motor load-curve test on PWM test

Temp [°C]	Torque [Nm]	Speed [rpm]	Voltage [V]	Current [A]	Power [W]	Freq [Hz]
112.3	321.8	1472.7	400.9	91.6	55699.2	50.0
112.5	291.9	1475.5	401.2	84.0	50547.2	50.0
110.2	219.5	1481.9	401.7	66.6	38359.6	50.0
107.3	146.4	1487.9	402.2	51.3	26347.5	50.0
103.2	74.0	1493.8	403.1	38.9	14486.9	50.0

Table A4.3 55 kW motor load-curve test on PWM supply

Temp [°C]	Torque [Nm]	Speed [rpm]	Voltage [V]	Current [A]	Power [W]	Freq [Hz]
126.98	530.50	1446.99	389.45	152.62	91812.79	49.99
130.75	443.26	1458.11	391.05	125.12	76152.51	49.99
130.29	356.30	1467.71	391.58	100.32	61034.93	49.99
127.64	265.89	1476.97	393.13	76.32	45722.29	49.99
123.97	176.88	1484.82	393.91	54.94	31078.56	49.99
117.90	88.64	1492.11	393.87	36.82	16823.70	49.99

APPENDIX B: INSTRUCTIONS FOR AUTOMATED TESTING PROCEDURE

B.1 No-load test on sinusoidal supply using MX 60 Power supply

The automated no-load test program is intended to start-up the motor from rest, accelerate it to rated voltage and frequency and then apply the required no-load voltages. The procedure outlined below assumes the MX60 output is initially set to deliver Zero volts. To run the automated no-load test on sinusoidal supply using the MX60 programmable power supply, the procedure outline below must be followed:

- Run the virtual panels software on the windows PC and make sure the MX60 power supply unit is recognized by selecting the appropriate serial connection. It is preferred to use LAN connection as it provides faster data transfer rates than USB.
- Once the MX60 is connected, shown by a green flashing indicator in the top right corner of the home screen, open transient lists tab and select the file '***Automated no-load test with modified start-up ramp***' from the available list of transient files.
- Before executing the transient list file, ensure the appropriate power supply configuration is selected on the Power supply configuration panel (white panel) and that the last contactor is energized.
- Also ensure that a signal interface cable is connected from the MX60 master's ***external trigger out*** port to the ***external start in*** connector of the Genesis 7i DAQ. Note that at the initial connection, the DAQ may trigger as it is set on ACTIVE-LOW.
- Run the transient list execution and wait until all data is captured and the transient list gives a notification that the operation is completed successfully.

B.2 No-load test on PWM supply (Test Drive)

The automated no-load test program is intended to apply the required no-load voltages to the motor when it is already running at rated voltage and frequency. Therefore, the motor must be started normally using the front panel controls on the drives panel (orange). Once the motor is running at rated voltage and frequency on drive supply, execute the automated no-load test by following the procedure outlined below:

- Ensure the serial communication cable (with a serial-to-usb converter) is connected between the Load drive and the windows PC, and that the ***external start in*** connector of the Genesis 7i DAQ is connected to the normally-open contacts of the 24V dc relay.

- On the windows PC, open ***Sypt Pro*** software and allow it to scan all connected ports. Once it establishes a communications link with all connected ports (under a yellow background), open the ***project*** tab and add all detected nodes by allowing each node to build/ upload.
- Open the test drive node DPL code and on the left task bar, find the ***automated no-load test*** in the background tasks. Since this code is in the background tasks (i.e continuously running), it is recommended to first stop the background task execution and turn contact switch ***#18.35*** **ON** by inputting a digital on (bit 1).
- Now restart the background task and wait for the automated no-load test to complete and automatically turn switch #18.35 OFF. Note that stopping the execution before turning #18.35 ON ensures the no-load test starts from the top, otherwise it may start from anywhere depending on which line of code the background task is executing.

B.3 Load-curve test (Load Drive)

The automated load-curve test program is intended to apply a sequence of torque references to the load motor when it is applying rated load torque to the motor under test. To perform this test well, the operator is required to familiarise him/herself with the torque control mechanism of the load motor shown in the block diagram in Fig. B1.

As shown in Fig. B1, the torque reference applied to the load motor is a summation of the analogue torque reference and the torque offset. Since the automated load test inputs torque references using the torque offset parameter ***(#4.09)***, it is advisable to set the analogue torque reference (front panel knob) to zero to avoid overloading the test motor. The required torque references can be obtained manually at the end of the load-curve test or can be roughly estimated using the graph presented in Fig. 6.2. To perform the automated load curve test, follow the instructions outline below:

- Setup the serial communications and cyclic-link node detection as described under appendix B2 for the automated no-load test execution.
- Open the Load Drive node DPL code and on the left task bar, find the ***automated load-test*** in the background tasks. Prior to executing the load-curve test, go into offline mode and update the torque references as required for the specific test motor. Remember to switch-off all motors before updating the Load Drive DPL as it is the main code that links all the three drive modules. Therefore, all drives become disabled when it is updating.
- With rated load applied to the test motor, run the load test by setting ***#4.10*** and ***#18.35*** to 1

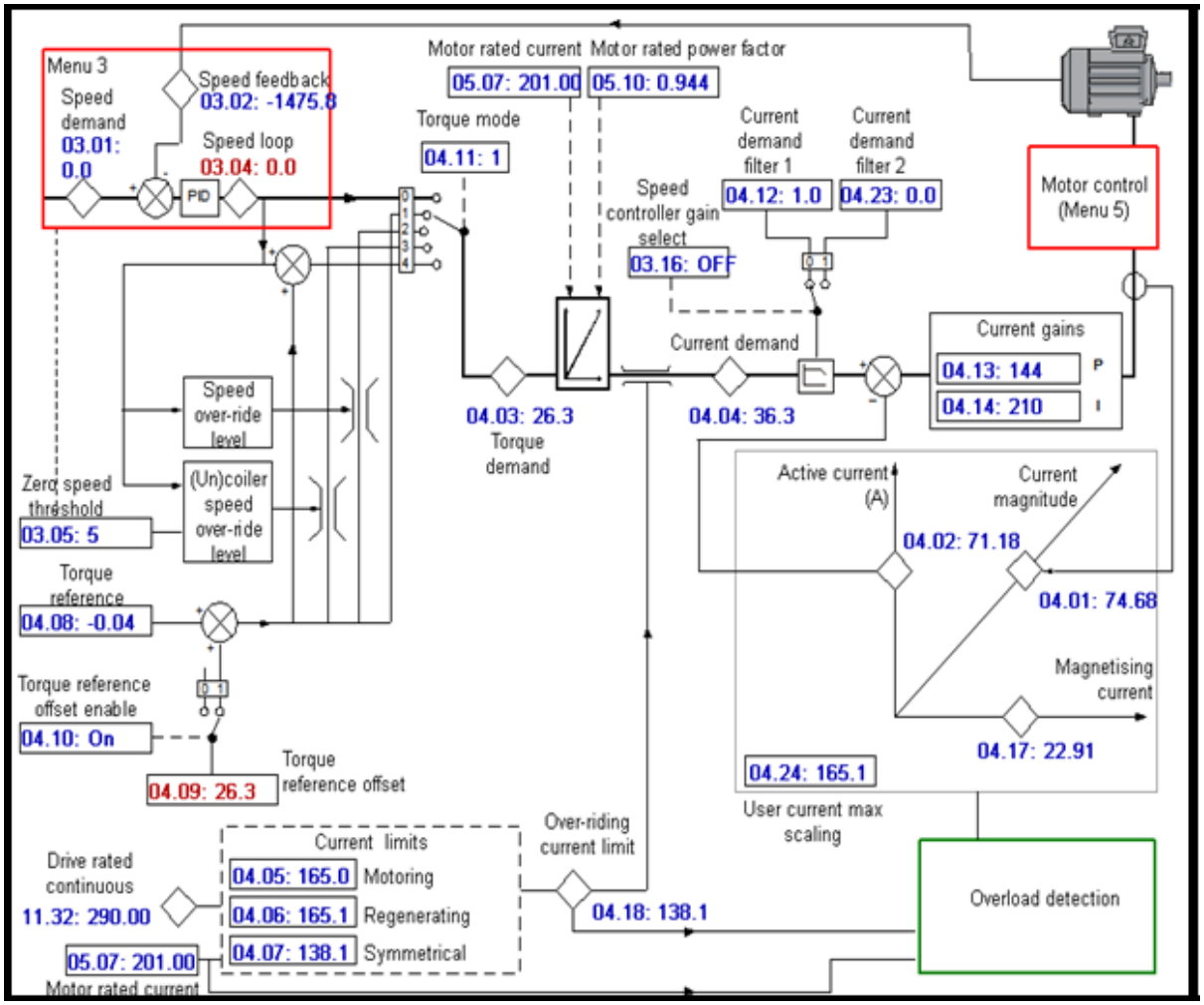

Fig.B1 Torque control block diagram of the Load motor

APPENDIX C: CODES FOR AUTOMATED TESTS

C.1 MX 60 Power supply Transient list file

Transient List Report

Transient Type	Dwell	Frequency	Volt A	Function A	Volt B	Function B	Volt C	Function C	Repeat	IsTriggerAppl
VoltageFrequencyStep	0.001	17	30	SINE	30	SINE	30	SINE	0	False
VoltageFrequencySweep	3	20	92	SINE	92	SINE	92	SINE	0	False
VoltageFrequencySweep	10	50	230.9	SINE	230.9	SINE	230.9	SINE	0	False
VoltageStep	0.001		254	SINE	254	SINE	254	SINE	0	False
Delay	0.001			SINE		SINE		SINE	0	True
VoltageStep	0.001		230.9	SINE	230.9	SINE	230.9	SINE	0	False
Delay	0.001			SINE		SINE		SINE	0	True
VoltageStep	0.001		219.3	SINE	219.3	SINE	219.3	SINE	0	False
Delay	0.001			SINE		SINE		SINE	0	True
VoltageStep	0.001		207.8	SINE	207.8	SINE	207.8	SINE	0	False
Delay	0.001			SINE		SINE		SINE	0	True
VoltageStep	0.001		138.6	SINE	138.6	SINE	138.6	SINE	0	False
Delay	0.001			SINE		SINE		SINE	0	True
VoltageStep	0.001		115.5	SINE	115.5	SINE	115.5	SINE	0	False
Delay	0.001			SINE		SINE		SINE	0	True
VoltageStep	0.001		92.4	SINE	92.4	SINE	92.4	SINE	0	False
Delay	0.001			SINE		SINE		SINE	0	True
VoltageStep	0.001		69.3	SINE	69.3	SINE	69.3	SINE	0	False
Delay	0.001			SINE		SINE		SINE	0	True

C.2 DPL code for Unidrive SP no-load test (Syptrol)

(* Set the drive output voltage to 110% ff motor rated voltage, wait for 5sec for the motor to stabilize then use #86.03 to start/stop the acquisition
N:B #18.35 is just a switch to run/ halt the program *)

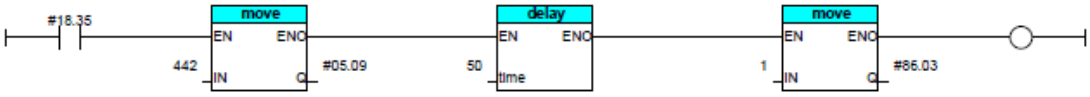

(* reset the relay and wait 7s for the acquisition to complete *)

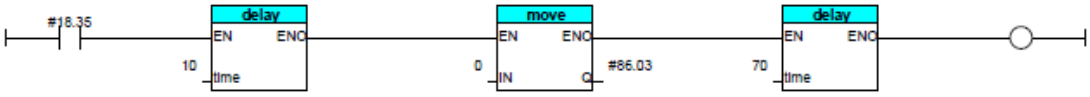

(* Set the drive output voltage to 100% 0f motor rated voltage and start the acquisition after 5 sec *)

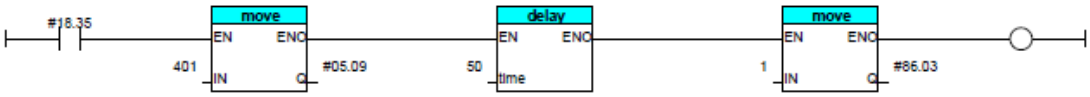

(* reset the relay and wait 7s for the acquisition to complete *)

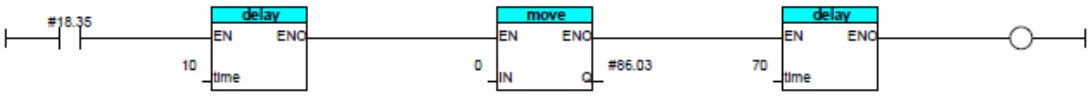

(* Set the drive output voltage to 95% 0f motor rated voltage and start the acquisition after 5 sec *)

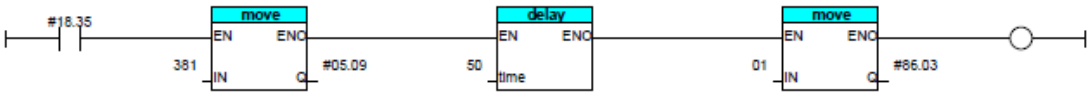

(* reset the relay and wait 7s for the acquisition to complete *)

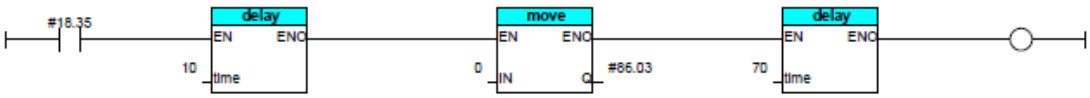

(* Set the drive output voltage to 90% 0f motor rated voltage and start the acquisition after 5 sec *)

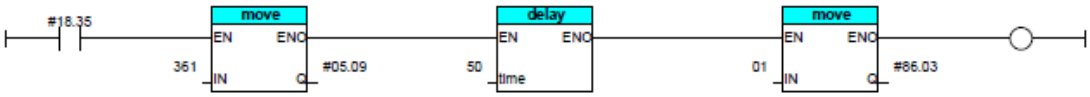

(* reset the relay and wait 7s for the acquisition to complete *)

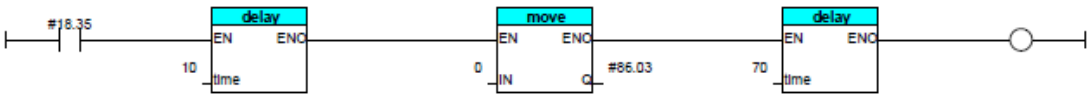

(* Set the drive output voltage to 60% 0f motor rated voltage and start the acquisition after 5 sec *)

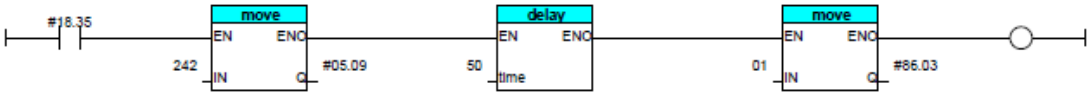

(* reset the relay and wait 7s for the acquisition to complete *)

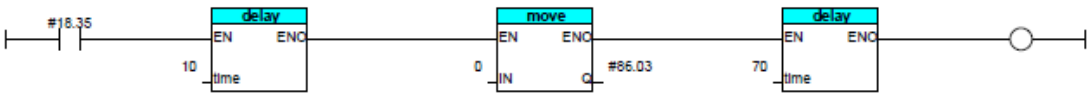

(* after 5 sec set the drive output voltage to 50% 0f motor rated voltage *)

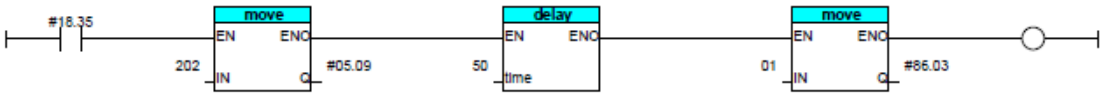

(* reset the relay and wait 7s for the acquisition to complete *)

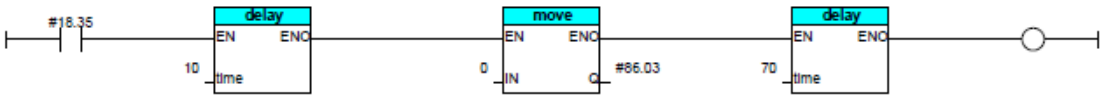

(* after 5 sec set the drive output voltage to 40% 0f motor rated voltage *)

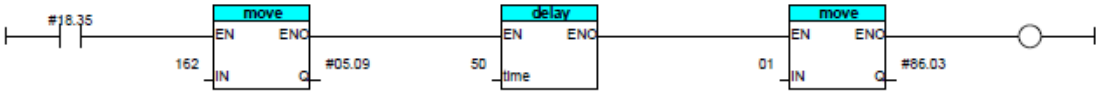

(* reset the relay and wait 7s for the acquisition to complete *)

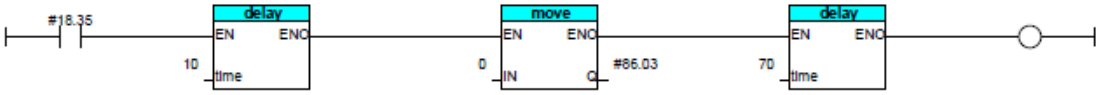

(* after 5 sec set the drive output voltage to 30% 0f motor rated voltage *)

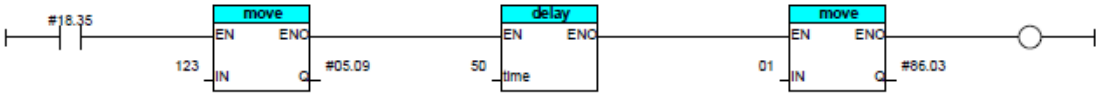

(* reset the relay and wait 7s for the acquisition to complete *)

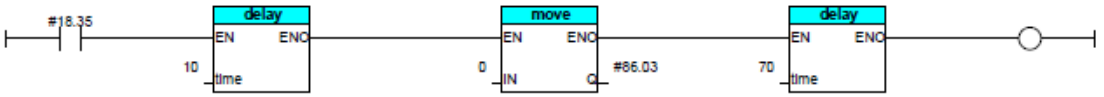

(* after 5 sec reset the acquisition and halt the program *)

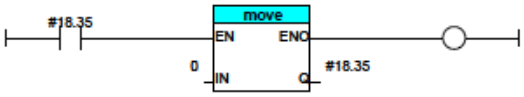

C.3 DPL code for Unidrive SP Load-curve test (Syptrol)

(* Set the load drive torque offset to a value that applies a torque of 125% of motor rated torque of the test motor, wait for 10 sec for steady state operation then start the acquisition using #86.05
N:B #18.35 is just a switch to run/ halt the program and #4.10 enables the torque offset *)

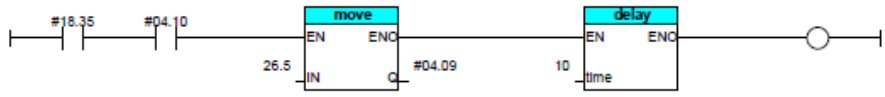

(* Double-click to enter a rung comment *)

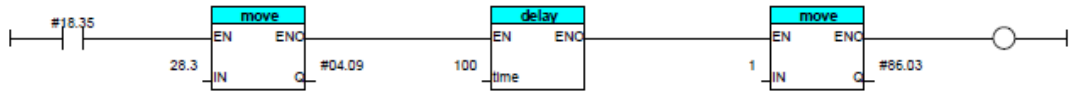

(* Wait for 10 sec and reset the acquisition *)

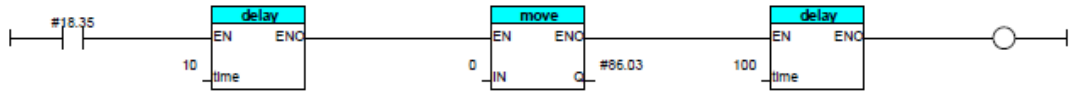

(* Set the drive torque offset to a value that applies 115% of motor rated torque and start the acquisition after 5 sec *)

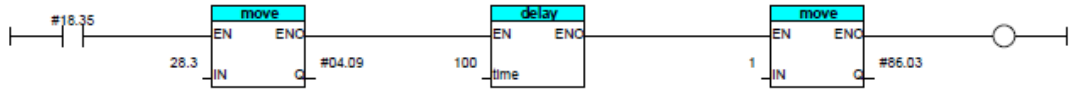

(* Wait for 10 sec and reset the acquisition *)

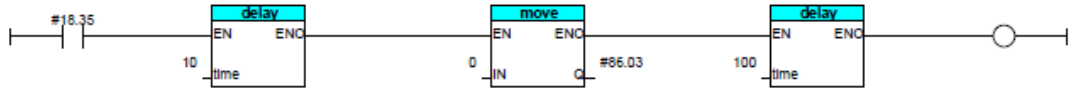

(* Set the drive torque offset to a value that applies 100% of motor rated torque and start the acquisition after 5 sec *)

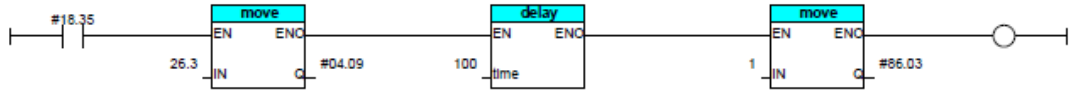

(* Wait for 10 sec and reset the acquisition *)

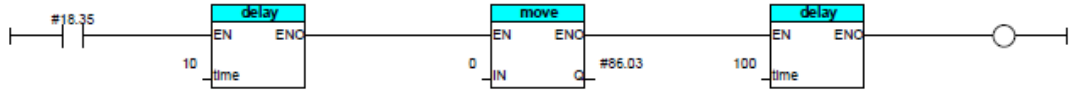

(* Set the drive torque offset to a value that applies 75% of motor rated torque and start the acquisition after 5 sec *)

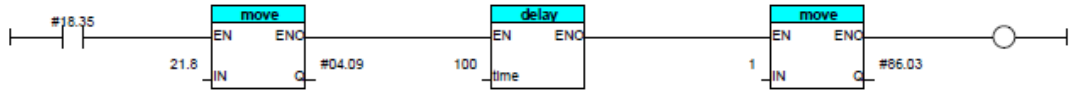

(* Wait for 10 sec and reset the acquisition *)

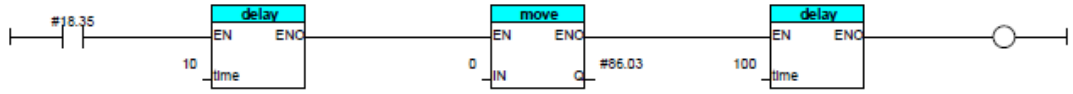

(* Set the drive torque offset to a value that applies 50% of motor rated torque and start the acquisition after 5 sec *)

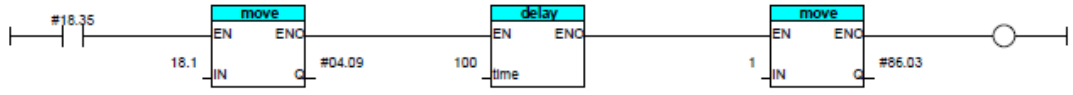

(* Wait for 10 sec and reset the acquisition *)

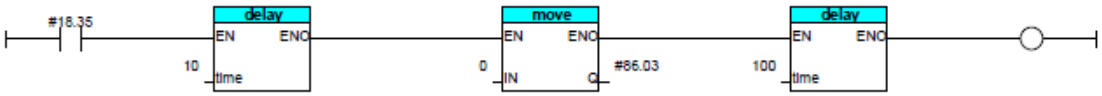

(* Set the drive torque offset to a value that applies 25% of motor rated torque and start the acquisition after 5 sec *)

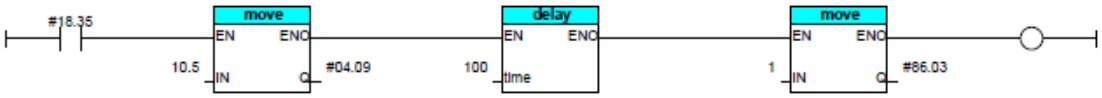

(* after 5 sec reset the acquisition and halt the program *)

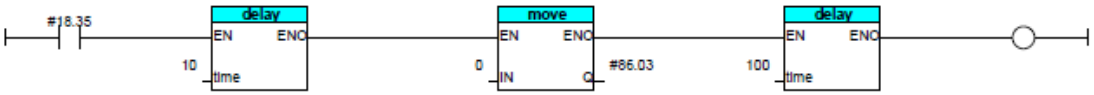

(* Double-click to enter a rung comment *)